Architecture and geodynamic evolution of the Svalbard Archipelago, the Yermak Plateau and the Fram Strait oceanic Province from deep seismic experiments

Aufbau und geodynamische Entwicklungsgeschichte des Svalbard-Archipels, des Yermak Plateaus und der ozeanischen Provinz der Framstraße aus tiefenseismischen Experimenten

---

Oliver Ritzmann

Ber. Polarforsch. Meeresforsch. 439 (2003)
ISSN 1618-3193

Oliver Ritzmann

Alfred-Wegener-Institut für Polar- und Meeresforschung
Geosystem
Sektion Struktur und Dynamik der Lithosphäre und Polarer Eisschilde
Columbusstraße
D-27515 Bremerhaven

Die vorliegende Arbeit ist die inhaltlich unveränderte Fassung einer Dissertation, die im September 2002 dem Fachbereich 5 - Geowissenschaften - der Universität Bremen vorgelegt wurde.

Eine elektronische Version dieser Dissertation kann unter
http://www.awi-bremerhaven.de/GPH/dissertationen.html
bezogen werden.

TABLE OF CONTENTS

ADDITIONAL WORK

LIST OF FIGURES AND TABLES

Chapter 4

Chapter 5

Chapter 6

ABSTRACT

Between 1997 and 1999 new seismic refraction data were acquired in the region of the Svalbard Archipelago. These experiments were carried out by a German, Polish, Norwegian and Japanese cooperation. The resultant seismic velocity profiles give new insight into the general crustal structure of Svalbard, its western continental margin, the Yermak Plateau and the adjacent Fram Strait in the northern Atlantic oceanic realm.

A fundamental observation of this study is that the Yermak Plateau north of the Svalbard Archipelago exhibits no evidence for elevated magmatic activity due to the presence of a mantle plume. The seismic velocity structure reveals none of the characteristic features of a rifted-volcanic margin. The southern Yermak Plateau shows instead a mid-crustal detachment that supports theories of Oligocene extensional movements and parallel development of pull-apart-like basins. Only slight amounts of melt have been intruded due to crustal thinning and subsequent decompressive melting.

Svalbard's different Caledonian terranes cannot be distinguished on the basis of their seismic structure. Stretching of continental crust, associated with the Cenozoic rifting of western Svalbard, is confined to the western terrane. The boundary between the western and central Caledonian terranes is overprinted by the Cenozoic Western Spitsbergen Orogenic Belt. This belt exhibits remarkably low seismic velocities within the upper brittle crust down to a depth of ~20 km, that leads to the assumption that the rock fabric is intensively sheared and faulted. Proposed flower structure models, in a transpressive tectonic regime, seem plausible for the evolution of the orogenic belt. The coincidence of Caledonian and Cenozoic (sinistral and dextral) shear zones may indicate the possible reactivation of old sutures.

The continental margin off western Svalbard is more segmented than previously thought. Off Van Mijenfjorden a rifted margin is observed. The continent-ocean transition off Kongsfjorden reveals a steep and abrupt change in Moho-depth that is interpreted as a sheared margin. The evolution of this sheared margin is associated with the Spitsbergen Fracture Zone of the southern Fram Strait. A rifted continental margin segment is observed off the northern margin of western Svalbard.

Oceanic crust off western Svalbard is very thin compared to the global mean. This is associated with slow spreading rates in the North Atlantic and the Fram Strait. The absence of oceanic layer 3, and low mantle seismic velocities, attributed to slight serpentinisation of upper mantle peridotites, are characteristics of the entire observed region.

The continental margins presented in this study are characterised by slight amounts of melt within the continent-ocean transition zone, regardless of having a rifted or sheared nature. At the sheared segment of the western Svalbard margin a possible source of melts is the large thermal contrast between cool continental crust and the hot oceanic mantle, which may have enhanced convective partial melting. The injection of melts is supposed to have occurred during the northward propagation of the Knipovich Ridge, or the passage of the Molloy Ridge along the (sheared) continental margin. The ancient Tertiary shear zones between Svalbard and Greenland (Spitsbergen Shear Zone) provide possible pathways for channelling and distribution of these melts along the western margin.

The zones of slight intrusion within the continent-ocean transition coincide with magnetic anomalies along Svalbard's western coast. At least one further anomaly is observed at the western Yermak Plateau, at the southern termination of a transform fault in the Fram Strait (Lena Trough). With regard to the proposed segmentation of the Svalbard margin, recent plate tectonic reconstructions, and the observed magnetic anomaly pattern, it follows, that the segmentation of the continental margin continues further north. The injection of melts is suggested to accompany the break-up. Sheared and non-sheared segments alternate along the margin.

KURZFASSUNG

In den Jahren 1997 bis 1999 führte das Alfred-Wegener-Institut für Polar- und Meeresforschung in Bremerhaven gemeinsam mit polnischen, norwegischen und japanischen Kooperationspartnern refraktionsseismische Experimente in der Region Svalbards durch. Die gewonnenen Tiefenprofile gewährleisten neue Erkenntnisse über den Krustenaufbau des Archipels, den vorgelagerten westlichen Kontinentalrand, das Yermak Plateau und die benachbarte ozeanische Provinz des Nordatlantiks.

Eine grundlegende Erkenntnis dieser Arbeit ist, dass keine Beweise für exzessive magmatische Aktivität aufgrund einer thermischen Anomalie in der Asthenosphäre (*mantle plume)* für das Yermak Plateau nördlich des Svalbard-Archipels geliefert werden können. Die seismische Struktur zeigt keine charakteristischen Elemente eines vulkanischen Kontinentalrandes (*rifted-volcanic margin*). Stattdessen ist die obere und mittlere Kruste des südlichen Yermak Plateaus durch eine Abscherungsfläche (*detachment*) getrennt, die Theorien über Dehnungsprozesse und Ausbildung von Aufreißbecken (*pull-apart basins*) während des Oligozän bestätigt. Während der Dehnung und Ausdünnung der Kruste sind wahrscheinlich aufgrund von Dekompression geringe Schmelzmengen aus dem Mantel in die untere Kruste intrudiert.

Die Kaledonischen Krustenfragmente Svalbards (*terranes*) können nicht anhand ihrer seismischen Struktur unterschieden werden. Krustendehnung wurde ausschließlich entlang des westlichen Kontinentalrandes innerhalb des westlichen Fragments beobachtet. Die Suturzone zwischen dem westlichen und dem zentralen Fragment ist maßgeblich überprägt durch das Känozoische Westspitzbergen-Orogen. Dieses Orogen zeigt bemerkenswert niedrige seismische Geschwindigkeiten in der oberen und mittleren, spröd-brechenden Kruste bis 20 km Tiefe. Dies führt zu der Annahme, dass der Gesteinsverband stark geschert und gestört ist. Geodynamische Modelle postulieren für die Auffaltung des Gebirgsgürtels eine Blumen-Struktur (*flower structure*) während der vornehmlich transpressiven Bewegung zwischen Svalbard und Nordgrönland. Diese Modelle werden durch die beobachtete seismische Struktur entlang des Westrandes unterstützt. Das Auftreten des Känozoischen (dextralen) Faltengürtels an der Position der (sinistralen) Suturzone der Kaledonischen Kontinentalfragmente beschreibt die Reaktivierung alter Bruchzonen.

Der Kontinentalrand Westsvalbards ist vielgestaltiger als bislang angenommen. Seewärts des Van Mijenfjorden zeigt die beobachtete Tiefenstruktur einen gerifteten (*rifted*) Kontinentalrand. Lediglich 200 km weiter nördlich, seewärts des Kongsfjorden (Ny Ålesund), ist der Kontinentalrand durch eine steile Stufe in der Kruste-Mantel-Grenze beschrieben. Diese Zone wird als gescherter Kontinentalrand interpretiert. Die Entwicklung des gescherten Kontinentalrandes wird der Spitsbergen Fracture Zone innerhalb der südlichen Framstraße zugeschrieben. Nördlich des Kongsfjorden am Nordrand Svalbards liegt wiederum ein normal gerifteter Kontinentalrand vor.

Die ozeanische Kruste jenseits des westlichen Kontinentalrandes von Svalbard ist aufgrund der Abwesenheit einer gabbroidischen Unterkruste (*oceanic layer 3*), im Vergleich zum beobachteten globalen Mittel, sehr geringmächtig. Die geringe Produktion von

ozeanischen Magmen ist ein Merkmal der extrem langsam spreizenden, mittelozeanischen Rücken des Nordatlantiks und der Framstraße. Die peridotitischen Gesteine des oberen Mantels unterhalb der ozeanischen Kruste sind wahrscheinlich serpentinisiert, da die seismischen Ausbreitungsgeschwindigkeiten hier unterhalb des allgemein beobachteten Mittels liegen.

Der in dieser Arbeit untersuchte Kontinentalrand Westsvalbards umfasst geringe Mengen an Intrusionen innerhalb der Übergangszone zwischen nicht gedehnter kontinentaler Kruste und der vorgelagerten ozeanischen Kruste. Dieses Phänomen tritt bei gescherten als auch bei normalen gerifteten Abschnitten auf. Entlang des gescherten Segments seewärts des Kongsfjorden ist ein möglicher Ursprung der starke Temperaturkontrast zwischen kalter kontinentaler Kruste und heißerer ozeanischer Lithosphäre. Diese Zonierung fördert die Bildung von Partialschmelzen aufgrund von induzierter Konvektion innerhalb des ozeanischen Mantels. Die Intrusionen können während der Ausbreitung des Knipovich Rückens in Richtung Norden stattgefunden haben. Weiterhin kann es zum Magmenaustausch gekommen sein, als der Molloy Rücken den gescherten Kontinentalrand passierte. Generell bieten die ehemaligen Hauptverwerfungen zwischen Svalbard und Grönland (Spitsbergen Shear Zone) entsprechende Kanäle für die Ausbreitung und Verteilung von Magmen.

Die Zonen des Kontinentalrandes entlang derer Intrusionen beobachtet werden, fallen mit positiven magnetischen Anomalien entlang der Westküste Svalbards zusammen. Darüber hinaus beobachtet fällt mindestens eine weitere magnetische Anomalie am Westrand des Yermak Plateaus auf, die die Südspitze einer Transformstörung innerhalb der Framstraße markiert. Unter Berücksichtigung der vorgestellten Segmentierung des Kontinentalrandes Westsvalbards, eines modernen plattentektonischen Modells und dem beobachteten magnetischen Anomalienmuster zeigt sich, dass die Segmentierung des Kontinentalrandes auch weiter nördlich gegeben ist. Entsprechend den Beobachtungen weiter südlich, kann auch hier angenommen werden, dass die Öffnung der nördlichen Framstraße von Intrusionen in die angrenzende kontinentale Kruste begleitet war.

INTRODUCTION

CHAPTER 1: INTRODUCTION

1.1 The aim of this thesis

The Svalbard Archipelago[1] (Fig. 1-1) is situated 650 km north of northern Norway at the northwest corner of the Barents Shelf. It is one of the furthest-flung accessible landscapes of the Eurasian supercontinent, and has been a source of intrigue for discoverers and researchers for centuries.

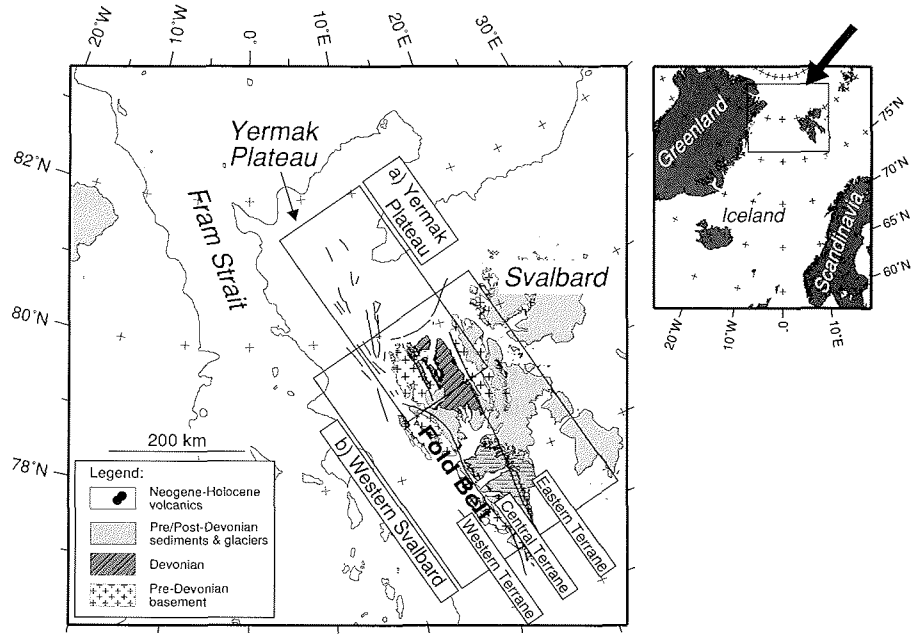

Figure 1-1: Overview map of the study area of Svalbard, the Yermak Plateau and the Fram Strait. Geology: Harland (1997a). Bathymetry (2000 m-contour): Jakobsson et al. (2000).

Geological research on Svalbard began in the early 19th century with Norwegian and British expeditions, in spite of Svalbard's harsh natural climate in the Arctic realm. The first geological maps, revealing the fundamental structure of the archipelago, were com-

[1]Svalbard means "cool coast" and was first mentioned in the Viking explorers' *Islandske Annaler* of 1194 and the *Landnámabók* of ca. 1230. The main island, Spitsbergen, was named by the Dutch Captain Barents in 1596 with reference to the mountain peaks that are visible on approach from the sea (Harland, 1997a).

piled in the late 19th century and early 20th century. It was the Norwegian geologist O. Holtedahl who first contributed between 1914 and 1925 to the understanding of the Caledonian age of some Svalbard rocks that were previously regarded as Archean.

Offshore geophysical exploration started in 1960 in response to industrial and political interests of the United States and the former Soviet Union. Systematic seismic surveying by western academic institutions began in the 70's (Eiken, 1994), also covering the neighbouring Fram Strait[1] oceanic gateway and Yermak Plateau[2] (Fig. 1-1). Wide-angle seismic experiments focused on the deeper crustal structure, and the acquisition of seismic reflection data were accomplished during the late 70's by Polish/Norwegian/German cooperations (e.g. Guterch et al., 1978). More recent deep seismic experiments were carried out in the 80's (Sellevoll et al., 1991). Due to the (simple) experimental setups, a detailed crustal model is not provided by any of these data.

Hence, a detailed view of the crustal structure of Svalbard and the adjacent oceanic province is still missing. As a consequence, a detailed joint interpretation with known onshore geological structures is missing, too. The recent geophysical database does not justice to Svalbard's outstanding scientific position. Questions concerning

- the Caledonian history of the Svalbard and the north Atlantic domain (e.g. terrane suturing),
- the structure of the Yermak Plateau,
- the Cenozoic break-up of the northernmost Atlantic between Svalbard and Greenland,
- continental rifting and the influence of intensive shear movements on the continental margins, and its relevance to the Western Spitsbergen Fold Belt,
- possible interactions between the mid-oceanic ridge and the continental margin off western Svalbard and
- the structure of oceanic crust generated at very slow-spreading rates

can be explored by suitable geophysical experiments on Svalbard and its neighbouring provinces.

The aim of this thesis is to report on a suite of such experiments, that contributes a detailed seismic structure, and to provide a geophysical and geological interpretation. The study area concentrates on two regions: (a) the Yermak Plateau and (b) the western Svalbard margin (Fig. 1-1).

---

[1]The Fram Strait is named after the research vessel *Fram* of Fritjof Nansen under the command of Captain Otto Sverdrup in the late 19th century. The *Fram* was the first research vessel built for use under sea ice conditions. Nansen saw the possibility to use the Arctic transpolar current to transport an icebound ship across the Arctic Ocean for the purpose of scientific studies (Weber & Roots, 1990).

[2]The Yermak Plateau is named after a Russian icebreaker captained by Admiral Makarov that reached Spitsbergen in 1899. The pioneering voyages of the *Yermak* showed that it was possible for icebreakers to sail through the Northeast Passage. The ship's name can be traced back to the conqueror Yermak Timofeyevich, the leader of a band of Cossacks, who were sent to protect the lands of the Stroganov family in West Siberia from local tribes.

The opening of the Fram Strait gateway is of special interest for polar research and global climatology studies (Boebel, 2000). The Fram Strait provides the only deep water exchange to the Arctic Basin and has therefore major influence on the North Atlantic Deep Water (NADW) budget and the global thermohaline circulation. With respect to this, the present thesis treats also the spatiotemporal development of the Fram Strait, as the acquired geophysical data derive proper constraints.

1.2 Used geophysical methods and the principle of interpretation

1.2.1 Seismic methods

The fundamental geophysical method treated in this thesis is seismic refraction profiling. The principle of seismic refraction surveying is to measure the traveltimes of refracted and wide-angle reflected seismic waves that have propagated through the Earth's interior. This information can provide a detailed picture of the distribution of compressional and shear wave velocities (p- and s-waves) within the solid earth. Since these waves behave differently according to the medium they travel in, refraction profiling gives us a window into the Earth's deeper interior. In the case of complex sub-surface structures, that are difficult to treat analytically, it is useful to apply a raytracing technique in order to model the acquired seismic data (*rayinvr*, Zelt & Smith, 1992; Kearey & Brooks, 1999). Structural p- and s-wave models are postulated and the traveltimes of seismic waves are calculated for comparison with the observed traveltimes. In the forward problem, iterative adjustments to the model approach an acceptable fit within a given tolerance.

The aim of seismic data discussed in this thesis (Jokat et al., 1997; Mjelde et al., 1998; Jokat et al., 2000) was to provide a detailed model of the subsurface down to the upper mantle (~50 km). In order to resolve structural elements smaller than 20 km of lateral extent (e.g. fracture zones, sutures) with reversed travelpaths, the spacing of recording stations was set to 5-10 km if possible. The applied source comprise 2 or 3 large volume airguns with a total charge of 92/152 l. The peak frequency of such a source is approximately 8 Hz, revealing a formal vertical resolution of ~190 m at 6 km/s ($\lambda/4$). The experimental setup comprise off- and onshore seismic receivers and the general operating platforms were *RV Polarstern* (Alfred Wegener Institute) and *RV Håkon Mosby* (University of Bergen). The marine seismic source forced the seismic transects to follow the coastlines and the fjords of Svalbard. Onshore seismic receivers were deployed using the helicopters of *RV Polarstern* in order to provide the best conditions for selecting receiver locations within an efficient time schedule. Ocean-bottom devices were deployed and recovered by sailing the profile lines before and after the actual shooting, which enlarges the time range for a single transect to about 3 to 4 days.

Additional structural information was given by seismic reflection surveying (parallel to only one transect; Mjelde & Johansen, 1999). The seismic reflection section reveals a direct view of the reflective nature of the crust, and can be linked to the velocity-depth profile coming from the seismic refraction experiment.

1.2.2 Potential field methods

To derive further physical properties of crustal and upper mantle rocks, the seismic structure is complemented by the free-air gravity anomaly. The subsurface geology can be explored on the basis of variations in the Earth's gravity field that are caused by density contrasts between subsurface rocks (Kearey & Brooks, 1999). The process starts with the seismic velocity distribution inferred from seismic modelling. Using common velocity-density relationships for sedimentary, igneous and metamorphic rocks (e.g. Gardner et al., 1974; Christensen & Mooney, 1995) the velocity model is converted to density. A forward modelling technique, using similar (see above) iterative adjustments to the model is performed in order to derive a fit of calculated and observed free-air anomalies (with the use of *LCT*; LCT user's guide, 1998).

The demands of the gravity modelling are that it should confirm or refine the crustal velocity structure within the given uncertainties of the seismic technique. Since the lateral and vertical resolution is limited in the seismic refraction experiments, gravity field variations exhibiting wavelengths smaller than 5 km are discarded. Gravity field observations were carried out with *RV Polarstern* (Jokat et al., 1997; Jokat et al., 2000) using the ship's onboard gravity meter. Boebel (2000) linked these data to airborne gravity measurements acquired by the Alfred Wegener Institute, and further satellite derived gravity field information, to create a regional grid of the Svalbard, Fram Strait and northeast Greenland region. This grid is the source of data for density modelling within the entire realm of the seismic refraction profiles.

Magnetic field observations provide information about anomalous magnetised bodies within the Earth that also cause local perturbations to the magnetic field. Upon cooling beneath the Curie temperature (for magnetic minerals such as haematite or magnetite this is 580-680°C; Fowler, 1995) part of the anomalous magnetisation is a remanent magnetisation. This remanent magnetisation describes the orientation of the field at the time of cooling below the Curie temperature. A further component of magnetisation is achieved by magnetic induction proportional to the rock's susceptibility. But thermoremanent magnetisation is generally many times stronger than induced magnetisation (Fowler, 1995). Within this thesis the regional magnetic anomaly field is used to extrapolate structures with similar suggested remanent magnetisation into regions not covered with seismic lines, in order to constrain the regional tectonic evolution.

1.2.3 Geological interpretation of geophysical data

The geophysical data describe physical properties of Svalbard's crust and upper mantle (i.e. seismic velocities v_p, v_s and density ρ). Since the experiments are carried out on- and offshore, direct information from the onshore geology can be linked to the seismic velocity and density structure and is extrapolated laterally and vertically. Despite extensive ice-cover and harsh climate Svalbard's geology is well known (e.g. Harland, 1997a-f). With reference to the resolution of the geophysical studies only major features, like large sedimentary basins or major sutures, are of interest for geological interpretation. Mantle xenoliths from northern Svalbard provide a view of Svalbard's deep structure, as do the seismic experiments. Direct measurements of physical properties of Svalbard rocks are published by Kurinin (1970) and Howells et al. (1977). Hence, there

is a direct link between local field samples and the modelled seismic and density structure.

Offshore geological information is limited to local dredge samples (Jackson et al., 1984; Neumann & Schilling, 1984; Hellebrand, 2000). Only oceanic rocks are expected to be representative of local structures since continental lithologies might have been delivered by former grounded ice-masses. Offshore drilling surveys (ODP Leg 151; Myhre, Thiede & Firth et al., 1995) only penetrate the upper sedimentary section to depths of ~500 m and are therefore of little significance for the crustal studies of this thesis.

1.3 Structure of this thesis

The crustal structure of northwestern Svalbard and the adjacent Yermak Plateau is discussed in chapter 2 (Fig. 1-1; region a). The interpretation is focused on the crustal nature of the plateau which is currently insufficiently understood. The tectonic interpretations drawn at the end of the chapter concern its magmatic history and sedimentary basin evolution in the light of detachment tectonics. This chapter yields a framework for the magmato-tectonic interpretations of the western Svalbard continental margin, since extensive volcanism during rifting is excluded. Chapters 3 and 4 (Fig. 1-1; region b) treat two east-west striking parallel profiles crossing the western continental margin of the Svalbard Archipelago. The profiles trend perpendicular to the Caledonian sutures of the Svalbard terranes, the Western Spitsbergen Orogenic Belt and the continental margin and provide a detailed characterisation of these structures. The mid-oceanic ridge system off Svalbard is characterised by oblique spreading, so that the profiles are neither perpendicular to the spreading ridges nor parallel to flowlines of plate motion. Therefore, the interpretation treats the age-independent general construction of oceanic crust, including its regional tectonic elements, e.g. fracture zones. The conclusions drawn for these profiles concern the evolution of the continental margin only locally. In order to augment the interpretation, chapter 5 introduces a further seismic transect, that covers the northernmost Svalbard margin. Hence, the discussion in chapter 5 is confined to the continental margin.

In chapter 6, seismic refraction data is used to evaluate and refine the most recent plate tectonic break-up model of the North Atlantic and Fram Strait (Boebel, 2000). The tectonic features inferred from seismic profiling are linked to the regional magnetic field, which enables extrapolation of the observed structures to the Fram Strait region. Chapter 7 summarises the thesis, and describes some of the outstanding problems, and specifies proposals for future projects.

This thesis contains the original text and figures of three manuscripts that were submitted to professional journals. The first manuscript (chapter 2) was accepted in August 2002 by the *Geophysical Journal International* (Blackwell Science UK; Ritzmann & Jokat, 2003). Two further manuscripts (chapters 3 and 4) were submitted to *Geophysical Journal International* and *Marine Geophysical Researches* (Kluwer Academic Publishers Netherlands) in September 2002 and January 2003.

ACCEPTED/SUBMITTED PUBLICATIONS

CHAPTER 2:
CRUSTAL STRUCTURE OF NORTHWESTERN SVALBARD AND THE ADJACENT YERMAK PLATEAU: EVIDENCE FOR OLIGOCENE DETACHMENT TECTONICS AND NON-VOLCANIC BREAK-UP

Oliver Ritzmann[1] & Wilfried Jokat[1]

[1]Alfred Wegener Institute for Polar and Marine Research, Bremerhaven, Germany

Reprinted from Geophysical Journal International 152, 139-159, Blackwell Science UK, January 2003

2.1 Summary

In 1999 new seismic refraction data were collected off northwestern Svalbard and the adjacent Yermak Plateau. A 260 km long profile provides detailed velocity information for the northeastern edge of the Eurasian Continent and the adjacent Yermak Plateau.

North of Forlandsundet Graben the depth of the Moho varies between 23 and 28 km, and remains at this depth to the northern edge of the profile at 81°N. The crustal lithology off western Svalbard can be related to the basement province west of the Raudfjorden Fault Zone. Off the northern shoreline of Svalbard the structure of the Tertiary Danskøya Basin is mapped. Below this, a Late Silurian/Early Devonian basin, with seismic velocities between 5.1 and 5.8 km/s and a thickness of up to 8 km is present. A Paleozoic sequence of up to 6 km thickness is expected below the Tertiary cover north of the Danskøya Basin. An earlier suggestion, that Oligocene rift processes affected the southern Yermak Plateau (Eiken, 1993), is confirmed. A detachment structure is situated below the Paleozoic Basin below Danskøya Basin, which is likely the consequence of simple shear tectonics. The middle crust exhibits low seismic velocities above the detachment fault. The lowermost crust beneath is slightly contaminated by mantle derived melts, which is deduced by the slightly elevated velocities of the lowermost crust. These melts can be attributed to decompressive melting caused by modest uplift of the Moho during stretching. The velocity-depth model provides no evidence for large magmatic activity that implies a non-volcanic rifted margin history. This leads to the assumption that the proposed Yermak Hot Spot during the break-up of Svalbard from northern Greenland did not exist.

2.2 Introduction

The Cenozoic opening of the North Atlantic resulted in the inception of a complex pattern of mid-ocean ridges and fracture zones in the Fram Strait along the northeastern rim of the Eurasian continent (Boebel, 2000). Seafloor spreading history in the Fram Strait is probably younger than 20 Ma, and was preceded by oblique stretching and

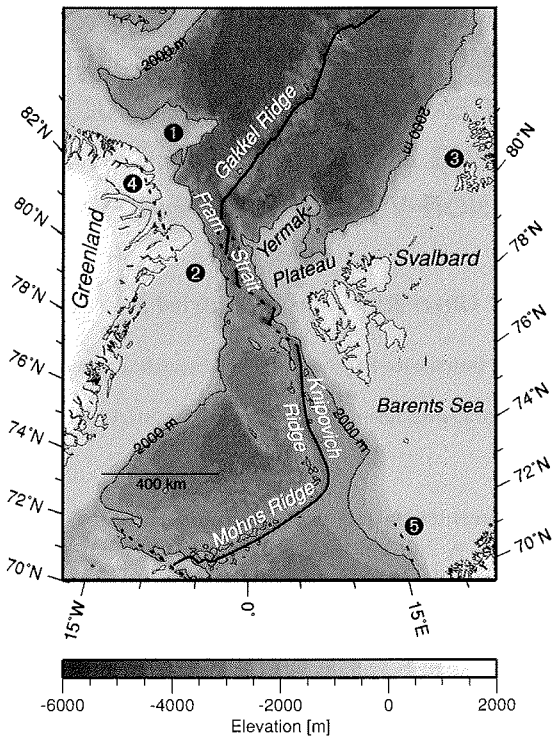

Figure 2-1: Overview map of the study area.
Thick black lines are mid-oceanic ridges, dotted lines indicate transform faults and fracture zones. (1) Morris Jesup Rise; (2) Ob-Bank; (3) Franz-Josef Land; (4) Trolle-Land Fault Zone; (5) Senja Fracture Zone. Bathymetry: IBCAO (Jakobsson et al., 2000). Fram Strait plate boundary after Boebel (2000).

strike-slip movements between Svalbard and northern Greenland (Eldholm et al., 1987; Boebel, 2000). It has been suggested that the Yermak Plateau and the Morris Jesup Rise (Fig. 2-1) are both related to Hot Spot activity during this separation, being two parts of an oceanic plateau found at the Gakkel Ridge plate boundary (Feden et al., 1979; Jackson et al., 1984).

According to models and observations, where hot spots (mantle plumes) interact with continental margins, their effects are manifested over large distances from the plume head (e.g. 2000 km for the North Atlantic; White & McKenzie, 1989; Barton & White, 1997). At the outer edges of the plume head magmatism can terminate abruptly leading to local segmentation of the margin (Barton & White, 1997; Skogseid et al., 2000). Although a large amount of seismic reflection data exist along Svalbard's western and northern margins, deep seismic data are sparse. Assumptions about the crustal structure,

and tectonic interpretations of the region are based on limited deep seismic information and airborne potential field measurements (e.g. Jackson et al., 1984; Sundvor & Austegard, 1990). The objective of this project is to provide new deep crustal information for Svalbard and the Yermak Plateau in order to further constrain their evolution.

Thus, during summer 1999 a deep seismic sounding experiment was performed along the coast of northern Svalbard (Fig. 2-2) with the German research ice-breaker *RV Polarstern*. The experimental setup, a dense pattern of onshore and offshore seismic stations in combination with a close spacing of airgun shots, was chosen to determine the local velocity distribution of the crust of northern Svalbard and the Yermak Plateau, to better constrain the Paleozoic to Cenozoic history of the Svalbard region.

2.2.1 Geological setting of western Svalbard and the Yermak Plateau

The archipelago of Svalbard is situated at the northeastern corner of the Barents Shelf of the Eurasian continent (Fig. 2-1). Northwest of Svalbard's shoreline the shelves are 50-80 km wide forming Sjubrebanken, Norskebanken and the Nordaustlandet margin (Fig. 2-2). Further seawards the hook-shaped submarine Yermak Plateau extends 200 km NNW to 5°E/81.5°N, and then proceeds further 200 km in ENE to 20°E/83°E. (Eiken, 1993). The northeastern arm of the Yermak Plateau is separated from the Eurasian continental shelf to the south by a 2000-3000 m deep abyssal plain (Fig. 2-2). To the west of the plateau the 3000 m deep Fram Strait gateway facilitates deep water exchange between the North Atlantic and the Eurasian Basin of the Arctic Ocean (Kristoffersen, 1990a; Boebel, 2000).

The onshore geology of northwestern Svalbard exhibits a Pre-Devonian metamorphic basement province, mainly west of the Breibogen Fault (Fig. 2-2). In the south this province consists of metasedimentary rocks, and in the centre and north of gneissic, migmatic and related igneous rocks. Overlying this basement is a Late Silurian/Early Devonian sequence best seen to the east and south of the Woodfjorden area (Hjelle, 1979; Harland, 1997c). Many authors use the generic term "Hecla Hoek" for the basement rocks occurring in northern Svalbard. This is a misconception regarding the terrane hypothesis, in which Svalbard is a composite of three allochthonous terranes originating in Greenland, and merged during Caledonian sinistral strike-slip movements. The present relative positions of the terranes were achieved in Late Devonian. The eastern terrane, related to east Greenland, and central terrane, related to north Greenland, constitute northwestern Svalbard, i.e. our investigated area. Both terranes are bounded by the postulated Kongsfjorden-Hansbreen Fault Zone (Fig. 2-2; Harland & Wright, 1979; Harland, 1997b).

A dredge haul from the central Yermak Plateau yielded high-grade Precambrian gneisses similar to the basement rocks of northern Svalbard (Jackson et al., 1984). Further rock samples were collected in 1999 on the northeastern Norskebanken at 16°E and provide low-grade metamorphic rocks (slate dolomite bands) which are suggested to be autochthonous material (Hellebrand, 2000).

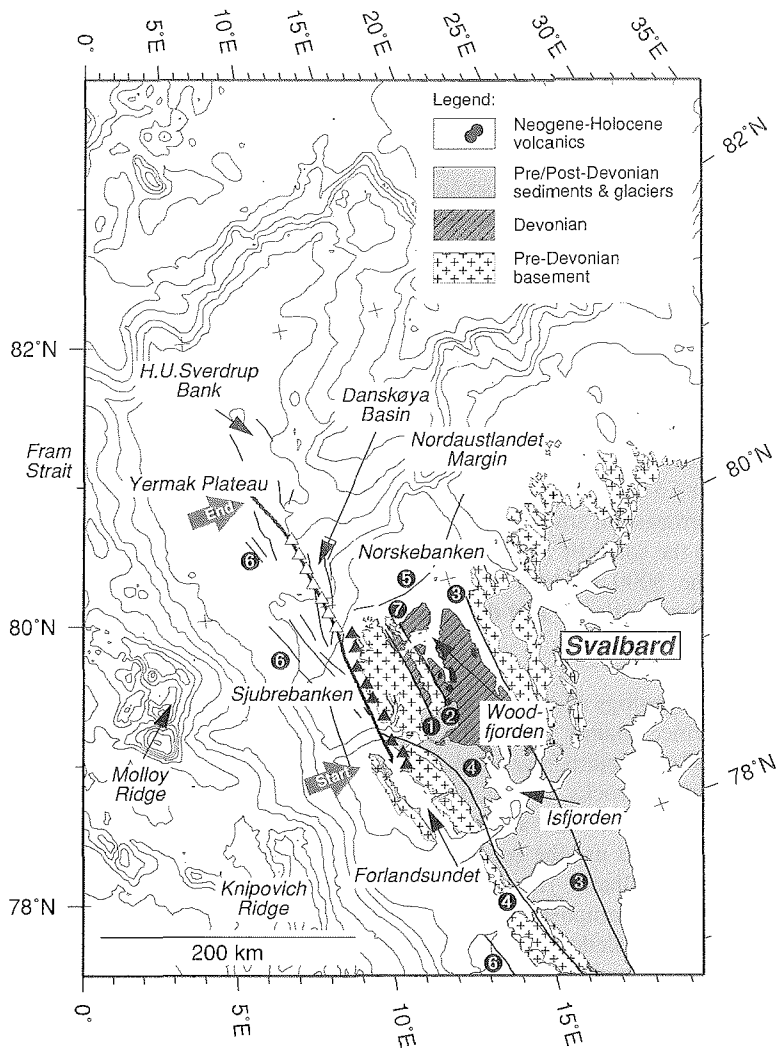

Figure 2-2: Location of seismic refraction profile AWI-99300.
The profile is marked by a thick black line (offshore), RefTek- and OBH stations by black and white triangles, respectively. Geology: Harland (1997a). Black lines are major faults onshore and offshore, numbered circles mark the following structures: (1) Raudfjorden Fault Zone, (2) Breibogen Fault Zone, (3) Billefjorden Fault Zone, (4) Kongsfjorden-Hansbreen Fault Zone, (5) Moffen Fault, (6) Hornsund Lineament, (7) Siktefjellet Strike-Slip Zone. Note, that the (sinistral strike-slip) faults (3) and (4) are proposed to subdivide Svalbard into the western-, central- and eastern terrane. Bathymetry: 500 m-interval + 200 m-contour (IBCAO; Jakobsson et al., 2000).

2.2.2 Offshore geophysical experiments and results

Sparse seismic reflection profiles resolve the sedimentary structure and upper basement character of the continental shelves and the Yermak Plateau. The western tectonic boundary of western Svalbard and the Yermak Plateau is marked by the Hornsund Lineament (Fig. 2-2; Eiken & Austegard, 1987). Structurally, it is a series of blocks, downfaulted to the west between 75°N-79°N along the continental margin. It forms a complex region of crustal transition (Myhre & Eldholm, 1988). On northern Sjubrebanken the lineament continues as two separate NNW-trending blocks, approximately 30 km wide, as far as at least 80.5°N (Eiken, 1993; Geißler, 2001). Eastward, along strike from the lineament on Sjubrebanken a 10 km wide graben filled with Tertiary sediments is probably the northward equivalent of the Tertiary Forlandsundet Graben (Eiken, 1993).

The southern Yermak Plateau is generally covered by sedimentary deposits more than 1000 m thick. Only one local outcrop of basement or Pre-Cenozoic sedimentary rocks is known, the north-trending H.U. Sverdrup Bank (Fig. 2-2). Its composition is poorly known. Suggestions range from Precambrian rocks to highly consolidated sedimentary strata of various ages and tectonic origin (Eiken, 1993). A striking feature of the southern plateau is the 4000-5000 m deep Tertiary Danskøya Basin, which strikes obliquely (30-35°) to the main fault pattern of the Hornsund Lineament (Fig. 2-2). Subsidence and sedimentation is believed to start the end of Eocene (36 Ma) and was superimposed by syn- and post-depositional uplift of northwestern Svalbard. Eiken (1993) suggests a transtensional mechanism with resemblance to pull-apart for the Danskøya Basin. Between 12°E-18°E at the landward reaches of Norskebanken the Moffen Fault acts as a hinge between continental crystalline rocks and the shelf sedimentary layers.

Deep seismic investigations were first performed in 1976 to investigate the crustal structure of Svalbard and its adjacent regions (Guterch et al., 1978). The area investigated (central Svalbard and Isfjorden) is located 50-80 km beyond the southern edge of our new profile AWI-99300. This provides basic information on crustal thicknesses in an area not affected by Tertiary rift events.

Chan & Mitchell (1982) published a three layer crustal velocity model with a total thickness of 27 km beneath northern Isfjorden. This 1D model was correlated with a petrological model derived from deep crustal and mantle xenoliths of the Neogene volcanic centres in northwestern Svalbard (Amundsen et al., 1987). In the model the rock types change from gneissic to granulitic at depths of approximately 14 km, which correlates well with the velocity model. Above the crust-mantle boundary lies a 6 km thick transition zone that is suggested to include significant interlayered mantle pyroxenites and/or lherzolites. 2D velocity models were published by Sellevoll et al. (1991), presenting a crustal thickness of 36 km for the Isfjorden area, based on the same data set used by Chan & Mitchell (1982). A thickness of 26 km was modelled below the Forlandsundet Graben. Due to an insufficient number of shots and receivers it was not possible to resolve a detailed velocity-depth function along the profiles. Despite this setup, lateral velocity variations in the deeper crust, occurring below the major fault zones of Svalbard, are reported.

Czuba et al. (1999) compiled Polish research activities on the crustal structure of Svalbard from 1978 to 1985 and proposed a two-layer model for the Isforden/Forlandsundet area. A significant difference with respect to older models is a 12 km thick lower crustal layer, of high seismic velocities up to 7.2 km/s. This layer is modelled up to western Norskebanken, where seismic velocities increase to 7.35 km/s. Gravity modelling (Myhre & Eldholm, 1988; Sundvor & Austegard, 1990; Austegard & Sundvor, 1991) confirms the seismic crustal thicknesses for the western Svalbard and coastal regions, but could neither confirm nor disprove the existence of a high velocity/density body in the lower crust.

Jackson et al. (1984) published two unreversed seismic refraction lines north of 81°N on the Yermak Plateau. Two crustal layers, showing seismic velocities of 4.3 and 6.0 km/s and a crust-mantle boundary at approximately 20 km were modelled. According to this model, the crust thins sharply north of 82°N. Velocities of the basement of the southern Yermak Plateau, derived from sonobuoy data suggest continental crystalline crust for this area (Sundvor et al., 1982). Boebel (2000) provides additional evidence for the continental nature of the southern and central Yermak Plateau from gravity modelling.

2.2.3 Cenozoic tectonic evolution

The earliest dextral strike-slip movements between Svalbard (Eurasia) and Greenland began 80 Ma ago (chron 33) in Late Cretaceous, along the Trolle-Land Fault Zone in northeast Greenland (Fig. 2-1; Håkansson & Pedersen, 1982). Eldholm et al. (1987) propose this fault to be the continuation of the Senja Fracture Zone of the North Atlantic. Throughout this strike-slip zone, local pull-apart basins developed. A short-lived change of spreading direction in the Labrador Sea west of Greenland gave rise to a brief period of Paleocene compression (59-56 Ma; chron 25, 24), affecting the juvenile transpressive fold belt of western Spitsbergen (Müller & Spielhagen, 1990). Simultaneously, true seafloor spreading to the south occurred only at Mohns Ridge, while rifting and crustal extension continued in the juvenile Norwegian-Greenland Sea. Later strike-slip movements occurred along the Hornsund Lineament, east of Trolle-Land Fault Zone (Eldholm et al., 1987). Immediately following Early Eocene times (56 Ma; chron 24) the western margin of Svalbard entered a transpressive regime, which sustained orogenic activity in the fold belt (Steel et al., 1985). The development of the juvenile Eurasian Basin began with spreading at the Gakkel Ridge (56 Ma; chron 24; Kristoffersen, 1990b). Transpression in western Svalbard was replaced by transtension in the Middle Eocene (49 Ma, chron 21). For this period Crane et al. (1991) suggest pull-apart and (later) spreading processes at the Molloy Ridge as an extensional relay zone in response to the readjustment of Nansen Ridge and/or Mohns Ridge.

Transtensional movements dominate since the Earliest Oligocene (36 Ma, chron 13). Authors agree that the lithosphere west of the Hornsund Lineament was stretched and later rifted (e.g. Eldholm et al., 1987; Müller & Spielhagen, 1990; Crane et al., 1991; Boebel, 2000). In addition, Feden et al. (1979) and Jackson et al. (1984) propose mantle plume activity (Yermak Hot Spot) at a former triple junction position at the eastern end of the Gakkel Ridge during this period. This triple junction was formed by the juvenile Gakkel Ridge and Hornsund Lineament and a transform fault cutting Ellesmere Island

from northern Greenland. It is suggested that excessive magmatism, associated with the mantle plume built up the northern Yermak Plateau and Morris Jesup Rise. The northeastern plateau shows a pronounced high-amplitude, long wavelength magnetic anomaly (the Yermak Anomaly; Feden et al., 1979). This anomaly, compared to the quiet magnetic signature south of 82°N, leads to the suggestion that the plateau had a dual origin. The northeastern part consists of thickened oceanic crust created by hot spot activity, whereas the southern part is continental (Jackson et al., 1984). Since 36 Ma transtensional processes led to the beginning of subsidence in the Danskøya Basin on the southern plateau, which resembles a pull-apart structure (Eiken, 1993).

The precise geodynamic history of the Fram Strait oceanic province west of the Yermak Plateau is still under debate (e.g. Srivastava & Tapscott, 1986, Sundvor & Austegard, 1990; Lawver et al., 1990; Boebel, 2000).

According to the model of Boebel (2000), a transtensional tectonic regime lasts up to the Middle Miocene (12 Ma, chron 5) at the western rim of the Yermak Plateau (Hornsund Lineament). Seafloor spreading began at the northern Knipovich Ridge in the Late Oligocene (25 Ma) and on Molloy Ridge in the Early Miocene (20 Ma). The generation of new crust along two proposed oblique spreading mid-ocean ridges in the northern Fram Strait, balanced the dextral movements of Svalbard relative to Greenland since the Late Miocene between 12-9.5 Ma (chron 5). Feden et al. (1979) suggested renewed plume activity along the western segment of the Gakkel Ridge since chron 5, which is supposed to stimulate Tertiary/Quaternary volcanic activity, i.e. basaltic flows/upper mantle xenoliths in northern Svalbard.

2.3 Geophysical data

2.3.1 Acquisition of seismic refraction data

Seismic refraction data along profile AWI-99300 were acquired by the German polar icebreaker *RV Polarstern* in August 1999. The seismic source, fired every minute (ca. 150 m interval), consisted of 2 large volume airguns with a total volume of 92 l. The 260 km (=1475 shots) long seismic transect follows the coastline of western Spitsbergen north of Prins Karls Forland towards the Yermak Plateau (Fig. 2-3). 9 RefTek seismometer stations with a receiver spacing of 9-20 km were deployed on the coast of Spitsbergen to record the seismic energy. This setup resulted in minimum shot-receiver offsets of 6-10 km for RefTek land stations, as the source (*RV Polarstern*) was situated offshore. The chosen station locations did not exceed altitudes of 70 m asl. Each station was equipped with 18 single coil geophones (4.5 Hz) which signals were stacked. On the southern Yermak Plateau 7 ocean-bottom hydrophone systems were deployed with a mean spacing of 13 km in water depths of 400-950 m bsl (Fig. 2-3).

Beside the use of airguns as an energy source the Polish ship *El Tanin* performed 20 TNT-shots with a charge of 25/50 kg north of 79.8°N and a shot distance of approximately 7 km. The seismic energy of the airgun source was strong enough to provide a high S/N-ratio on the recordings, so that the TNT-shots give no supplementary information for crustal studies. Therefore, the seismic sections presented in this publication contain recordings of airgun source only.

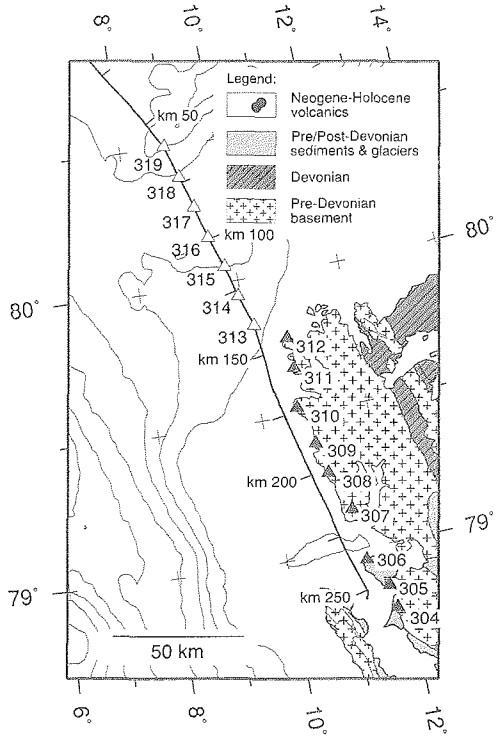

Figure 2-3: Locations and names of deployed seismic stations during the AWI-99300 experiment.
Black triangles mark the position of onshore RefTek seismometer stations. White triangles mark the positions of offshore ocean-bottom hydrophone systems. Geology: Harland (1997a). Bathymetry: 250 m-interval (IBCAO; Jakobsson et al., 2000).

2.3.2 Examples of seismic refraction data

In this section we present 6 (of totally 16) seismic sections recorded during the AWI-99300 experiment. The shown sections are representative examples, which explain the main features of acquired data (Fig. 2-4 to Fig. 2-6; ref304, ref306, ref311, obh313, obh317 and obh319).

The seismic refraction data recorded by the RefTek stations onshore (ref304-312; for locations see Fig. 2-3) are generally of good quality over almost the entire profile length on either side of the receivers (up to 140-240 km offset; Fig. 2-4a and b, Fig. 2-5a). The ocean-bottom receiver systems on the Yermak Plateau (obh313-319; for locations see Fig. 2-3) provide variable quality between 40-140 km offset and a S/N-ratio of about 1

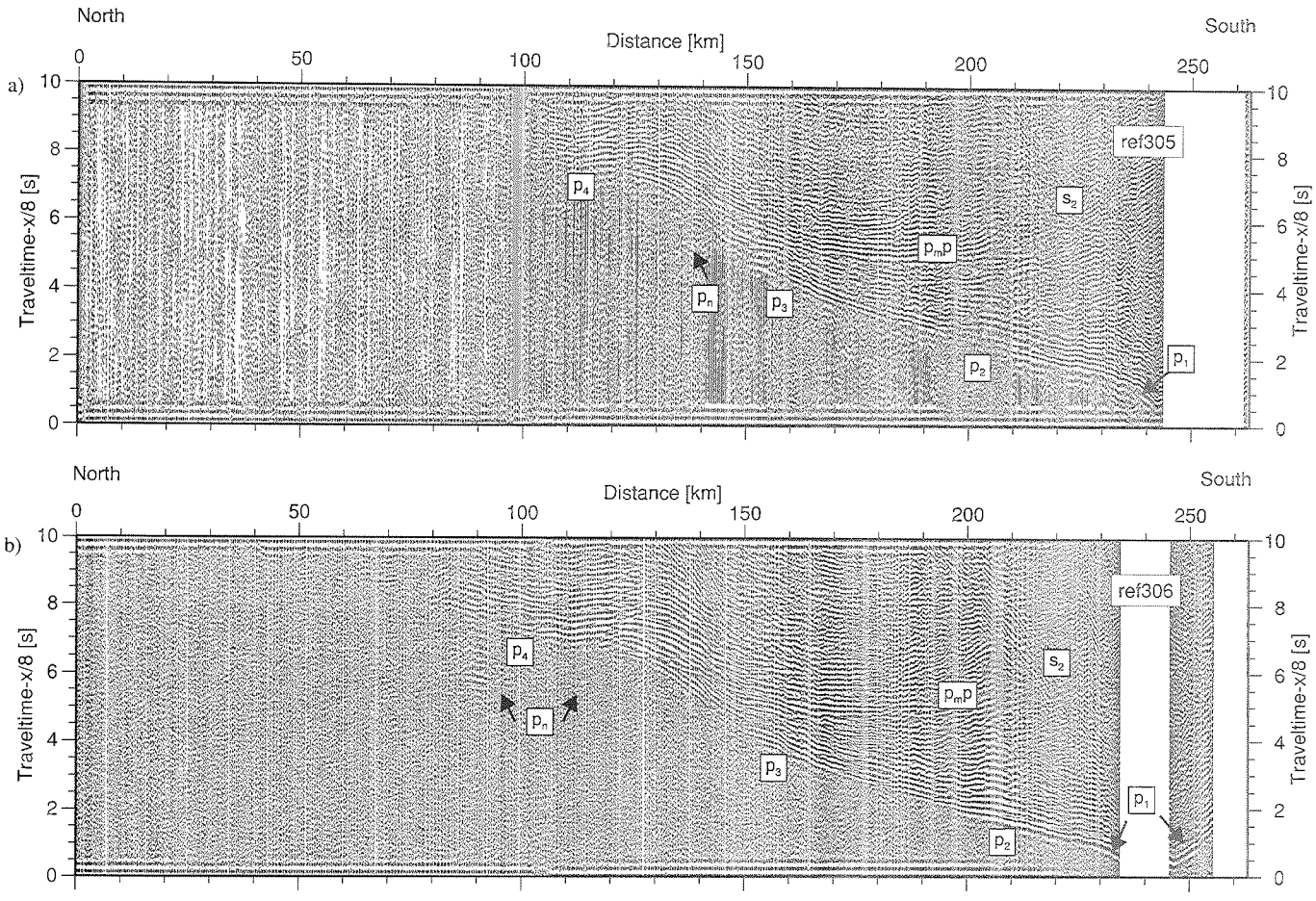

Figure 2-4: Record section examples for onshore and offshore receivers.
RefTek seismometer systems (a) ref305 and (b) ref306. For processing details see text.

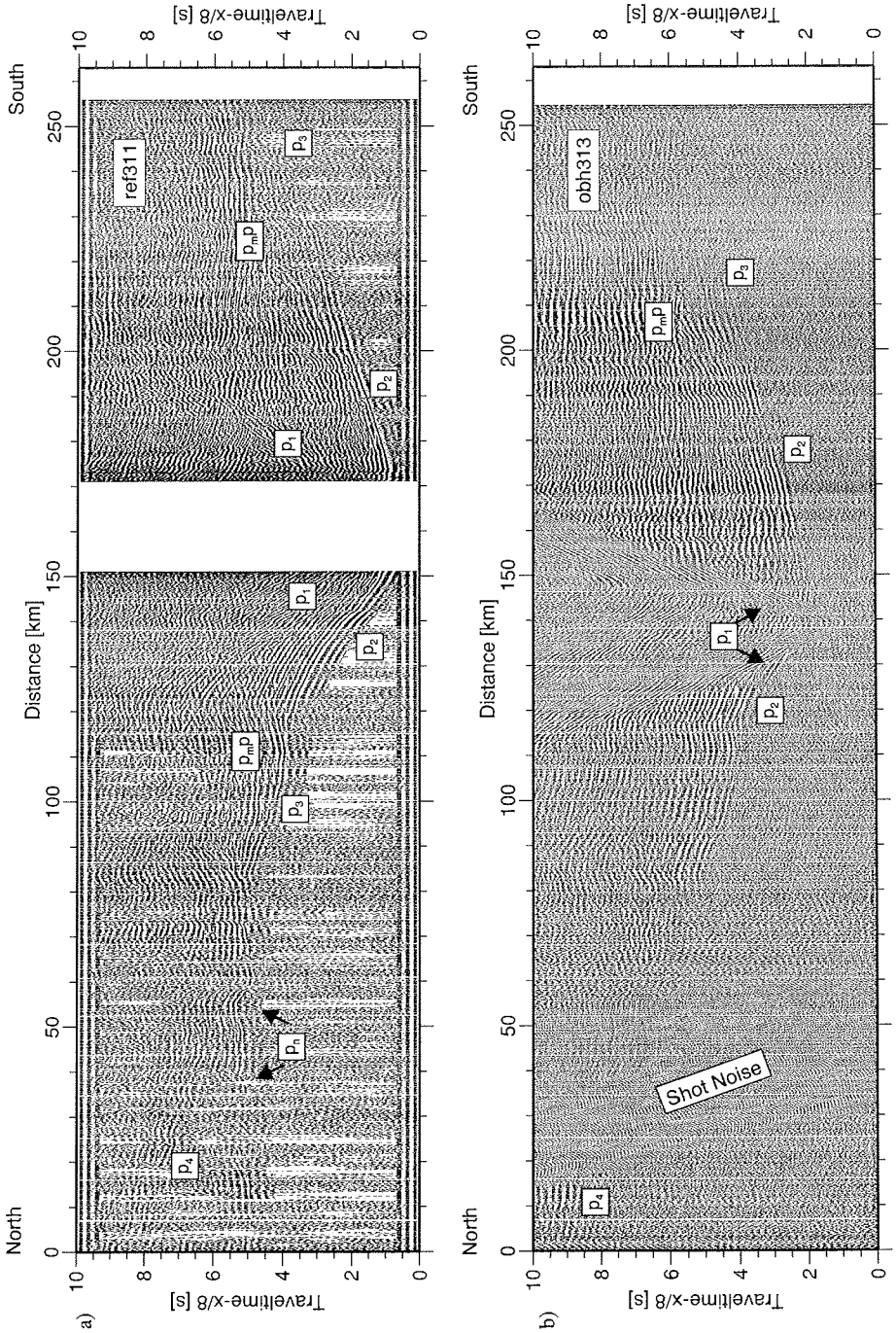

Figure 2-5: Record section examples for onshore and offshore receivers.
RefTek seismometer system (a) ref311 and ocean-bottom hydrophone system (b) obh313. For processing details see text.

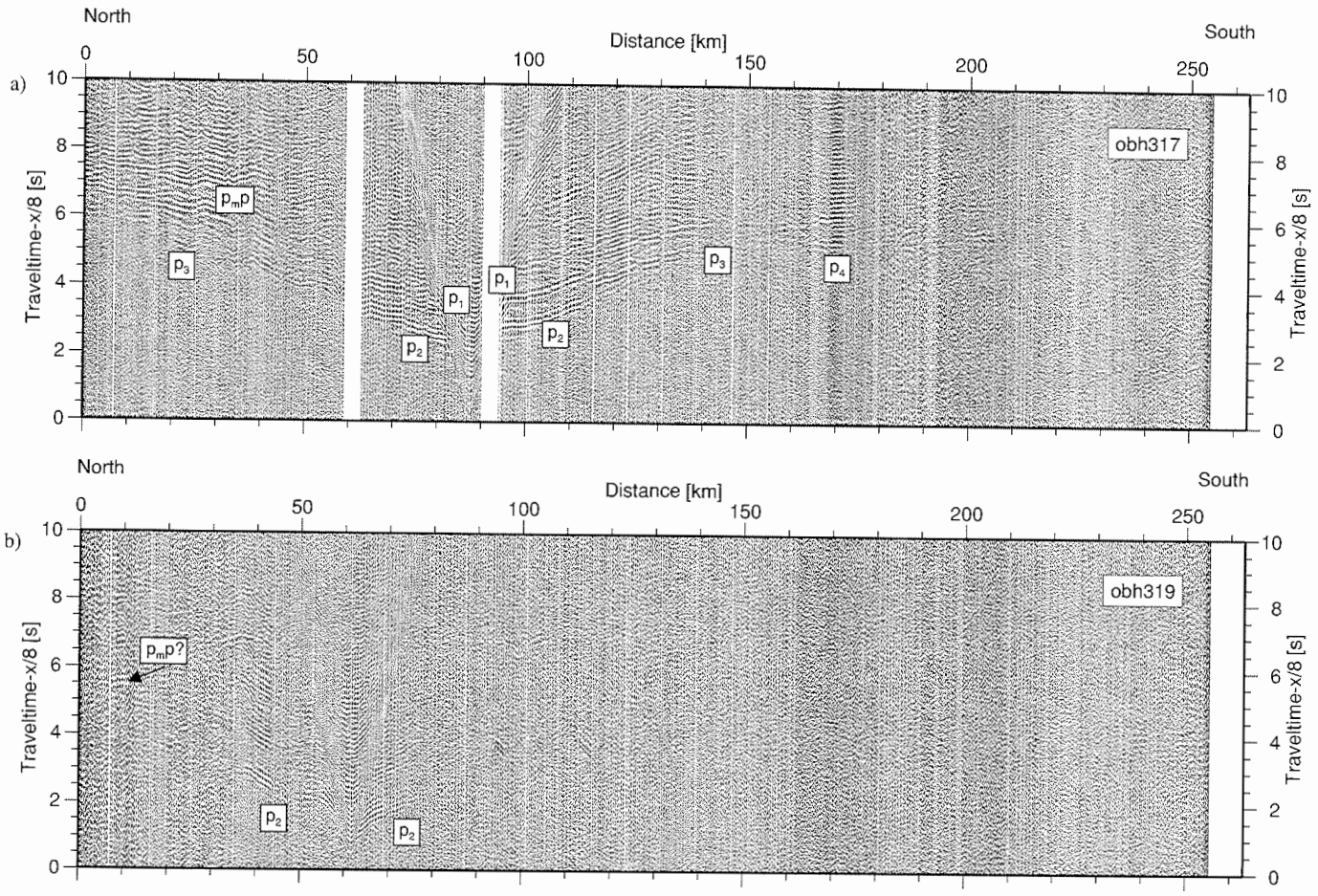

Figure 2-6: Record section examples for onshore and offshore receivers.
Ocean-bottom hydrophone systems (a) obh317 and (b) obh319. For processing details see text.

on some stations (Fig. 2-5b, Fig. 2-6a and b). Thus, arrivals were only detected by phase correlation, facilitated by the close shot spacing.

The frequency spectra of the recorded data are in the range of 5-15 Hz with a dominant peak at 8 Hz. A bandpass filter passing frequencies from 5-17 Hz (exception is obh315: 11-20 Hz) was applied to the data. For further enhancement of reflected and refracted arrivals at offsets greater than 20 km, the data was scaled by automatic gain control within a window of 1000 ms.

The recorded wave field is characterised by a strong reverberation pattern, probably created by the multiple reflection of the source signal off the ocean floor in shallow water. A large impedance contrast is given by known high velocity gas hydrate cemented sediments on the ocean floor off northwestern Svalbard (Posewang & Mienert, 1999). In addition, high seafloor velocities are supposed to result from overconsolidation associated with Late Cenozoic uplift of the shelf areas (e.g. Eiken & Austegard, 1987). Peg-leg type propagation of seismic energy can further be induced by the occurrence of low-velocity gas bearing sediments below these horizons at depths of 100-200 m bsf. Despite this, first arrivals as well as sedimentary and crustal reflections are clearly observed on many of the sections (e.g. obh313; Fig. 2-5b).

Due to the chosen shot interval of 60 sec, noise from the previous shot overprints useful signals at distances of approximately 90 km in the case of some of the ocean-bottom receivers, e.g. obh313 (km 15-60; Fig. 2-5b). The recordings of the RefTek stations are not affected by this kind of noise energy.

At the southern end of the profile at Kongsfjorden the recordings ref304-306 show refracted phases at near offsets (<15 km) with a high gradient and seismic velocities of 4.5-5.0 km/s (Fig. 2-4a and b). At larger distances to the receiver the gradient decreases and crustal p-phases are only affected by moderate lateral heterogeneity of the crust on the southern Yermak Plateau. These undulations of the apparent velocity, i.e. positive or negative slope changes occur between km 110-180 along the profile (e.g ref306; Fig. 2-4b). Crustal p-phases (diving waves) often remain beyond the crossover distance of mantle phases as secondary arrivals and give reliable information about seismic velocities and gradients in the deeper crust, e.g. ref311 (Fig. 2-5a).

On the southern Yermak Plateau the near offsets (<15 km) of the recordings ref312-obh316 (example: Fig. 2-5c and d; p_1) show arrivals from the sedimentary cover on the shelf and Danskøya Basin identified by low seismic velocities of 2-3 km/s and a high velocity gradient. Due to the thinning of the Tertiary sediments north of Danskøya Basin crustal p-arrivals occur increasingly earlier on more northern stations.

On all stations deployed on Spitsbergen and on some ocean-bottom stations (e.g. obh314/317) refracted seismic signals from the upper mantle (p_n; >7.8 km/s; Fig. 2-4 and Fig. 2-5b), as well as mantle wide-angle reflections, were recorded. The crossover distance remains rather constant at 90-110 km on all stations which points to a uniform Moho depth. Amplitudes of p_n-arrivals are, in relation to crustal p-arrivals obviously lower. This is probably caused by a very low velocity gradient in the upper mantle.

Converted s-wave energy is recorded only on some of the receivers (Fig. 2-4a and b; s_2). S-wave arrivals, which occur in a diffused pattern of high energy p-wave reverberations of reflections, are not easy to define on these stations (Fig. 2-4a). Due to only a few

s-wave arrivals and described difficulties we can not derive an s-wave velocity model and poisson's ratio, which would have given further constraints for a rheologic interpretation.

2.3.3 Gravity data

Gravity data were acquired in parallel with seismic measurements by the shipboard gravity meter KSS31 (Bodenseewerke). The data were linked to the International Gravity Standardization Net 1971 (IGSN71) using harbour measurements in Tromsø (Norway). The observed gravity was resampled to a 2 km-interval, which is reasonable for resolving large scale sedimentary structures and crustal structures. The applied processing sequence comprises latitude and Eotvoes correction to calculate the free-air anomaly.

Since the ship passed significant coastal topography at distances of about 10 km, possible terrain effects had to be checked. A test was conducted on the free-air anomaly grid of the Fram Strait, Svalbard and northeast Greenland (Boebel, 2000). A terrain correction was calculated by fast-fourier transformation (Forsberg, 1984). The calculated influence on gravity measurements at 10 km distance was less than 0.75 mGal, less than 1.5 percent of the maximum gravity variation in the measured ships gravity along our profile track. Furthermore, this correction is smaller than the gravity variations, caused by the uncertainty of the initial density model, which is itself derived from wide-angle data modelling. The effect of the surrounding terrain on the ships gravity is therefore insignificant for crustal investigations.

2.4 Velocity modelling

2.4.1 Modelling procedure

For modelling the RefTek/OBH wide-angle data we used the following strategy:

- (1) Traveltimes of refracted and reflected arrivals with good correlation were picked on each of the 16 recordings.
- (2) 1D velocity profiles were calculated for each station and gathered to a 2D velocity section, which was used as the initial model for raytracing.
- (3) The program *rayinvr* (Zelt & Smith, 1992) was used to perform 2D raytracing with a forward modelling technique. The modelling procedure took place layer by layer, starting from the top. The parametrisation of the velocity model (depths and velocities), was held fixed when the next layer was modelled. To fit the traveltimes taken from the seismic recordings some additional velocity or boundary nodes were implemented in the velocity model. During modelling more emphasis was put on matching the slope and shape of the observed traveltime branches than on minimizing the traveltime residual provided by the program *rayinvr*.
- (4) After producing a reliable model, traveltimes were calculated for phases of stations which reveal poorer quality due to lower S/N-ratios. A second inspection of the data was conducted to search for "hidden" information, such as low amplitude arrivals.
- (5) The final fit of observed traveltimes was derived by two runs of the inversion method of *rayinvr* to the velocity model.

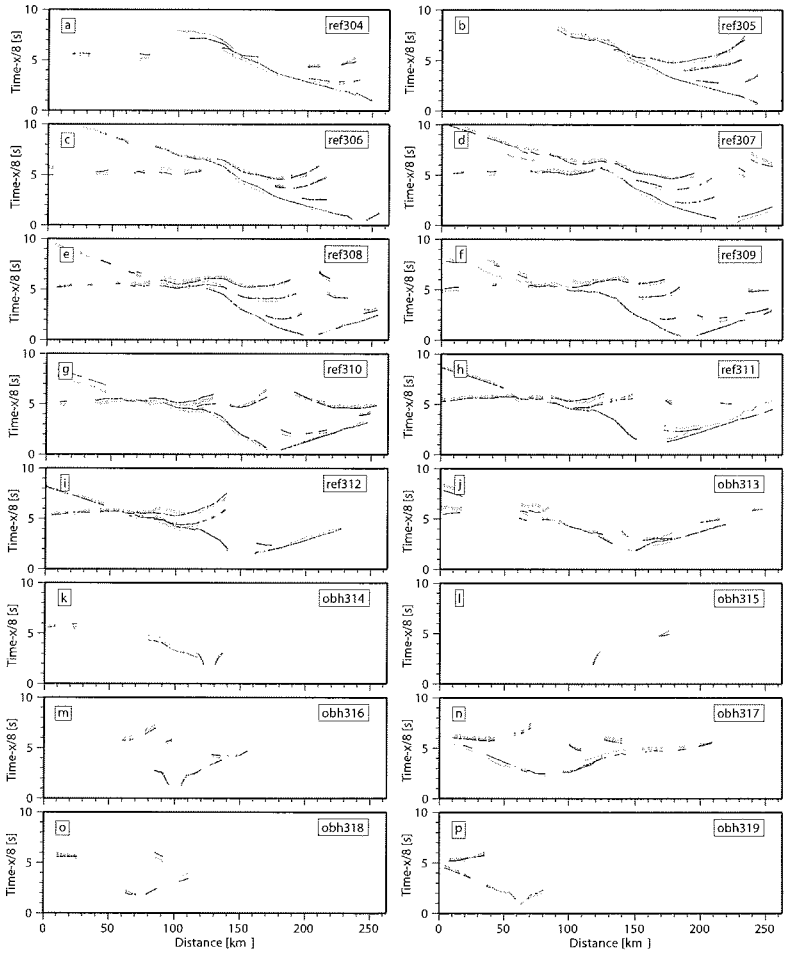

Figure 2-7: Observed and calculated p-wave arrivals for profile AWI-99300.
a-i: RefTek seismometer systems; j-p: ocean-bottom hydrophone systems. Grey errors bars indicate the assigned error to the picked traveltimes. The black lines show the traveltimes calculated using the final velocity model shown in Fig. 2-10.

The observed and calculated traveltimes of the final p-wave velocity model are shown in Fig. 2-7. In total about 4200 traveltimes of refracted and reflected energy were picked from the seismic section and used for raytracing. The corresponding raypaths are shown in Fig. 2-8.

Several seismic record sections show diffraction arrivals at traveltimes before and after p_mp-arrivals, which are concentrated on the southern Yermak Plateau. Attempts to

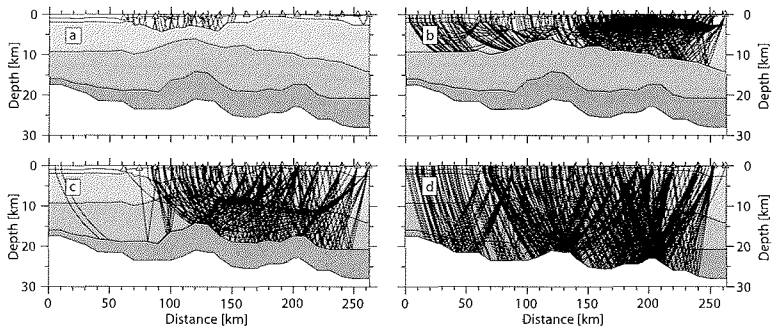

Figure 2-8: Raytracing for the four modelled crustal layers of profile AWI-99300
(a) Tertiary sediments. (b) Upper crust. (c) Middle Crust. (d) Lower Crust and Mantle. Every 5th ray is shown. Vertical exaggeration x3.

model the locations of diffraction origins, derived no consistent results. This may point to a complex 3D structure in the central section of the profile.

2.4.2 Final velocity model

The final velocity model for the profile AWI-99300, shown in Fig. 2-9 and Fig. 2-10, is composed of five layers excluding the water column. The uppermost of four crustal layers was inserted for the sedimentary section (Fig. 2-9), while below, three layers represent the crystalline section and highly consolidated sedimentary rocks of the crust (Fig. 2-10). The lowest layer represents the upper mantle. Within each layer, the seismic velocities vary both horizontally and vertically.

Tertiary sedimentary section

Seismic velocities for the 2 km thick sedimentary sequence on the shelf (km 145-160) vary between 2.6-3.0 km/s at the seafloor and 4.1-4.8 km/s at the lower boundary. Tertiary sediments thicken towards the north in the southern Danskøya Basin to a maximum of 3.0-4.5 km (Fig. 2-9). The base of the sediments in the Danskøya Basin is formed by a 70 km wide w-shaped boundary. Seismic velocities of 2.0-3.0 km/s at the top, and 3.3-4.3 km/s at the base of the sequence are calculated. The thickness of the Tertiary sedimentary section north of Danskøya Basin (km 60) is not well constrained, due to the lack of seismic stations. It decreases to approximately 1.2 km, while the seismic velocities vary in the range of 2.5-3.6 km/s (top/bottom). The different seismic structure of the sedimentary sections along the profile is also obvious in the 1D velocity profiles (Fig. 2-11a-c, ①-③).

For the residual crustal part of the model, the profile can be split (horizontally) into four segments S1-S4 for a better structural interpretation (see Fig. 2-10 and Fig. 2-11a-d):

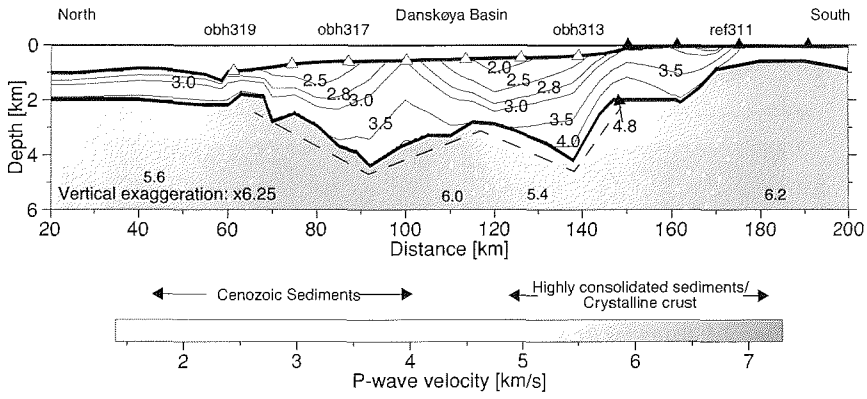

Figure 2-9: Final p-wave velocity model for the Tertiary sedimentary section of Danskøya Basin. Black and white triangles mark the positions of deployed seismic stations (RefTek-seismometer systems and ocean-bottom hydrophone systems). The dashed line marks the w-shaped surface of the basement below the Tertiary Danskøya Basin. For further explanations see Fig. 2-10.

Segment S1 (Northwestern Svalbard)

The uniform, 80 km wide southern segment S1 extends up to the northern coastline of Spitsbergen Island. Seismic velocities in the top layer are 4.8-5.3 km/s, which thins to the north from 2.5-1.5 km (Fig. 2-11d, ④). As the profile is located at an acute angle to the strike of Forlandsundet Graben, this layer could represent the eroded and crushed cap of the eastern basement graben shoulder. Note that this layer of the velocity model is identical with that representing the Danskøya Basin (see above.; Fig. 2-10). The boundary between both structures is realised by a large lateral velocity gradient in the model.

Below this layer the crust is composed of three units of similar velocity gradient (Fig. 2-11d, ⑤), subdivided by different seismic velocities and strong wide-angle reflections. The thickness of the upper layer decreases from 12-8.5 km towards the north. Seismic velocities range from 6.1-6.3 km/s. The middle unit, showing velocities of 6.4-6.6 km/s varies in thickness from 7-10 km and is characterised by a slight 2 km high uplift (km 200), which pushes through the lower layer down to Moho level. The lowest layer, with a uniform thickness of ca. 6 km and seismic velocities of 6.7-6.8 km/s, rests on the crust-mantle boundary. The total crustal thickness for this segment varies between 23-28 km.

Segment S2 (Southern Yermak Plateau)

A narrow, 50-60 km wide segment S2 is situated below the shelf break and the southern Danskøya Basin. This trough-shaped segment narrows to 30 km at a depth of 18 km. It is characterised by decreased seismic velocities of 5.1-5.8 km/s in the upper crustal part (6-10 km) compared to the segment S1. These velocities belong most likely to Paleozoic sediments (Fig. 2-11c, ⑥). Seismic velocities increase constantly with a high gra-

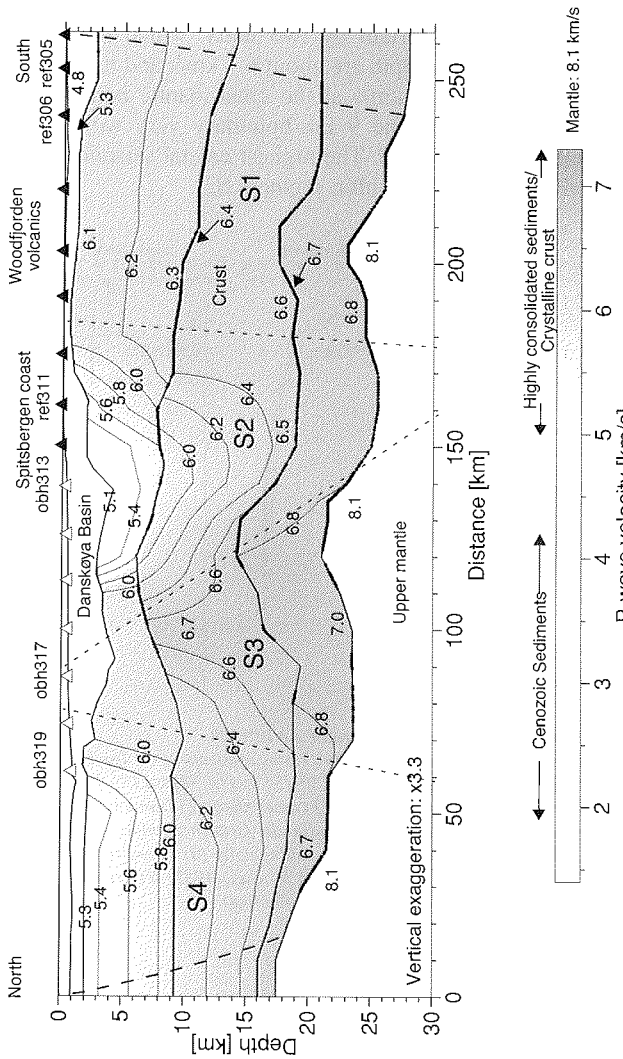

Figure 2-10: Final p-wave velocity model for profile AWI-99300.
The grey shade and the contour lines (0.2 km/s-interval from 5.4-6.8 km/s) show the crustal velocity field. Station locations along the profile are marked by white (obh) and black (ref) triangles. The dotted lines indicate the boundaries of the four crustal segments S1-S4 described in the text. The southern and northern maximum extents of penetrating rays are marked by thick dashed lines.

dient between 0.04 and 0.1 1/s to a value of 6.5 km/s at a depth of 18 km (Fig. 2-11c, ⑦). Only weak reflections mark a boundary at 7-9 km depth. The lowest crustal layer exhibits the same seismic structure like observed in segment S1. The Moho is lifted up by about 4 km at the northern end of this segment so that the entire crustal thickness decreases to 21 km.

Segment S3 (Southern Yermak Plateau)

Below the northern Danskøya Basin a 3-5 km thick layer with a constant seismic velocity of 6.0 km/s is observed. It is underlain by two units, which broaden with increasing depth. Seismic velocities at 9 km depth are about 6.7 km/s and increase gradually with a low gradient of 0.02 1/s to 7.0 km/s at the crust-mantle boundary (Fig. 2-11b, ⑧). Wide-angle reflections constrain the 9 km-boundary very well, while at greater depth no continuous reflector is observed. The highest crustal seismic velocities (7.0 km/s) along the entire profile are observed within segment S3.

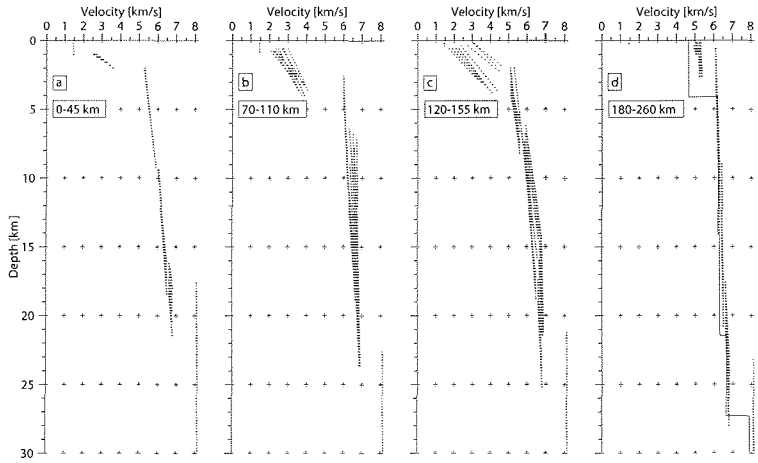

Figure 2-11: Seismic velocity-depth functions for profile AWI-99300.
The velocity-depth functions are separated into the four crustal segments S1-S4 specified in the text. (a, S1) km 0-45, (b, S2) km 70-110, (c, S3) km 120-155 and (d, S4) km 180-260, see also Fig. 2-10. Numbered circles: Tertiary sediments: (1) inner shelf, (2) Danskøya Basin, (3) outer Yermak Plateau. Crustal sections: (4) Forlandsundet Graben shoulder, (5, 7, 8) continental crust, (6) Paleozoic sediments (9) mantle. Additionally (d) shows the velocity-depth profile for northwestern Spitsbergen from Chan & Mitchell (1982) derived by traveltime- and waveform analysis of seismic refraction data (solid line).

Segment S4 (Central Yermak Plateau)

The northern, 60 km wide segment is only sampled by non-reversed shots, due to the absence of stations north of 80.5°N. Notwithstanding this, the seismic structure down to depths of 10 km and the entire crustal thickness are well constrained. Velocities at the top of the sub-Tertiary section of 5.3 km/s increase with a high gradient of 0.07 1/s to 6.0 km/s at 9 km depth. As in segment S2 these velocities are suggested to be likely for Paleozoic sediments (Fig. 2-11d, ⑥). The crust-mantle boundary is well constrained between km 45-65. The curvature of reflected arrivals indicate moderate seismic velocities of 6.7 km/s at the Moho boundary. Station obh319 shows a weak reflection (Fig. 2-6b and Fig. 2-7p), which supports the assumption that the crust-mantle boundary is shallowing north of km 40. Fig. 2-7p shows the observed traveltimes for this reflection

(km 10-40), which is best fitted with a shallowing Moho. Therefore, the final p-wave velocity model includes this shallowing, although this is in opposition to the results of gravity modelling (see below).

Upper mantle

Seismic velocities in the upper mantle are well constrained between km 40-220 along the profile, due to numerous of p_n-arrivals at the different seismic stations. The best fit of mantle refracted phases was reached at a velocity of 8.1 km/s along the profile. The phases were modelled as head waves, due to the absence of a velocity gradient in these phases (Fig. 2-11a-d, ⑨).

2.4.3 Resolution and uncertainty of the p-wave velocity model

The following procedures were applied to determine the quality of the final velocity model:

- (1) The formal resolution of the velocity field parameters of the sedimentary and sub-sedimentary section was calculated by the inversion method of Zelt & Smith (1992). This quantitative approach is based on the relative number of rays which determine or assign the parametrisation, i.e. the velocity-depth nodes. In the case of this study we determine only the resolution of the velocity nodes in certain depth. Fig. 2-12 shows the resolution of the final model. Resolution values of 0.5 or greater are considered to be well resolved (Zelt & Smith, 1992). The sedimentary section is well constrained in the region of Danskøya Basin (Fig. 2-12a). The lack of stations on the northernmost 50 km of the profile, results in extremely low values for the sedimentary layer. The parametrisation of this part of the model was kept fixed north of obh319 (km 61.3), as the velocity resolution is satisfying at this position. The seismic velocities of the shallow graben shoulder south of km 180 are not well resolved, but the resolution enhances to greater depths at the southern edge of the profile to values greater than 0.6. Generally the resolution satisfies for the preponderance of the sub-sedimentary section (km 50-220; Fig. 2-12b) as resolution values are mostly greater than 0.6. Due to reduced ray coverage, the resolution decreases towards the northern flank of the model, where the values do not exceed 0.4. Resolution values for the deepest crustal layer decrease, due to the small amount of direct velocity information from refracted energy traversing this layer. Upper mantle velocities are well resolved, values greater than 0.6 are calculated.
- (2) For the uncertainty of the depth level of the layer boundaries, which are mostly defined by wide-angle reflections (see Fig. 2-10, thick lines), the depth values of the individual reflectors were shifted both up and down until the calculated traveltime no longer fitted. The method depends strongly on the assigned size of the traveltime error (±100-200 ms) and the rms-velocity of the penetrated crustal section. Determined uncertainties for the crustal reflectors

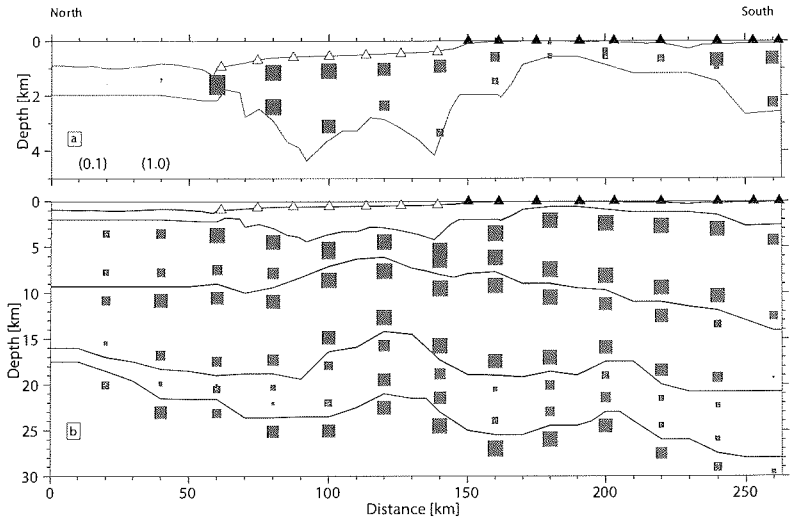

Figure 2-12: Resolution of the p-wave velocity field along profile AWI-99300.
Resolution was calculated according to Zelt & Smith (1992) and resampled to 20 km-intervals along the profiles. The upper figure (a) shows values for the (Tertiary) sedimentary section (km 0-180) and the Forlandsundet Graben shoulder (km 180-263), the lower figure (b) for the underlying crust. The sizes of the grey squares are proportional to the quantified resolution. The black and white triangles mark the position of the seismic stations.

are about 5-10 percent of the absolute depth level. The error estimations are listed in Table 1.

Table 1: Errors in depth level of the layer boundaries.

Boundary	Assigned error	Max. error in depth level	% of absolute depth
upper/middle crust	± 100 ms	± 0.7 km	5.0-11.0%
middle/lower crust	± 150 ms	± 0.8 km	3.8-5.8%
lower crust/mantle	± 200 ms	± 0.8 km	2.9-4.5%

- (3) Depth-dependent uncertainties of the seismic velocities were derived by varying velocity values at certain depths, until the slope of a phase is significantly altered. Furthermore the shifts in seismic velocity were performed within each modelled layer since the main parts of the traveltime branches do not fall outside the assigned errors of picked data. Although the technique is

highly subjective, it gives a further evaluation criterion for the final velocity model. The determined uncertainties are listed in Table 2.

Table 2: Errors in depth depended seismic velocity.

Layer	Velocity Range	Max. error in seismic velocity
sedimentary section	2.0-4.8 km/s	± 0.10 km/s
upper/middle crust	5.1-6.3 km/s	± 0.15 km/s
middle/lower crust	5.9-6.7 km/s	± 0.20 km/s
lower crust	6.7-7.0 km/s	± 0.25 km/s
mantle	8.1 km/s	± 0.10 km/s

2.5 Gravity modelling

Further constraints on the geological model of profile AWI-99300 is provided by 2D gravity modelling, performed with LCT interpretation software (LCT User's Guide, 1998). Density of the water column was assumed to be 1.03 g/cm^3. For the densities of crystalline rocks the non-linear velocity-density relationship of Christensen & Mooney (1995) was used. Based on global studies this solution is suitable to calculate depth dependent densities for crustal and peridotitic (mantle) rocks. All bodies were assumed to be 2D, and have an infinite extent at each end of the density model.

The final p-wave velocity field was gridded and transformed to density. Blocks were digitised within an interval of 0.05 g/cm^3 and used for the initial density model. For the main part of the profile, i.e. km 40-260, this starting model fits the observed gravity well. After slightly shifting some boundaries within the determined depth uncertainties of the velocity model boundaries (Table 1), the resulting gravity field fits all observed anomalies well (Fig. 2-13).

For the northern part of the profile, i.e. km 0-40, a coarse downward shift of 4 km in Moho level is necessary to fit the long wavelength decrease of the observed gravity in northward direction (Fig. 2-13). This is contrary to the final seismic refraction modelling result, in which reflection signals suggest possible shallowing of the Moho (Fig. 2-7p).

The observed gravity anomaly pattern (Fig. 2-13; 1-4) is explained by the following features of the final density model:

- (1) The northward shallowing of mid-crustal rocks (2.75-2.80 g/cm^3) and slight shallowing of the Moho (km 160-260).
- (2) The interplay of the deepening basement (Danskøya Basin) and low-density rocks (2.60-2.70 g/cm^3) in upper- and mid-crustal levels (km 120-160).
- (3) The relatively dense rocks (2.85-2.95 g/cm^3) in mid-crustal levels (km 60-120).
- (4) The low-density material (2.55-2.60 g/cm^3) in upper-crustal levels accompanied with a deepening Moho (km 0-60).

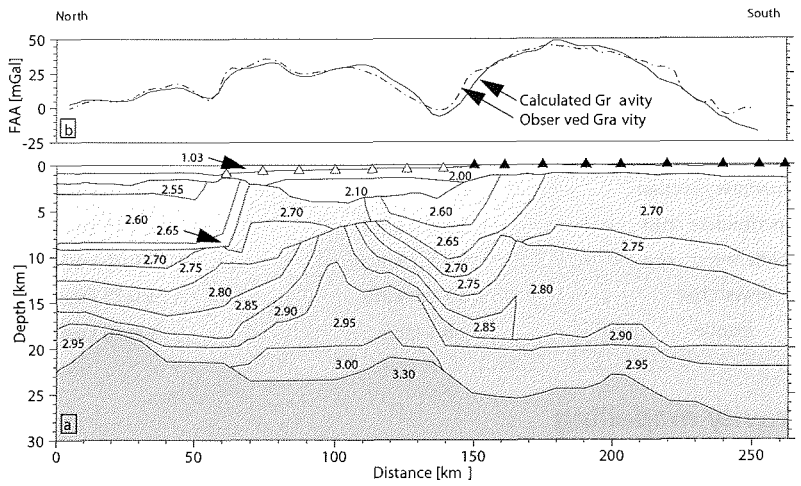

Figure 2-13: Final density model for profile AWI-99300.
The upper figure (a) shows the observed (dashed line) and modelled (solid line) free-air gravity. Density values (g/cm³) are calculated by the non-linear regression of the velocity-density relationship of Christensen & Mooney (1995). Black and white triangles mark the positions of seismic station locations. At km 0-40 the fit to the observed gravity is achieved by an arbitrary 4 km downward shift of the crust-mantle boundary! This region is not well constrained by seismic refraction data, but the gravity modelling gives a reliable estimate for Moho topography.

For the main part of the profile the density distribution confirms the crustal structures derived from seismic refraction modelling. At the northern end a downward correction in Moho depth is achieved.

2.6 Geological interpretation and discussion

The following section is structured according to the segmentary structure of profile AWI-99300 (S1-S4; Fig. 2-9 and Fig. 2-10). Fig. 2-14 summarises the interpretation and shows a geological cross-section of northwestern Svalbard and the adjacent Yermak Plateau.

2.6.1 The geology of segment S1 (Northwestern Svalbard)

The segment S1 (Fig. 2-10 and Fig. 2-14), located adjacent to the shoreline of northwestern Svalbard (Fig. 2-2) is built up of stretched continental crust, and shows similar thicknesses to these below the outer Isfjorden (e.g. Sellevoll et al., 1991; Czuba et al., 1999). Compared to the results of Chan & Mitchell (1982) we found a similar crustal structure, consisting of three lithological units, defined by seismic velocity (6.1-6.3, 6.4-6.6 and 6.7-6.8 km/s) and rock density (2.70-2.75, 2.80-2.90 and 2.95 g/cm³). According to the work of Amundsen et al. (1987), on xenoliths from the Woodfjorden

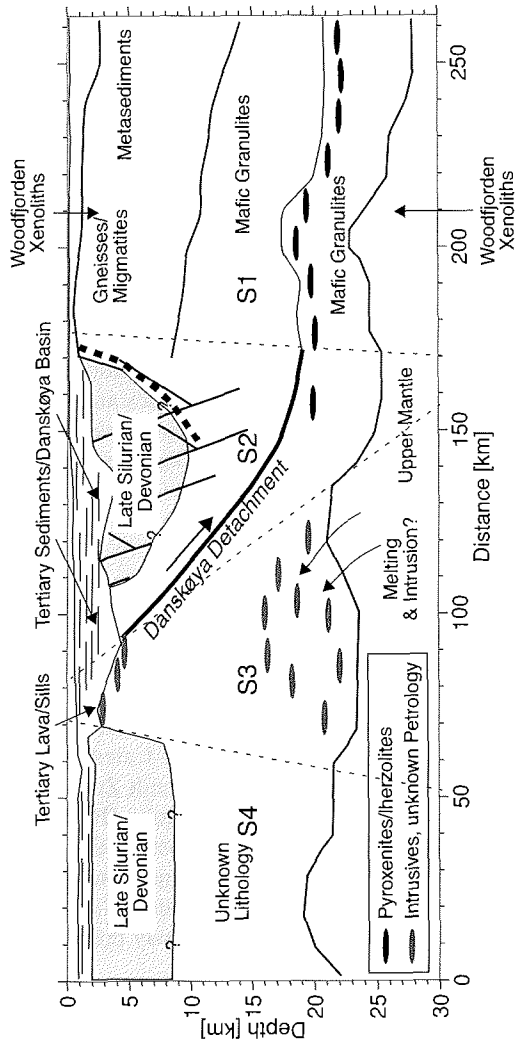

Figure 2-14: Final interpretation of the velocity model of profile AWI-99300. *The dotted lines mark the boundaries of the four crustal segments S1 to S4 as described in the text. Grey shaded regions mark the position of inferred Late Silurian/Devonian sedimentary basins. Between segments S2/S3 a thick black line marks the location of the proposed Cenozoic detachment fault. A possible north-dipping Caledonian Fault is marked by a dashed black line.*

area (Fig. 2-2), and onshore geology structural information compiled by Harland (1997c), we propose the following rock types for the seismic units:

Upper unit (0-14 km depth)

This unit consists of gneisses, migmatites and metasedimentary rocks, which are not covered by Paleozoic sedimentary rocks as in the central part of northern Svalbard (Amundsen et al., 1987; Fig. 2-2). The final velocity model provides no evidence for a separation of less mafic granulites for this unit as proposed by Amundsen et al. (1987). The seismic data indicate a more or less homogeneous upper-crustal unit. Following the definition of "Hecla Hoek"-basement rocks (Harland, 1997d), located to the east of the Billefjorden Fault Zone (Fig. 2-2) we do not use the term "Hecla Hoek" adopted by Amundsen et al. (1987) for our interpretation of the basement origin. Instead, we relate this upper unit to the unified basement province (terrane) west of the Raudfjorden Fault Zone (Fig. 2-2), which dips gently to the south, thus exposing deeper structural levels in the north. The southward dip of this unit is constrained by the observed seismic velocity structure, which shows a northward shallowing of the upper layer from 14-9.5 km depth along segment S1 (Fig. 2-10). The great variations in lithology throughout this basement province, from predominantly metasediments in the south to gneisses and migmatites in the north (Hjelle, 1979; Harland, 1997c) is not visible in the smooth velocity structure (Fig. 2-10). Therefore, we also exclude further batholiths, as found further west in the northwestern Svalbard province along the seismic profile (i.e. Hornemantoppen Batholith).

Middle unit (14-21 km depth)

At about 14 km depth Amundsen et al. (1987) define the boundary to mafic granulites. The seismic velocity of 6.4 km/s at depths of 10-14 km is rather lower than that for granulites at suitable p/T conditions observed in laboratory studies (approximately 6.7 km/s; Christensen & Mooney, 1995). Instead, the observed seismic velocities of the mid-crustal unit are in better agreement with Paleozoic orogenic areas, showing velocities of approximately 6.4 km/s (Holbrook et al., 1992). Earliest timing of Caledonian deformation found for the geologic provinces west of the Raudfjorden Fault Zone (Fig. 2-2) is dated to the Mid-Silurian, within the Paleozoic Caledonian orogeny (Harland, 1997c). After Holbrook et al. (1992), likely compositions for the mid-crustal units are more felsic, e.g. granitic or granodioritic. The Woodfjorden xenoliths undoubtedly bear mafic two-pyroxene granulites, so we favour this composition for the mid-crustal unit, despite its slightly inconsistent velocity. We suggest, that this deviation may point to a stronger tectonic overprinting, due to the Cenozoic rifting processes.

Lower unit (21-28 km depth)

According to Amundsen et al. (1987), the lower crust consists of mafic granulites, like these of the middle crust, with interlayered mantle pyroxenites and/or lherzolites. The observed velocity range along the profile is consistent with the interpretation of Amundsen et al. (1987) that the lower crust consists most probable of mafic granulite rocks interbedded with pyroxenite lenses. From the seismic data it seems that these lenses occur at a depth level of 6.5 km above the crust-mantle boundary, which may reflect certain p/T conditions, forming a distinct lithological unit. At this level a strong reflector (6.6 to 6.7 km/s; Fig. 2-10) separates the lower-crustal portion along segment S1. Here the transition between the brittle and ductile crust is also expected. This may provide fur-

ther good conditions for the accumulation of low amounts of mantle derived pyroxenites/lherzolites.

Seismic velocities of 6.7-6.8 km/s at the crust-mantle boundary are characteristic for Paleozoic orogenic regions. Furthermore, this is in agreement with velocities found below central Isfjorden, located 50-80 km to the southeast (Sellevoll et al., 1991).

A comparison to a seismic model for the lower-crustal structure of northwest Svalbard published by Czuba et al. (1999) shows obvious differences. The 10-15 km thick lower-crustal section of Czuba et al. (1999) showing seismic velocities of approximately 7.3 km/s, is not confirmed by this study. The large discrepancies to Czuba's model (1999) may be due to the experimental setup. The sparse shot-receiver distribution and non-reversed profiles were not able to provide non-ambiguous seismic data. Velocities greater than 7.2 km/s are typical for continental shield provinces (Holbrook et al., 1992) or passive (volcanic) margins influenced by mafic to ultramafic underplating (White & McKenzie, 1989). We exclude magmatic underplating processes within segment S1, based on the observed low seismic velocities. Further, no evidence for excessive volcanism during break-up at 36 Ma has been found onshore. Our model combined with geology observations suggest that more likely a non-volcanic continental structure is present.

2.6.2 The geology of segments S2/S3 (Southern Yermak Plateau)

Off the northwestern tip of Svalbard (Fig. 2-2) the upper and middle crustal velocities of segment S1 (Fig. 2-10 and Fig. 2-14) are replaced by a zone of lower seismic velocities (>5.1 km/s) of segment S2. Further north, slightly higher velocities of 6.7-7.0 km/s in the middle and lower crust define segment S3.

The trough-like structure in segment S2, underlying the southern Danskøya Basin, shows seismic velocities of 5.1-6.0 km/s, which we interpret as Paleozoic, i.e. Late Silurian/Devonian sediments. We suggest, that the trough is bounded by faults, which may have been reactivated to facilitate Tertiary rifting. The base of the Paleozoic sedimentary section in the trough is marked by velocities of 5.6-6.0 km/s at depths of 8-11 km. Thus the Paleozoic sequence has a thickness of 4-7 km (Fig. 2-14), which is comparable to onshore observations on northwestern Svalbard (Harland, 1997b). Younger Post-Devonian sediments are not suggested here, since we assume similar sedimentary-erosional processes onshore and offshore for the northern central terrane.

According to onshore geological interpretations subsiding Paleozoic basins of the central terrane were the result of transtension tectonics since Late Silurian (Friend et al., 1997). Pull-apart structures are interpreted to have developed in the vicinity of the Raudfjorden-, Hannabreen- and Breibogen Fault Zones, indicating Late Silurian/Devonian sedimentation in northern Svalbard. The occurrence of the Paleozoic sequences to the north is poorly known, due to the small number of offshore seismic investigations. Eiken (1994) suggests Devonian strata east of Danskøya Basin and south of the Moffen Fault (Fig. 2-2). Seismic velocities for Devonian strata on Svalbard are poorly known, although velocities of 4-6 km/s were recorded for younger Permian-Carboniferous sediments (Eiken, 1994). Fechner & Jokat (1996) and Schlindwein & Jokat (1999) found seismic velocities of 5.5 km/s and 5.3/5.7-6.0 km/s (surface/base) for Devonian sedimen-

tary rocks to the east of the Caledonian orogen for the deeper Jameson Land Basin of the East Greenland Fjord Region, whose structure is well known from onshore geology mapping.

Jokat (2000) mapped highly compacted Paleozoic sedimentary rocks of a possible Caledonian foreland basin (Surlyk, 1991; sedimentary deposits are not preserved onshore) below the Ob-Bank off northern Greenland showing seismic velocities of up to 5.8 km/s. According to tectonic reconstructions and geological records (e.g. Harland & Wright, 1979; Håkansson & Pedersen, 1982) northern Greenland and Svalbard together occupied a wide depositional realm of the Caledonian orogen. The density model (Fig. 2-13) shows density values of 2.55-2.60 g/cm^3 for the respective crustal section. In fact, this is a reasonable range for highly-consolidated sedimentary rocks. It is therefore likely, that the crust below the Danskøya Basin of segment S2 consists of Late Silurian/Devonian strata. The northern edge of this Paleozoic basin is marked velocities ranging between 6.0-6.1 km/s. These seismic velocities are similar to those observed along segment S1 for crystalline basement.

At depths of 20 km, below the Paleozoic basin of segment S2, seismic velocities are lower in comparison to the same level in segment S1. Further north seismic velocities along segment S3 increase to 6.6 km/s indicating a pronounced lateral velocity variation at a depth of 20 km. Eiken (1993) emphasised the resemblance of the Danskøya Basin to a Tertiary pull-apart structure, due to the fact that the bounding faults strike slightly oblique to the Hornsund Lineament (Fig. 2-2). Eiken (1993) proposed a simple shear rifting history as the origin for the Danskøya Basin. As a consequence of rifting, thin crust off the northwestern tip of Svalbard was suggested. Thinned crust cannot be confirmed by this study. But the pronounced asymmetry in seismic velocity structure between the segments S2/S3 can be consistent with such a view. Following the detachment extension models of Lister et al. (1991), based on Wernicke's (1985) simple shear concept, the boundary between the segments S2/S3 might be interpreted to be a deep penetrating fault or detachment. According to Wernike's (1985) concept the upper plate (consisting here of the segments S1/S2) trends to brittle block-faulting, while the lower plate's (segments S3/S4) crust-mantle boundary behaves in a ductile fashion forming a Moho uplift.

The zone of lower seismic velocities within the middle and lower parts of segment S2 (Fig. 2-10) may be therefore block-faulted and partly mylonitised, due to extension. Faulted (acoustic) basement was found for the landward side of the southern Danskøya Basin (Eiken, 1993). The low velocities in segment S2 at depths of 12-18 km can be attributed to ancient domino faults suspending and cracking the actual lithological structure of suggested mafic granulites (segment S1).

Stretching and uplift of the upper mantle can lead to its subsequent decompressive melting. The rising magma can crystallise at the base of the crust (underplating) or within its lower and middle parts, following zones of weakness (Lister et al., 1991). Thus, the lower parts of segment S3 may be interpreted as slightly contaminated with mantle derived melts, increasing the seismic velocity here (Lister et al., 1991). Eiken (1993) interprets strong and smooth reflections at the base of the sediments in the northern Danskøya Basin (below segment S3) as sills or lava flows; a further indicator of

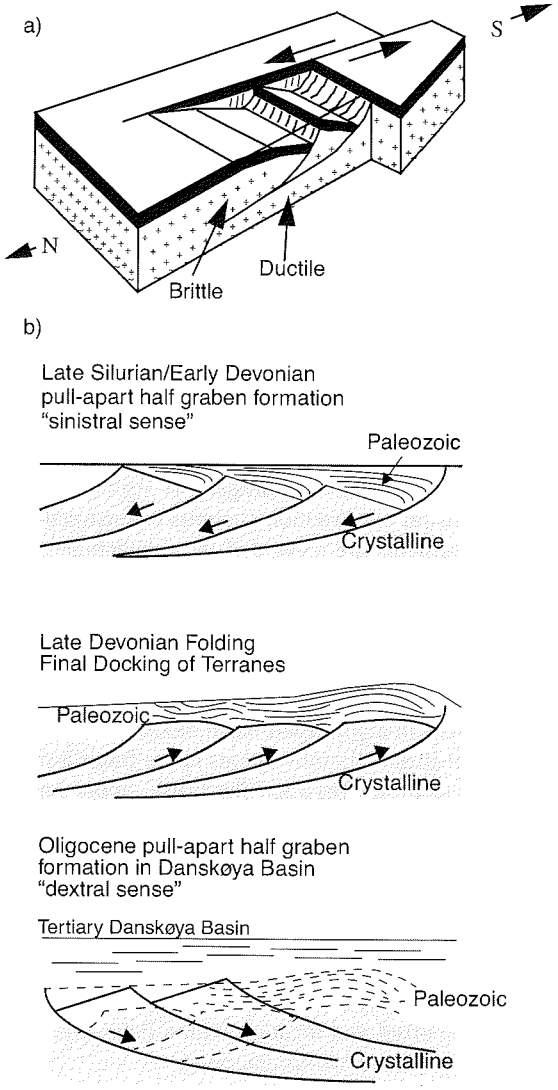

Figure 2-15: Block Diagram showing the principal growth of pull-apart half grabens in a sinistral strike-slip zone (a) and schematic evolution of the Danskøya Basin (b).
This geometry is supposed for the depositional setting of the Devonian Siktefjellet Strike Slip Zone (Fig. 2-2; after Friend et al., 1997). The same tectonic is considered for the formation of the Paleozoic Basin below Danskøya Basin, which is located 50 km to the northwest. Paleozoic schematic evolution of the Danskøya Basin crustal section after Friend et al. (1997).

slight volcanic activity. Generally, the magmatism along segment S3 was essentially subdued, since the magnetic field pattern (Feden et al., 1979) appears rather smooth.

The seismic refraction data along profile AWI-99300 yield no consistent evidence for the suggested reflectivity of a mylonitic detachment or fault zone at the base of the Paleozoic sedimentary section (Etheridge & Vernon, 1983; Fountain et al., 1984). Here, the boundary between the segments S2 and S3 shows no significant impedance contrast. The wave length of seismic signals is ~750 m at seismic velocities of 6 km/s and a frequency of 8 Hz. Thus, if the velocity distribution and the geometry of the segments S2 and S3 are due to the presence of a detachment fault, a discrete mylonite zone on this plane must have a very low thickness of less than ~190 m according to the formal vertical resolution. But a gradual transition from the mylonite zone to the (undisturbed) surrounding rock units is probably more natural resulting in a not sufficient impedance contrast.

Summarising the discussion for the segments S2/S3 we conclude that a Late Silurian/Devonian basin exists within segment S2. The p-wave velocity range found for shore rocks deposited after the Caledonian orogeny is very similar to those we found. The strong asymmetry in crustal construction supports extensional detachment tectonics so it is possible that the segments are separated by a detachment fault. Regarding the pull-apart character of the Oligocene Danskøya Basin (Eiken, 1993) we support models that require simple shear processes for the Mid-Cenozoic rifting.

The existence of a deeper seated Devonian Basin indicates that extensional movements took place during the Caledonian orogeny. Striking support is given also by recent geological mapping (Friend et al., 1997) at the Siktefjellet Strike-Slip Zone (Fig. 2-2), which discovered half-grabens in a pull-apart basin of Late Silurian/Early Devonian age. These grabens are related to strike-slip movements along Raudfjorden Fault and Breibogen Fault and detachment tectonics between the brittle upper and ductile lower crust (Fig. 2-15a). Similar tectonic origin is considered for the formation of the Paleozoic Basin below Danskøya Basin, which is located 50 km to the northwest (Fig. 2-15b). Thus it is required that the Raudfjorden Fault (or a related major fault) extents further to the north to enable Paleozoic half-graben formation below the Danskøya Basin. The subsequent Tertiary extension and formation of Danskøya Basin was accompanied by the reversal of the strike-slip motion from sinistral (Caledonian terrane accretion) to dextral sense (Cenozoic break-up of Svalbard from northeast Greenland; Fig. 2-15b). It seems, that Tertiary transtension occurred at a location with a Paleozoic faulting history which provided possible zones of weakness within the crust.

2.6.3 The geology of segment S4 (Central Yermak Plateau)

Compared to the velocity structure along segment S1, segment S4 (Fig. 2-10 and Fig. 2-14) shows similar crustal thickness derived from seismic and gravity modelling. Lower seismic velocities of 5.3-5.8 km/s are present within the upper-crustal section. Following the interpretation of Paleozoic sediments in segment S2, we suggest the existence of Post-Caledonian sediments here, north of the Danskøya Basin. The observed acoustic basement in seismic reflection data (approximately 2 s TWT; Eiken, 1994) may represent

a sediment-sediment boundary. Assuming velocities up to 6.0 km/s for Paleozoic sediments, the actual sediment-basement boundary may be located at depths of 8-10 km.

The final velocity model (Fig. 2-10) constrains a reflective boundary, separating velocities of 6.0 from 6.1 km/s. The latter velocity seems likely to be related to northern Svalbard crystalline rocks, as observed along segment S1 and confirmed by onshore geological observations. The thickness of crystalline crust decreases to 10-14 km below the Devonian basin (Fig. 2-14). A lithological interpretation is difficult. Svalbard's central terrane of the Caledonian and Ellesmerian orogeny, might extent as a spur northwest of Norskebanken (Fig. 2-2). Therefore, a similar lithology as found for the central terrane onshore might be expected.

The northern edge of profile AWI-99300 adjoins the southern H.U. Sverdrup Bank, whose origin is the subject of speculations. Seismic refraction data from the H.U. Sverdrup Bank (Austegard, 1982) revealed seismic velocities generally greater than 5 km/s. Eiken (1993; 1994) interprets the H.U. Sverdrup Bank as a crystalline block, due to its smooth aeromagnetic character (Feden et al., 1979) and dredged Precambrian gneisses (Jackson et al., 1984). Our deep seismic profile AWI-99300 provides no new evidence concerning the nature of the bank. The direct juxtaposition of a Devonian basin (segment S4) with the H.U. Sverdrup Bank may point to a Paleozoic sedimentary origin for the uppermost section.

2.7 Tectonic implications

Following the interpretation and discussion of the resulting geological model of profile AWI-99300, two implications can be drawn: (1) The nature and magmatic history of the Yermak Plateau, with regard to the proposed Yermak Hot Spot (Feden et al., 1979; Jackson et al., 1984), must be revised, because the observed crustal structure exhibits no evidence for plume activity. (2) The proposed Cenozoic simple shear processes entail isostatic response on the lithosphere of northern Svalbard and the Yermak Plateau, and therefore uplift of the Svalbard region.

2.7.1 The nature and magmatic history of the Yermak Plateau

From Prins Karls Forland (Fig. 2-2) up to the northern edge of the profile AWI-99300 slightly thinned continental crust is present, showing a relatively constant crustal thickness. The southern section of the profile is associated with the basement province cropping out west of the Raudfjorden Fault on Svalbard (Fig. 2-2; Harland, 1997c). It is part of Svalbard's central terrane in the north of the Kongsfjorden-Hansbreen Fault Zone (Fig. 2-2; Harland & Wright, 1979). The Danskøya detachment fault separates this province from a further continental fragment, i.e. segment S4 that might also be related to the central terrane province. According to gravity field observations (Boebel, 2000) stretched continental crust on the western Yermak Plateau is bounded by strong gravimetric anomalies (see Fig. 2-16; i and ii). Most probably stretched continental crust reaches up to 82°N, separating the oceanic Fram Strait spreading system (anomaly i) from the oceanic Yermak Plateau province at 82°N (anomaly ii), the conjugate to the Morris Jesup Rise (Fig. 2-1 and Fig. 2-16; Boebel, 2000). Southward, the eastern anomaly ii intersects with the profile where stretched continental crust is present. We con-

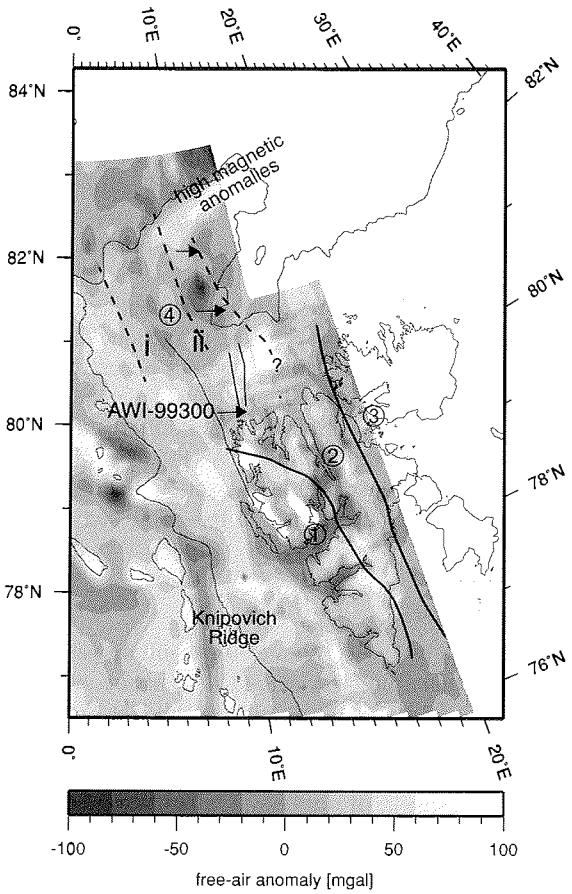

Figure 2-16: Free-air anomaly grid of Boebel (2000).
Thick black lines on Svalbard separate the three proposed terranes: (1) western, (2) central, (3) eastern terrane. The gravity high anomaly i is suggested to express the western continent-ocean transition of a stretched continental fragment (4; Boebel, 2000). The gravity low ii indicates its proposed eastern boundary. Note, that profile AWI-99300 (thin line) is located to the east of anomaly ii, so that the transition probably occurs further east (arrows). The continental fragment of the Yermak Plateau probably belongs to the central terrane of Svalbard. Zone of enhanced magnetic anomalies after Feden et al. (1979). Bathymetry: IBCAO (Jakobsson et al., 2000; 2000 m-contour).

clude, that anomaly ii reflects rather the summit of a stretched fragment than the eastern boundary to a oceanic province south of 82°N as proposed by Boebel (2000). The actual continent-ocean boundary occurs probably 30 km further east (Fig. 2-16).

Up to 81°N, the observed crustal structure along profile AWI-99300 provides no evidence for increased magmatic activity, due to the presence of the Yermak Hot Spot (Feden et al., 1979; Jackson et al., 1984). Plume-related features like volcanic wedges, numerous intrusions or underplating as found for North Atlantic continental margins (e.g. Barton & White, 1997) are missing here. For the case of the North Atlantic the influence of the mantle plume extends up 2000 km distance from its head. The distance from the northern tip of profile AWI-99300 to the strong magnetic anomaly pattern in the northeast (Fig. 2-16), which was interpreted as a result of plume activity on the Yermak Plateau (Feden et al., 1979) is just 150 km. A stretching factor of β=1.2-1.6 is calculated between the mean crustal thickness of the central terrane (35 km; Sellevoll et al., 1991) and the observed values along profile AWI-99300 (21-28 km). Applying these factors the distance between the northern termination of profile AWI-99300 and the high magnetic anomalies shortens to 100 km.

Further it has to be considered that western Svalbard adjoins the Spitsbergen Shear Zone which marks the plate boundary between Svalbard and Greenland in Oligocene times (Crane et al., 1991). Lithospheric thinning is suggested along the fracture (Crane et al., 1991) which would therefore lead to channelling of the plume through this zone towards the south (Thompson & Gibson, 1991; Saunders et al., 1992). Decompressive melting due to a lesser lithospheric load would provide a simple path for distribution of large amounts of melts associated with the hot mantle plume. Further north-south striking major faults on the Svalbard Archipelago (Fig. 2-2) might also control the plume evolution. Although good boundary conditions are given only a slight amount of intrusives is observed below the central and southern Yermak Plateau. Therefore, the intrusives below the detachment fault in the lower crust, seem to be more consistent with decompressive melting (Lister et al., 1991) as a consequence of the extensional processes and subsequent slight uplift of the crust-mantle boundary.

The temperature of the asthenosphere determined on Neogene volcanics of the Woodfjorden area (Fig. 2-2) is 1350°C, slightly above that of normal asthenosphere (Vågnes & Amundsen, 1993). This is rather low, compared to temperature anomalies reported from other hot spots (+200-300°C; Vågnes & Amundsen, 1993). It seems more likely, that the Oligocene volcanic activity was a local phenomenon situated and restricted to the northeastern Yermak Plateau (Fig. 2-16 and Fig. 2-17) along an ancient section of the Gakkel Ridge. Therefore, we prefer a non-volcanic continental margin evolution for northwestern Svalbard and the Yermak Plateau continental margins investigated here.

Consequently, local volcanic activities further south, i.e. northern Danskøya Basin and Woodfjorden volcanics, appear to be not linked to any mantle plume influences. More likely, they seem to be also related to the extensional lithospheric shear processes below the Danskøya Basin during Cenozoic, destroying the internal structure of the continental crust and providing paths for mantle derived melts.

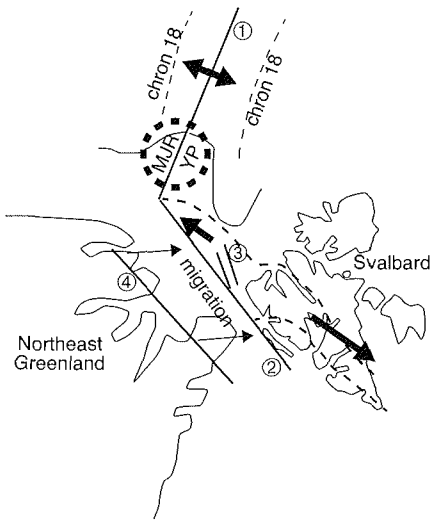

Figure 2-17: Oligocene schematic plate tectonic configuration (36 Ma).
The figure includes the boundary of the northern continuation of Svalbard's central terrane that results from this study (dashed). Thin dashed lines along the Gakkel Ridge mark the position of chron 18 (after Boebel, 2000). In Pre-Oligocene times northeast Greenland, Svalbard and the juvenile Gakkel Ridge (1) adjoined a triple junction (RFF-system). From 36 Ma onwards, Gakkel Ridge spreading and transtensional movements along the Hornsund Lineament (2; thick arrows) caused the break-up of Svalbard from northeast Greenland. The Danskøya Basin (3) as well as a detachment below developed (or was reactivated). Later, at 20 Ma, seafloor spreading started in the Fram Strait, to finally connect the North Atlantic MOR system (Mohns Ridge-Knipovich Ridge; Fig. 2-1) with the Arctic Gakkel Ridge. Local volcanism formed the northeastern Yermak Plateau (YP; position of enhanced magnetic anomalies) and the Morris Jesup Rise (MJR; thick dashed circle) during Oligocene. The actual constructions of these geological features (YP and MJR) are still subject of speculations. Broader plume activity which formed a large volcanic plateau consisting of thickened oceanic crust is excluded, since the continental spur of Svalbard's central terrane exhibits no evidence for higher magmatic activity. The transform fault systems between Greenland and Svalbard moved continuously eastwards (e.g. Trolle-land Fault Zone (4) to Hornsund Lineament) from Late Cretaceous onwards. Fault systems commonly feature pull-apart structures. The most recent of these is the Danskøya Basin on the southern Yermak Plateau. Thicker dashed lines on Svalbard and Yermak Plateau indicate terrane boundaries.

2.7.2 Cenozoic tectonics between Greenland and Svalbard and subsequent uplift

Since Late Cretaceous times the main transcurrence/transtension fault system between Svalbard and Greenland, migrated continuously eastwards (Håkansson & Pedersen, 1982; Crane et al., 1991). First movements started at the Trolle-Land Fault system, while later a jump to the Hornsund Lineament occurred (Fig. 2-17). The transfer movements were not limited to a single fault, but were rather spread over a broader region, so that local pull-apart basins developed (e.g. predestination of Molloy Ridge (Crane et al.,

1991), Trolle-Land Fault Zone (Håkansson & Pedersen, 1982)). The development of Danskøya Basin and the detachment tectonics fit to this interpretation, since it defines the eastern termination of migrating strike-slip tectonics. Eiken (1993) mentioned the pull-apart character of the Danskøya Basin, although its precise shape is unknown. The geological interpretation of the final velocity model (Fig. 2-14) supports this interpretation.

The continental Yermak Plateau fragment underwent extension from Oligocene onwards, so that a juvenile rift structure developed. Svalbard, as well as the surrounding Barents Sea region experienced uplift and erosion during the Cenozoic, as shown by geological records and model calculations (Doré & Jensen, 1996). A first uplift phase is supposed to have a tectonic origin, probably occurring in several episodes throughout the Cenozoic. A second phase is associated with the rebound from ice-sheets of the great glaciations of the Pliocene and Pleistocene (Doré & Jensen, 1996). Total erosion of 3000 m is supposed for the southwestern Svalbard region, mainly caused by glacial erosion (Dimakis et al., 1998). For the marginal rift flanks of the Barents Sea (i.e. Senja Fracture Zone-Western Svalbard and Nordaustlandet-Franz Josef Land; Fig. 2-1) only 500-1000 m of uplift is related to rifting, break-up and subsequent opening of the adjacent ocean basin. This is most probably due to (i) heat transfer defining temperature distribution and therefore flexural rigidity of the lithosphere and (ii) lithospheric shear mechanical flexure during break-up, respectively (Dimakis et al., 1998). Regarding the detachment models of Lister et al. (1991), we suggest an additional local component for the southern Yermak Plateau that interacts with rift induced tectonic uplift along the western rim of the Barents Sea. Mid-crustal detachments and crustal thinning (Lister et al., 1991) can lead to uplift during the rift phase followed by a post-rift subsidence phase. Model calculations with a detachment fault at 15 km depth and an initial crustal thickness of 35 km result in a maximum net uplift of 600 m (Lister et al., 1991). Since a full rifting phase was not completed at the southern Yermak Plateau, the maximum amount cannot be expected. With a stretching factor of β=1.2-1.5 a net uplift of up to 300 m is possible (Lister et al., 1991) superimposed on broader tectonic events.

2.8 Conclusions

Transtensional tectonics during the break-up of Svalbard and Greenland thinned the crust from 35 km below inner Svalbard, to 18-28 km as observed along the profile. The deep structure of the southern section of the profile can be related to the basement province west of the Raudfjorden Fault building up the central terrane of Svalbard. The character of the stretched continental crust remains similar on the northern Yermak Plateau, but the actual lithology of the middle and lower crust remains speculative.

North of Svalbard's coastline the velocity structure supports the existence of a detachment fault, although the fault plane is not resolved in the seismic data itself. Above this, the Tertiary Danskøya Basin is underlain by a Paleozoic sedimentary basin, of suggested Late Silurian/Devonian age. The Paleozoic sedimentary origin of that basin is constrained by low seismic velocities of 5.1-5.8 km/s, which are typical for Devonian rocks

of Greenland and Svalbard. Paleozoic sedimentary rocks may occur also in the upper section (6 km) between the H.U. Sverdrup Bank and the Danskøya Basin. The onset of extension in the Danskøya Basin above the detachment was in the Oligocene, while its duration is speculative. Due to the obvious asymmetric construction, simple shear rifting is supposed. This might have driven an uplift of maximum 300 m in the Cenozoic.

The final velocity model reveals no evidence for a large-scale influence and magmatism of a suggested hot spot during the break-up of Svalbard from northern Greenland (Yermak Hot Spot). The boundary conditions for a widespread distribution of mantle derived melts are generally given since thin lithosphere can control the evolution of the plume along the major fractures and would provide ideal paths.

We propose, that the observed crustal structure is typical for the entire western plateau up to 82°N, which is thus a stretched spur of the continental central terrane of Svalbard.

The volcanism that created the northeastern Yermak Plateau and the Morris Jesup Rise seems to have been local and short-lived, and is therefore unrelated to mantle plurne activity as proposed for the North Atlantic margins. Therefore non-volcanic continental margins for northern and western Svalbard may be expected. Known volcanic events further south are, according to our interpretation, related to melt generation caused by simple shear tectonics combined with a slightly increased asthenospheric temperature.

CHAPTER 3:
A DEEP SEISMIC TRANSECT IN NORTHWESTERN SVALBARD AT KONGSFJORDEN (NY ÅLESUND) AND THE IMPLICATIONS FOR THE CENOZOIC BREAK-UP FROM GREENLAND: A SHEARED MARGIN STUDY

Oliver Ritzmann[1], Wilfried Jokat[1], Wojciech Czuba[2], Alexander Guterch[2], Rolf Mjelde[3]& Yuichi Nishimura[4]

[1] Alfred Wegener Institute for Polar and Marine Research, Bremerhaven, Germany
[2] Institute of Geophysics, Polish Academy of Sciences, Warsaw, Poland
[3] Institute of Solid Earth Physics, University of Bergen, Bergen, Norway
[4] Institute of Seismology and Volcanology, Hokkaido University, Sapporo, Japan

Submitted to Geophysical Journal International, Blackwell Science UK, September 2002

3.1 Abstract

New seismic refraction data were collected across the western Svalbard continental margin off Kongsfjorden (Ny Ålesund) during the cruise leg ARK15/2 of *RV Polarstern*. The use of on- and offshore seismic receivers and a dense airgun shot pattern provide a detailed view of the velocity structure of Svalbard's continental interior, the continent-ocean transition, and oceanic crust related to the northern Knipovich Ridge and the Molloy Ridge.

The Caledonian central and western terranes of Svalbard are not distinguishable on the basis of seismic velocity structure. Below a 7 to 8 km thick Paleozoic sedimentary cover the crystalline crust reveals a three-layer structure with seismic velocities ranging between 6.1 and 6.9 km/s. The geological suture between the terranes is imperceptible. The middle and upper crust below the Tertiary Forlandsundet Graben shows striking low velocities. This can be related to the Early Paleozoic convergent transpressive movements between Svalbard and northern Greenland, followed by an extensional (relaxing) phase. We argue that a brittle-fractured rock formation is present below the graben, which also buries a sedimentary Paleozoic core.

The continent-ocean transition can be classified as a sheared margin formed at the continental part of the Spitsbergen Fracture Zone. Moderate crustal thinning is achieved only to the west of the low velocity zone below the Forlandsundet Graben. This leads to the assumption that transtensional rift movements since Oligocene were decoupled from the central terrane of Svalbard. The Moho dips with an angle of 45° eastwards at the continent-ocean transition that exhibits higher seismic velocities of 7.2 km/s on the continental side. These can be interpreted as minor mantle-derived intrusions, probably

induced by convection due to the juxtaposition of cool continental and hot oceanic lithosphere.

The oceanic crust generated at the Knipovich Ridge and the Molloy Ridge is thin (2 to 4 km), compared to the global mean, and is characterised by the absence of oceanic layer 3. These observations can be ascribed to conductive cooling of the ascending mantle due to the extremely low divergence rate and the neighbouring cool continental crust. The underlying mantle is slightly serpentinised below the Knipovich Ridge segment, reflected by low seismic velocities of ~7.7 km/s. A thicker sequence of syn- and post rift sediments and sedimentary rocks are observed on the Molloy Ridge oceanic segment, which results from greater subsidence relative to the Knipovich Ridge segment.

3.2 Introduction

The Paleozoic to Cenozoic tectonic history of western Svalbard is revealed onshore along a 150 km wide area of outcrops, that is morphologically intersected by large fjords (i.e. Kongsfjorden and Isfjorden; Fig. 3-1). This coastal strip and the adjacent continental margin were affected by various tectonic events, which are mostly associated with strike-slip movements. The earliest of these was the sinistral merging of Paleozoic basement terranes (Harland & Wright, 1979; Harland, 1997b). Later, in the Early Cenozoic, the West Spitsbergen Orogeny (e.g. Steel et al., 1985; Harland, 1997a) took place. The latest step in the tectonic history was the dextral transtensional rifting and break-up between Svalbard and northeast Greenland (Eldholm et al., 1987). The supposed spreading axes of the Knipovich Ridge and the Molloy Ridge within the Fram Strait are closely located to the newly developed margin, which might enhance magmatic interactions from the ridges to the continental crust.

Due to the absence of continuous and detailed deep seismic transects across the archipelago large gaps still exist in the knowledge about the deeper crustal composition of Svalbard. The western Barents Sea margin (Senja margin) and the western Svalbard/Yermak Plateau margin have been only locally explored (e.g. Guterch et al., 1978; Myhre & Eldholm, 1988; Faleide et al., 1991; Sellevoll et al., 1991). As a consequence, there is a lack of a velocity structure across the continental margin that is detailed enough to resolve the mentioned tectonic units.

This contribution provides new detailed background information on the crustal structure of the continental margin of northwestern Svalbard (Fig. 3-1). The evolution of the major tectonic elements will be discussed. This study is integrated in the newly derived seismic data along the eastern North Atlantic margin (this issue). We base our study on a seismic refraction experiment off Kongsfjorden (Fig. 3-1) with an integrated analysis of gravity data. This experiment was carried out by the Alfred Wegener Institute for Polar and Marine Research (Bremerhaven) in cooperation with Polish, Japanese and Norwegian scientists in August to September 1999 with the German Icebreaker *RV Polarstern*.

3.2.1 Caledonian geology

The Svalbard Archipelago (Fig. 3-1 and 3-2) is supposed to consist of three distinct terranes, that are bounded by major discontinuities (e.g. the Kongsforden-Hansbreen Fault Zone; Harland & Wright, 1979). These terranes merged during the Early

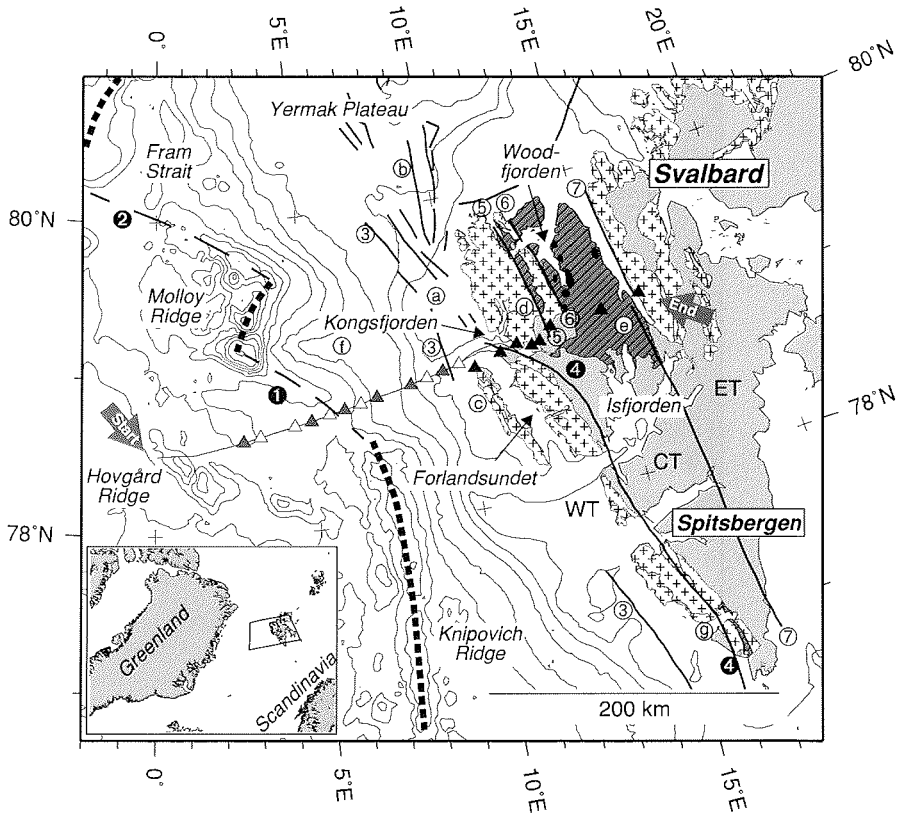

Figure 3-1: Location of seismic refraction profile AWI-99400.
Insert: Location in the North Atlantic. The profile track is marked by a thin black line, RefTek-stations (black), obh-stations (grey) and obs-stations (white) by triangles. The cross marks indicate Pre-Devonian basement outcrops (after Harland, 1997a: simplified geological map). Devonian sedimentary rocks are coloured dark grey (dash pattern). Local outcrops of Quaternary volcanics in the Woodfjorden area are plotted as black polygons. Thick black lines are major faults offshore (dashed) and onshore (solid): (1) Molloy Transform Fault, (2) Spitsbergen Transform Fault, (3) Hornsund Lineament, (4) Kongsfjorden-Hansbreen Fault Zone, (5) Raudfjorden Fault, (6) Breibogen Fault, (7) Billefjorden Fault. Spreading ridges are marked by a thick dotted line. Geographic locations used in the text: (a) Sjubrebanken, (b) Danskøya Basin, (c) Prins Karls Forland, (d) Albert I. Land, (e) Andrée Land, (f) Vestnesa, (g) Hornsund. Note, that the sinistral strike-slip faults (4) and (7) are proposed to subdivide Svalbard into the western-, central- and eastern terrane (WT, CT and ET). Plate boundary after Boebel (2000). Bathymetry: IBCAO (500 m-contour interval + 200 m-contour; Jakobsson et al., 2000).

Silurian-Devonian closure of the Iapetus Ocean by sinistral transform movements. Recent compilations of Svalbard's geology (e.g. Harland, 1997b) support this hypothe-

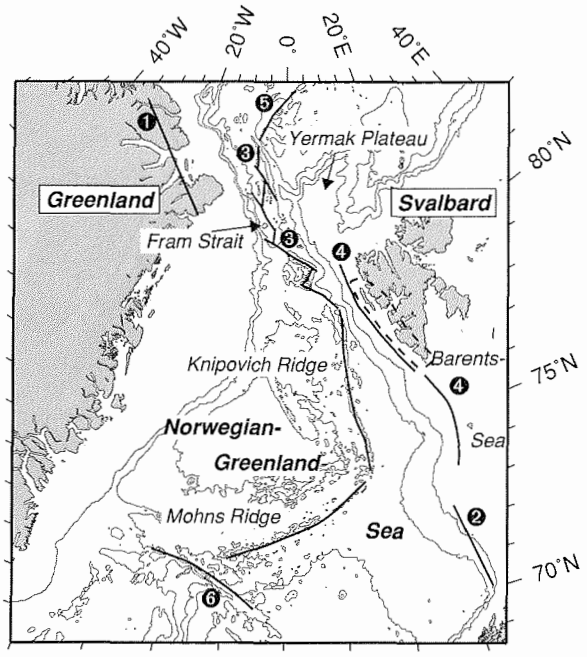

Figure 3-2: Tectonic structures in the North Atlantic region. *The thick dotted line indicates the approximate position of the West Spitsbergen Fold Belt. (1) Trolle-Land Fault Zone, (2) Senja Fracture Zone, (3) Mid-ocean ridges and transforms within the Fram Strait according to Boebel (2000), (4) Hornsund Lineament and Bjørnøya-Sørkapp Fault, (5) Gakkel Ridge, (6) Jan Mayen Fracture Zone.*

sis, although other authors continue to treat the Pre-Devonian of Svalbard as one province (e.g. Manby & Lyberis, 1992). The central terrane covers most of the northwestern part of Spitsbergen, the main island of the archipelago. The central terrane itself is separated into at least three subterranes (or basement provinces) which also docked in Silurian/Devonian times by sinistral movements along transform faults (e.g. Breibogen Fault; Friend et al., 1997). Primarily these faults controlled the Devonian sedimentation history of northwestern Svalbard (Harland, 1997b) between the Breibogen Fault and the Billeforden Fault Zone (Fig. 3-1). Further Devonian deposits are found along the Raudfjorden Fault Zone in the Woodfjorden region. Here, narrow half grabens occur along the fault, suggesting that simple shear tectonic accompanied the Paleozoic history. This results in extension and large-scale detachment tectonics (Friend et al., 1997). Locally, Devonian sedimentary rocks are also preserved within the West Spitsbergen Fold Belt (Hornsund; Fig. 3-1; Steel et al., 1985).

3.2.2 Tertiary break-up and Western Spitsbergen Fold Belt

Tertiary break-up of Svalbard and northern Greenland was initiated by the beginning of seafloor-spreading at the Mohns Ridge in the Norwegian-Greenland Sea (Fig. 3-2) about at chron 25 (~57 Ma; Talwani & Eldholm, 1977; Eldholm et al., 1987). Between Svalbard and Greenland shear movements took place along the Trolle Land-Senja Fault Zone (Håkansson & Pedersen, 1982; Eldholm et al., 1987) while later an eastward migration to the Hornsund Lineament (Eiken & Austegard, 1987) occurred. Crane et al. (1991) term this broad shear region the Spitsbergen Shear Zone, that also includes the Bjørnøya-Sørkapp Fault (Fig. 3-2) connecting the juvenile Senja-transform margin to the Hornsund Lineament. The mostly transpressive regime lasted up to chron 13 (36 Ma) and resulted in the development of the West Spitsbergen Fold Belt, that today is localised within a 50 km wide region along the western coast of Spitsbergen (Müller & Spielhagen, 1991). The Early evolution of this orogen is supposed to comprise also extensive movements, since subsidence of the Forlandsundet Graben prior to the Oligocene is verified (e.g. Steel et al., 1985).

Between chrons 13 and 5 (36 to 9.5 Ma) the very slow spreading Knipovich Ridge (< 10 mm/y; Eldholm et al., 1990) is supposed to have propagated northward into the shear zone, resulting in extremely asymmetric spreading (Eldholm et al., 1990; Crane et al., 1991; Crane et al., 2001). Further north the precise plate boundary between Svalbard and Greenland within the Fram Strait (Fig. 3-2) was defined by Boebel (2000) by modelling airborne gravity data. The associated reconstruction, based on the poles of rotation of Srivastava & Tapscott (1986) suggests the onset of seafloor-spreading at Molloy Ridge in the Early Miocene (20 Ma). Further north, two ancient ridge-transform pairs (Fig. 3-2) balanced the gradual opening of the Fram Strait oceanic gateway since chron 5 (12 to 9.5 Ma). The seafloor-spreading of these ridges within the Fram Strait is expected to be oblique, as observed for the Knipovich Ridge (Eldholm et al., 1990; Boebel, 2000).

3.2.3 The deeper structure of Svalbard and the adjacent oceanic province

Offshore seismic surveys have been conducted since 30 years ago, and comprise seismic reflection experiments and expanding spread profiling (Eiken & Austegard, 1987; Myhre & Eldholm, 1988; Faleide et al., 1991; Eiken, 1993; Eiken & Hinz, 1993) or larger refraction experiments using a small amount of seismic receivers and shots (Guterch et al., 1978; Sellevoll et al., 1991; Czuba et al., 1999). A first detailed crustal study along the northwestern shoreline and the southern Yermak Plateau was carried out by *RV Polarstern*, when seismic data of this study was acquired (Jokat et al., 2000; Ritzmann & Jokat, 2003; see chapter 2).

Guterch et al. (1978) and Sellevoll et al. (1991) defined the crustal thickness below central Svalbard to be 36 to 37 km and that below the Forlandsundet to be 26 to 27 km. Ritzmann & Jokat (2003) found similar crustal thicknesses of 28 km along the northwestern coast of Svalbard north of Prins Karls Forland. Sellevoll et al. (1991) and Czuba et al. (1999) report anomalously high seismic velocities at the crust-mantle boundary, assuming a transitional character of the Moho. This observation is not confirmed by Ritzmann & Jokat (2003), who assume a first-order crust-mantle discontinuity. The petrological constitution of the central terrane is derived from xenolith studies within the

Woodfjorden volcanics (Fig. 3-1). Amundsen et al. (1987) define a three-layered structure of gneisses, granulites and intrusive granulites (mantle pyroxenites and lherzolites) for northwestern Svalbard that supports the seismic model of Chan & Mitchell (1982) and Ritzmann & Jokat (2003). Sub-division into terranes after Harland & Wright (1979) is not possible since resolution of any seismic refraction experiment is too low.

Crustal models across the western continent-ocean transition were also deduced by velocity information of expanding spread profiles and gravity data (Sundvor & Austegard, 1990). Off Isfjorden a high velocity/density body is supposed to extend up to 2 km below the seafloor (Sundvor & Austegard, 1990). Published thicknesses of the oceanic crust associated to the Knipovich Ridge range between 8 and 12 km (Sundvor & Austegard, 1990; Czuba et al., 1999). The actual transition of continental and oceanic crust is mainly located using seismic reflection data. Up to 79°N the boundary is thought to be located at the Hornsund Lineament (Myhre & Eldholm, 1988; Sundvor & Austegard, 1990). It comprises a series of blocks downfaulted to the west, while on northern Sjubrebanken it separates into two distinct NNW-trending blocks (Myhre & Eldholm, 1988). The sedimentary structure off Svalbard is mapped by several seismic reflection lines (Eiken, 1994). According to the sedimentary distribution map of Austegard & Sundvor (1991), thicknesses vary between 1 and 3 km along the western Svalbard margin east of the Knipovich Ridge. Sedimentary deposits show a prominent depocentre at Vestnesa (up to 5 km), that is also a prominent feature in bathymetry (Fig. 3-1). The sedimentary structure of the offshore Tertiary graben, e.g. Forlandsundet Graben, was characterised by the work of Eiken & Austegard (1987). They conclude that structurally these graben are relatively small but deep basins (up to 5 km), which terminate north of Prins Karls Forland, but it is not possible to relate them to Tertiary transform movements or the continental break-up. Later, Eiken (1993) proposed an up to 10 km wide graben on northern Sjubrebanken to be similar to the Forlandsundet Graben structure.

3.3 New geophysical data

3.3.1 Seismic data acquisition

Seismic measurements were performed with the German icebreaker *RV Polarstern* during cruise leg ARK15/2 (Jokat et al., 2000). Two large volume airguns with a total volume of 92 l produced the acoustic energy and were fired every minute. In total the 1628 airgun shots extend from 0° to 12°E from Hovgård Ridge to Kongsfjorden over a distance of 250 km (Fig. 3-1 and 3-3). Additionally the Polish ship *El Tanin* participated with 5 TNT-shots with a charge of 50 kg between 8.5° and 9.5°E. Onshore, 8 RefTek seismometer stations, each equipped with 18 single coil geophones (4.5 Hz; vertical component) were used to record seismic energy. The easternmost station (ref401) was installed at 16.3°E, which results in an over-all length of profile AWI-99400 of 360 km. The spacing of the onshore receiver stations range from 5 to 35 km, and their deployment altitudes vary from 10 to 900 m. West of Prins Karls Forland 7 ocean-bottom hydrophone and 8 three-component seismometer systems (4.5 Hz geophones, gimbal mecha-

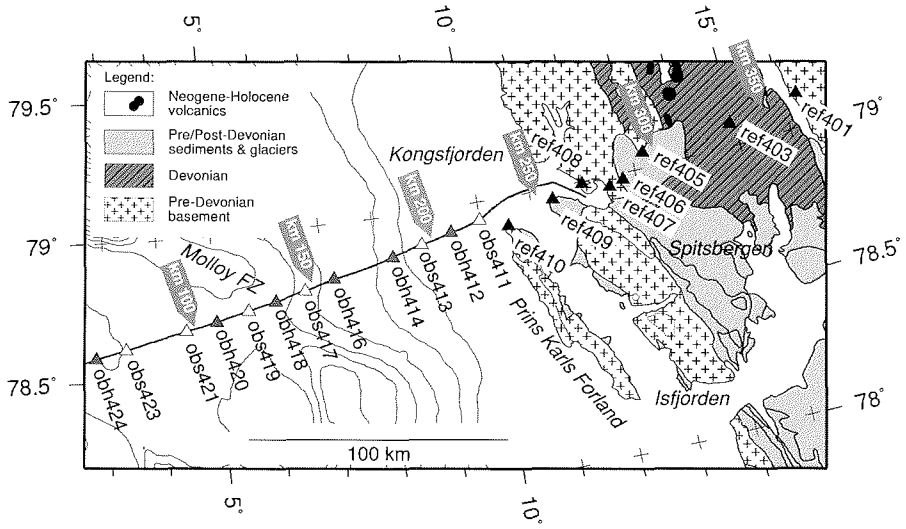

Figure 3-3: Detailed map of profile AWI-99400 and locations of receivers.
The profile track in the main figure is marked by a thin black line, triangles as for Fig. 3-1. Bathymetry: IBCAO (Jakobsson et al., 2000).

nism) were deployed in water depths of 200 to 2500 m. A receiver spacing of approximately 12 km was chosen for ocean bottom instruments. Failures of the stations obs425/obs415 and obh422 result in two larger gaps of 24 km along the profile (3°E and 7.7°E; Fig. 3-3). The profile AWI-99400 is unreversed west of station obh424 (2.8°E) as well as east of ref408 (12°E; Fig. 3-3; see also Jokat et al., 2000).

3.3.2 Characteristics of seismic refraction data

Figures 3-4 to 3-7 show 8 representative record sections of 20 successful registrations on- and offshore. The sections illustrate the main characteristics of the observed crustal velocity distribution. The data are filtered with a bandpass filter passing frequencies between 5 and 17 Hz. A 1 s-automatic gain control (agc) was applied for the evaluation and analysis of seismic refraction data. The data quality of the RefTek seismometers is in general excellent, e.g. p_n-arrivals were recorded up to distances of 220 km. Mostly, a low signal to noise ratio is compensated by the dense shot spacing yielding a good phase correlation.

Offshore, the ocean-bottom seismometer systems provide higher quality data than the neighbouring hydrophone systems. The recordings of the seismometer systems show up to twice the maximum distance of arrivals. Some hydrophone systems reveal extremely poor quality, so that data were ignored during picking and raytracing (obh414 and obh416).

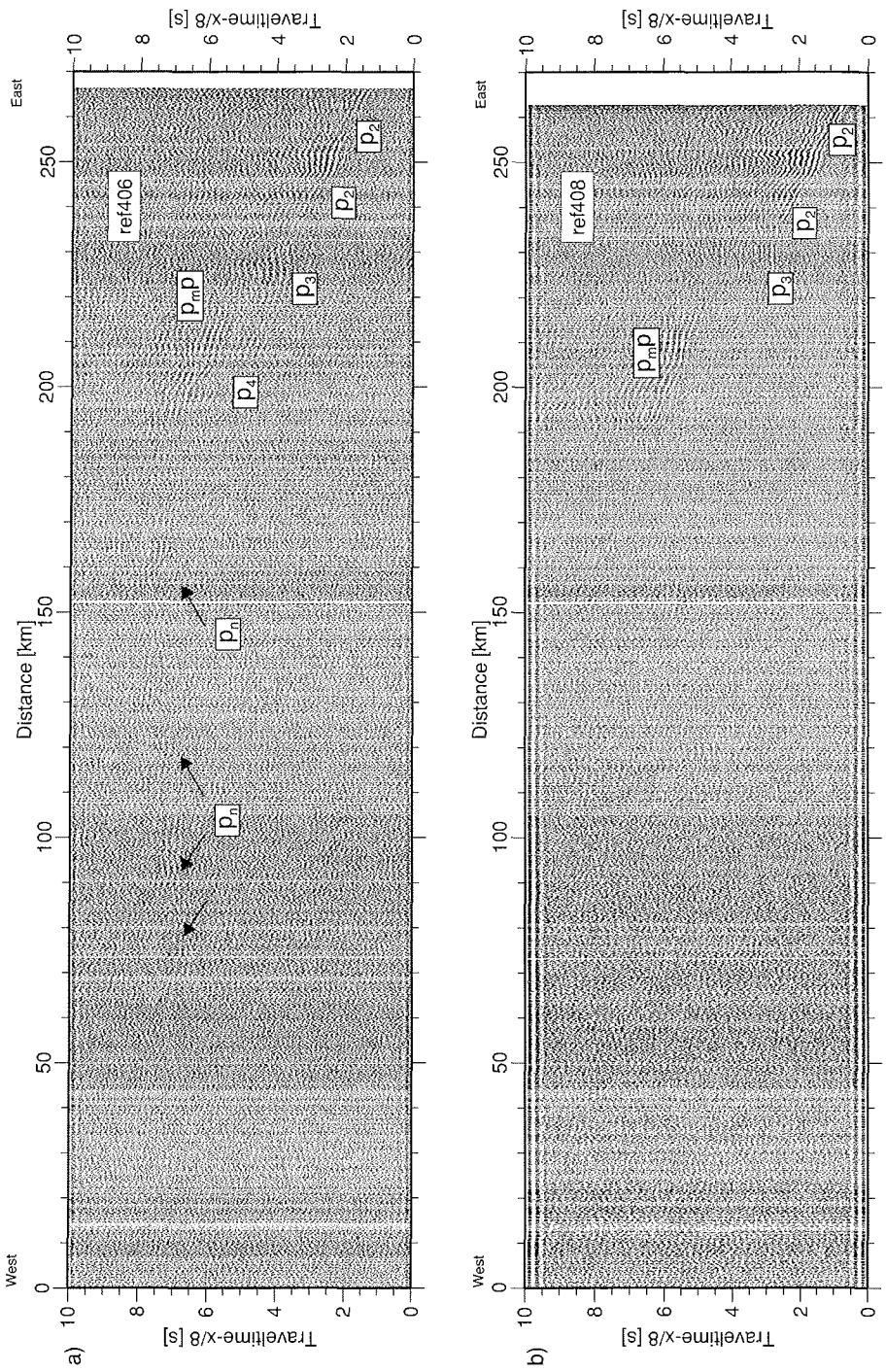

Figure 3-4: Record sections of onshore and offshore receivers.
RefTek seismometer systems (a) ref406 and (b) ref408.

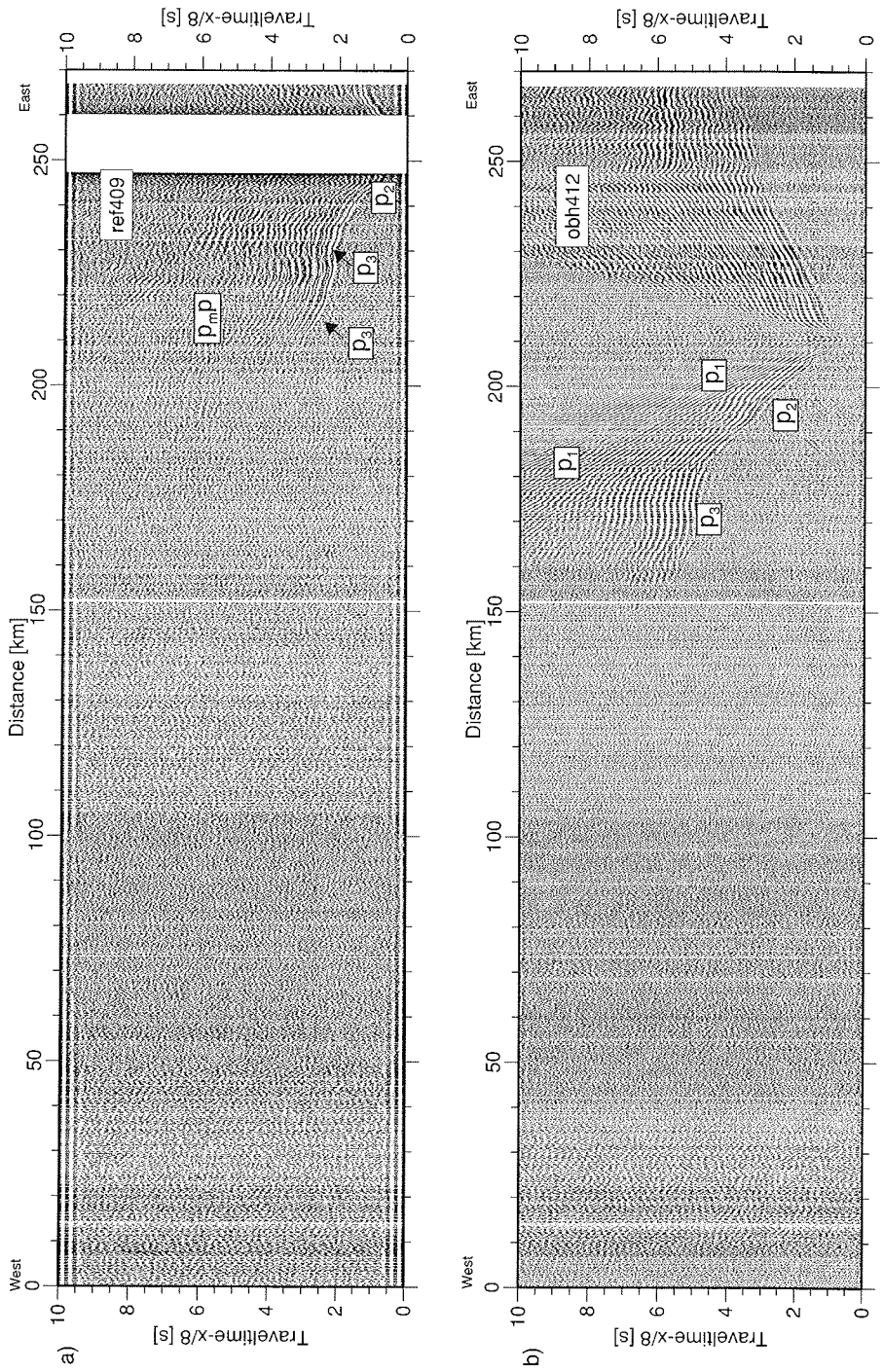

Figure 3-5: Record sections of onshore and offshore receivers.
RefTek seismometer system (a) ref409 and ocean-bottom hydrophone system (b) obh412.

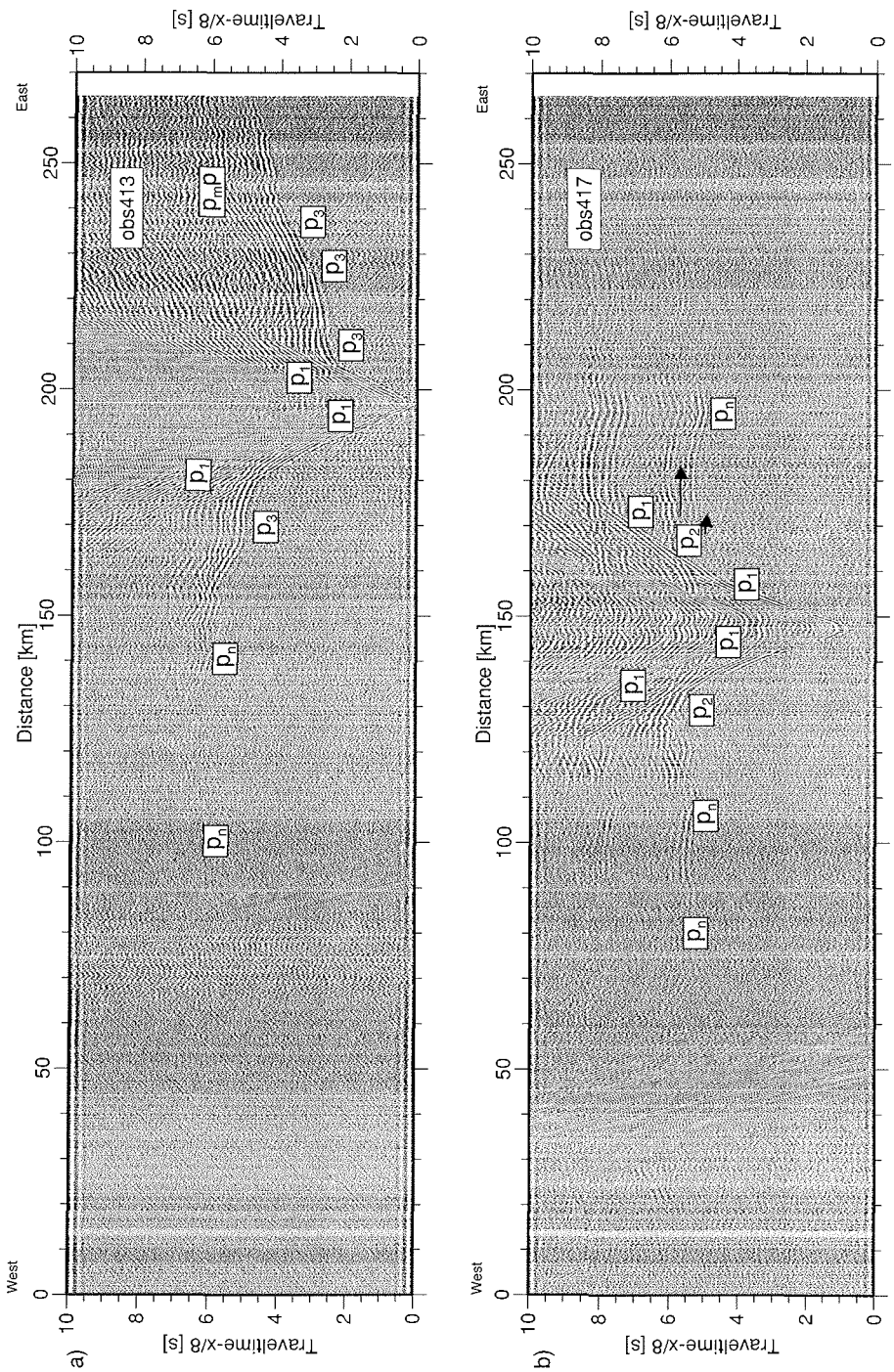

Figure 3-6: Record sections of onshore and offshore receivers.
Ocean-bottom seismometer systems (a) obs413 and (b) obs417.

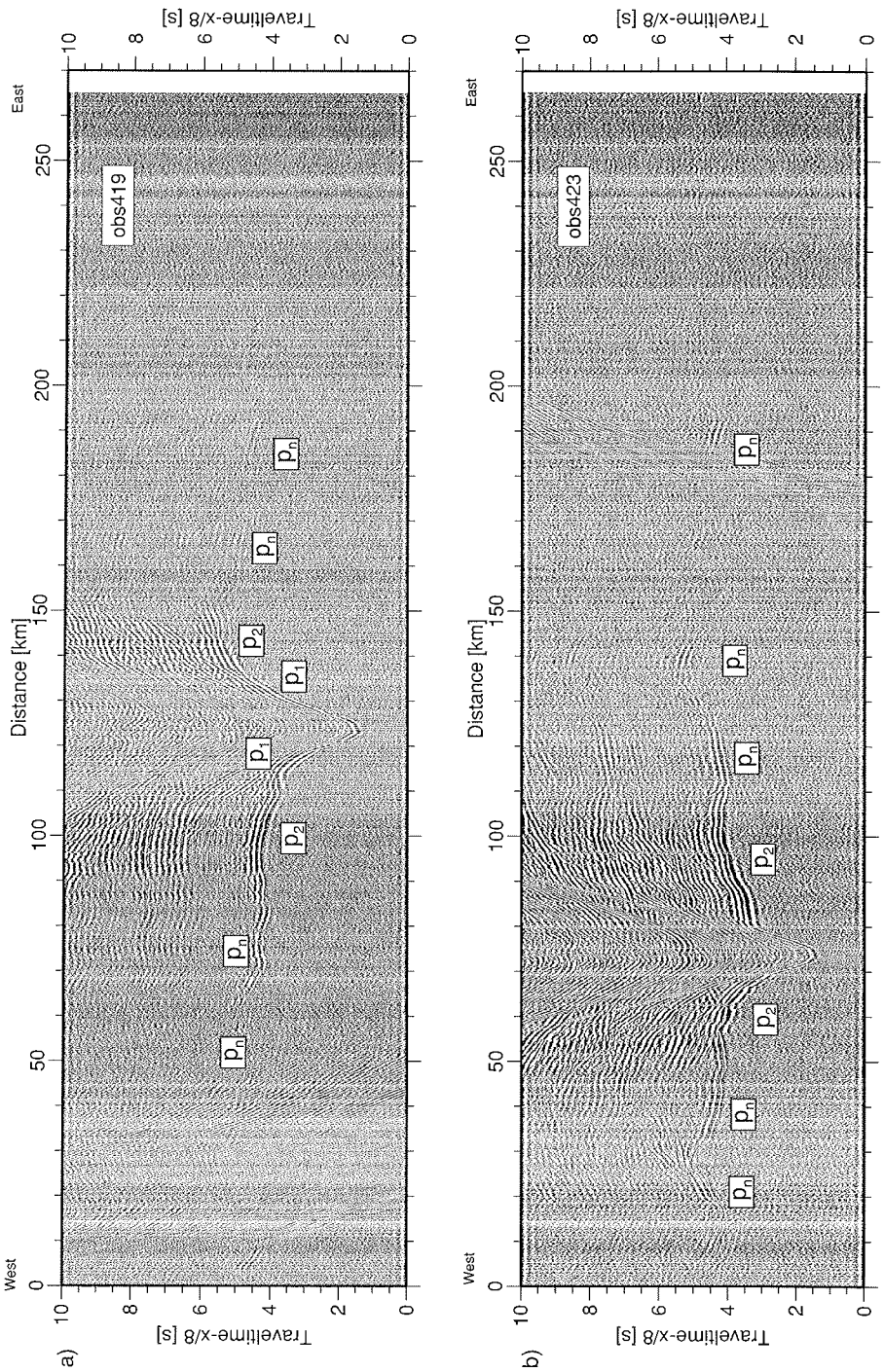

Figure 3-7: Record sections of onshore and offshore receivers.
Ocean-bottom seismometer (a) obs419 and (b) obs423.

First arrivals on seismic sections recorded by receivers east of Kongsfjorden at near distances (20 to 30 km offset) are upper crustal phases penetrating Devonian sedimentary rocks with p-wave velocities of 5.4 to 6.2 km/s (Fig. 3-4a and b; ref406, ref408; p_2). At greater offsets weak p-wave arrivals point to lower velocity gradients in the deeper crust (Fig. 3-4a and b; ref406, ref408; p_3, p_4). Strong p_mp-reflections mark the crust-mantle boundary on several onshore recordings (Fig. 3-4a and b; ref406, ref408; p_mp). At 90 to 100 km offset, mantle refracted arrivals become first arrivals at approximately 7 s traveltime using a reduction velocity of 8 km/s (Fig. 3-4a and b; ref406, ref408; p_n). Recordings from stations near Kongsfjorden (e.g. ref409; Fig. 3-5a) are characterised by $p_{2/3}$-phase undulations, i.e. the increase/decrease of apparent seismic velocity pertaining to lateral velocity variations in the middle crust at km 220 (Fig. 3-5a; ref409; p_3). The same effect is also observed on the reversed sections (e.g. obs413; Fig. 3-6a; p_3). Here, seismic velocities of 7.0 km/s are found at near offsets, while they are lower towards the east (6.0 km/s). Seismic data recorded off Prins Karls Forland provide further reliable velocity information of the Tertiary sedimentary section up to the Molloy Transform Fault (Fig. 3-5b and Fig. 3-6a; obh412, obs413, obs417; p_1) of 2.2 to 3.5 km/s. The seismic structure on both sides of the Molloy Transform Fault (km 120) differs, i.e. to the east crustal p_2-arrivals appear with lower seismic velocity than to west (Fig. 3-7a; obs419; p_2). Further, the arrival times of p_n-phases are up to 2 s delayed suggesting a thicker sedimentary cover and/or a deeper crust-mantle boundary. Mantle phases recorded by more distant stations, e.g. obs423 show characteristic phase undulations at the position of Molloy Transform Fault (Fig. 3-7b; p_n). Seismic velocities of mantle phases at the western edge of the profile are remarkable low and we assume a deepening crust-mantle topography towards the Hovgård Ridge, whose bathymetric expression is well defined by phase undulations of mantle arrivals (Fig. 3-7b; obs423; p_n).

Generally, the observed seismic energy is extremely low for deeper crustal phases at absolute profile distances of 150 to 180 km, i.e. the signal to noise ratio decreases to values below 1. This zone is roughly the northern continuation of the Hornsund Lineament, the supposed continent-ocean transition (Fig. 3-1). It seems that the crust-mantle construction of this transition is responsible for the damping/scattering of seismic energy. Despite this, the seismic velocities for the upper mantle are well resolved due to p_n-phase arrivals observed on either side of this geological complex zone.

3.3.3 2D kinematic raytracing

Modelling of the seismic refraction data was performed using the raytracing software *rayinvr* of Zelt & Smith (1992):

- (i) Traveltimes of reflected and refracted phases were picked on each record section. 1D velocity profiles were calculated and gathered to a 2D section along the profile track.
- (ii) The derived model was used as the initial source for 2D kinematic raytracing using a forward modelling technique. The modelling took place layer by layer and velocity-depth nodes were held constant when the next, deeper layer was modelled. To further enhance the fit of observed traveltimes additional velocity-depth nodes were implemented. Matching the slope and shape of the

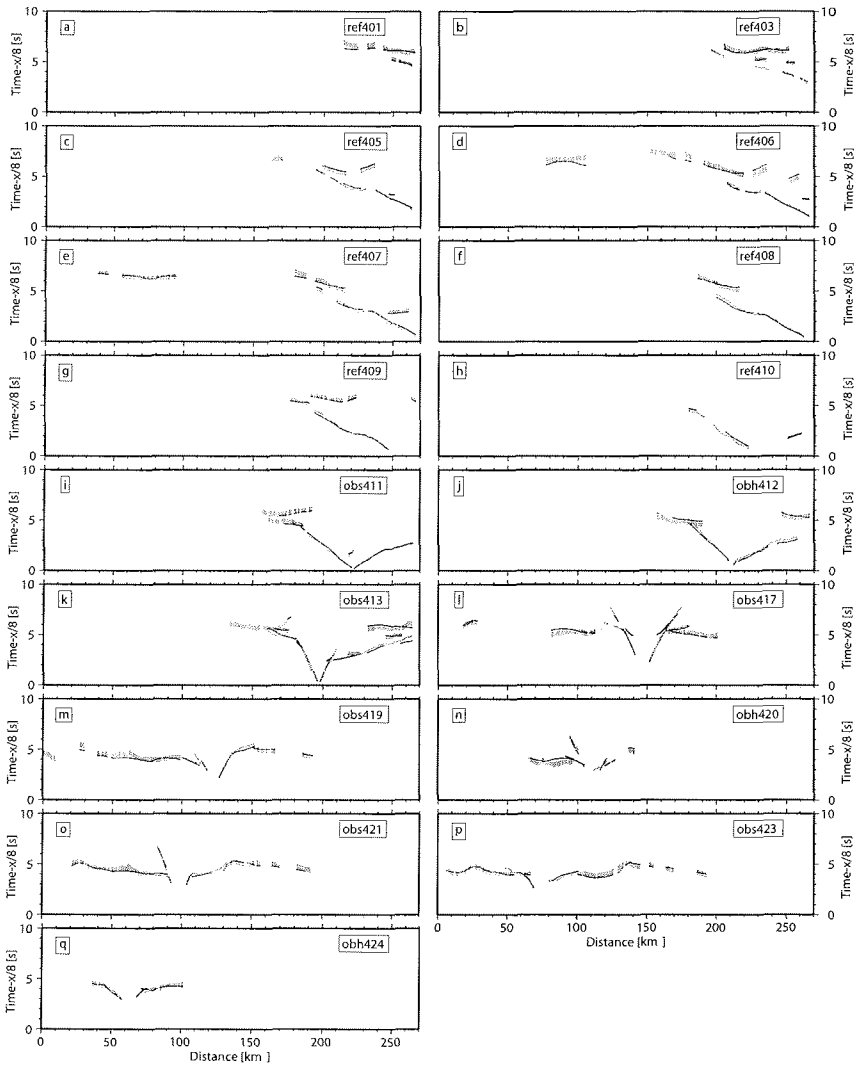

Figure 3-8: Observed and calculated p-wave arrivals for profile AWI-99400.
a-h: RefTek seismometer systems (ref). i-o: ocean-bottom seismometer/hydrophone systems (obs/obh). Grey errors bars indicate the assigned error to the picked traveltimes. The black lines show the travel times calculated using the final velocity model shown in Fig. 3-10 and Fig. 3-11.

observed traveltimes was paid more attention than reducing the rms-traveltime residual calculated by the program *rayinvr*.

- (iii) Once the model provided a reasonable overall fit of observed and calculated traveltimes, traveltimes of phases with poorer quality were calculated. Thus, it was possible to search for additional information on seismic sections, such as low amplitude arrivals due to low velocity gradients. This information was added to the existing traveltime observations. The final set of traveltime picks (in total 2862) are shown in Fig. 3-8 for each of the processed seismic stations. The appropriate ray traces for the modelled layers are shown in Fig. 3-9.
- (iv) Where possible, the final model was improved by two runs of the application of the inversion algorithm of *rayinvr* to enhance the match between calculated and observed traveltimes. This procedure was only possible for profile sections without any steep layer boundaries, i.e. the eastern continental as well as the western oceanic section of the profile, but not at the transitional section between obh412 and obs417 (Fig. 3-1 and 3-3).

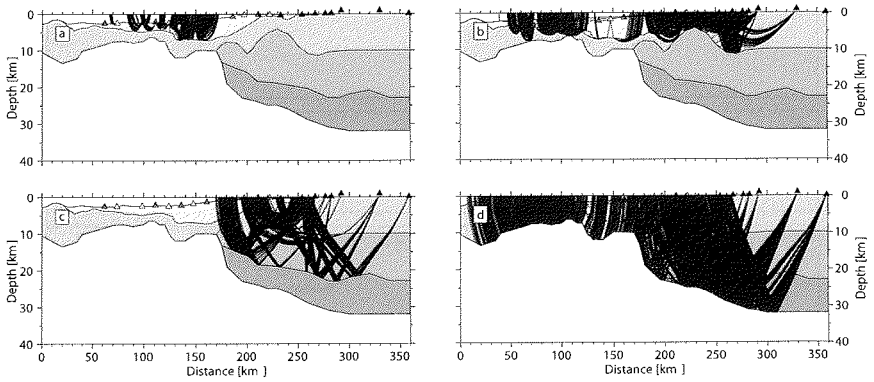

Figure 3-9: Raytracing for profile AWI-99400 for the modelled layers.
(a) Cenozoic sediments and sedimentary rocks. (b) Upper crust. (c) Middle Crust. (d) Lower Crust and Mantle. Vertical exaggeration x3.

3.3.4 The final velocity model

The final modelling result after raytracing is shown in Fig. 3-10 for the sedimentary section between km 20 and 260, and Fig. 3-11 for the entire crustal section. Generally, the oceanic section (km 0 to 180) fits well the observed traveltimes using a one layer-constant gradient model with an overlying sedimentary section. Further east, the observed traveltimes of stations on the continental crust were modelled by a three layer model.

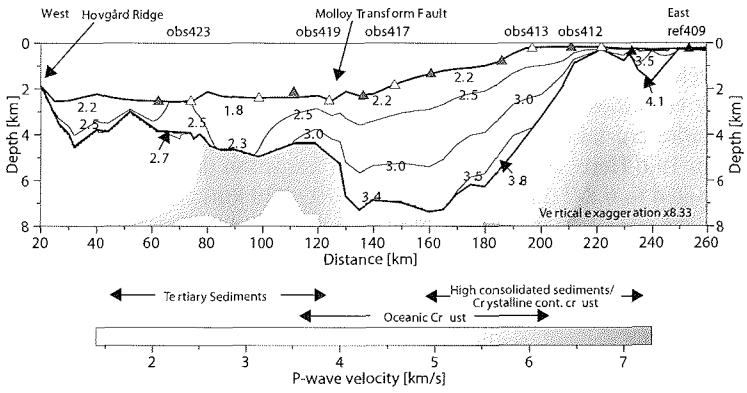

Figure 3-10: Final p-wave velocity model for the sedimentary cover along profile AWI-99400.
The contourlines (2.5, 3.0 and 3.5 km/s) and values shown in the figure indicate seismic p-wave velocity. Triangles as for Fig. 3-1. Vertical exaggeration: x8.33.

Cenozoic sedimentary section

The thickness of the Cenozoic sedimentary cover, which overlays partly oceanic-, transitional and continental crust varies from 1 km (close to the Hovgård Ridge) to approximately 6 km east of the Molloy Transform Fault (Fig. 3-10). Seismic velocities range from 2.2 km/s at the top to 3.8 km/s close to the basement at the continental slope. According to Eiken (1993), Eiken & Hinz (1993) and Geissler (2001) the seismic velocities of the uppermost sequences off northwestern Svalbard are in general lower than observed here (~1.7 km/s). This effect may related to the applied low-frequency energy source for our profile, which limits the vertical resolution. Although it has to be considered that seismic velocities are higher than previously suggested. To the west, sedimentary thickness does not exceed 2.3 km and the seismic velocities of the lower sections are 2.3 to 2.7 km/s at maximum. A remarkable decrease of seismic velocity occurs at km 90, where the upper sedimentary strata show seismic velocities of 1.8 km/s. Sedimentary rocks of the Tertiary Forlandsundet Graben at km 240 (Fig. 3-10) exhibit high velocities of 3.5 to 4.1 km/s, which mark the highest values for Tertiary sedimentary rocks along the entire profile.

Eastern continental section and the continent-ocean transition

The final velocity model of the eastern continental section of profile AWI-99400 consists of three units. The upper unit, with velocities between 5.4 and 6.2 km/s reveals a thickness of 10 km in the east, while it thins to the west to approximately 5 km, over the flanks of an updoming structure beneath the northern Forlandsundet Graben (Fig. 3-11). The underlying unit has a velocity of 6.4 to 6.6 km/s at depths of 20 to 23 km between

km 250 and 360. In the upper parts of a zone of lower velocity beneath Forlandsundet Graben, seismic velocities range between 5.8 and 6.0 km/s. This vertical feature has a width of 20 to 30 km along the profile and a maximum depth of 18 km, where the decreased velocity is 6.4 km/s. The lower unit of the eastern continental section is characterised by velocities of 6.7 to 6.9 km/s and thins slightly westwards from 9 to 5 km. Thus, the entire crustal thickness along the section decreases from 32 km in the east to 14 km at km 190. Here, at the continent-ocean transition (km 180 to 200) velocities are slightly elevated to 6.8-7.2 km/s (at depths of 10 to 20 km) compared to the section east of km 250. The transition itself is marked by a steep and abrupt decrease of Moho depth towards the west.

Western oceanic section and Hovgård Ridge

The crust of the oceanic section of the profile (50 to 180 km) is mostly thin, ranging from approximately 2 km west of Molloy Transform Fault to 4.5 km to the east, underlying a thick portion of Cenozoic sedimentary layers. Seismic velocities east of Molloy Transform Fault range from 5.3-5.4 km/s at the top to 5.5-5.8 km/s at deeper levels. The transform itself marks a transition to higher velocities in the crustal section. West of the transform velocities of 5.8-6.1 km/s are observed for the upper parts, while downwards they increase to approximately 6.3-6.6 km/s at the crust-mantle boundary. At the Hovgård Ridge (km 0 to 40) the crustal thickness increases to 11.5 km. Stations obs423 (Fig. 3-7h) and obh424 give a reliable view of a change in seismic velocities for upper basement at km 80. Velocities are markedly lower west of this point (3.3 to 3.6 km/s). Downwards, velocities increase to approximately 6.0 km/s at the crust-mantle boundary. Since the profile is unreversed west of obh424 (Fig. 3-3) the seismic velocity structure of the Hovgård Ridge remains speculative. West of the stations obs423/obh424 the velocity-depth function was held fixed, merely the basement and crust-mantle topography were altered to fit traveltimes.

Upper mantle

Upper mantle seismic velocities are highest below the eastern continental section of the profile. Velocities of 8.0 to 8.1 km/s are modelled at profile distances of km 190 to 360. Towards the Molloy Transform Fault velocities decrease to 7.9 km/s west of the steep rise of the crust-mantle boundary at km 175. Directly at the Molloy Transform Fault low seismic velocities between 7.6 and 7.7 km/s are modelled (km 65 to 120). Seismic velocities of the upper mantle increase again to 8.0 km/s below Hovgård Ridge.

3.3.5 Resolution and uncertainty of the final velocity model

The resolution of the crustal model presented above was assessed using the inversion method of Zelt & Smith (1992). The relative number of rays which determine the parametrisation of the velocity model (i.e. velocity and boundary nodes) are the principle of this quantitative approach. In this case we calculated only the numerical resolution of velocity nodes, which are counted among certain depths. The uncertainty of the depth levels of the modelled layer boundaries, that are mostly constrained by wide-angle reflections were tested by shifting the depth values of the individual layer boundaries up

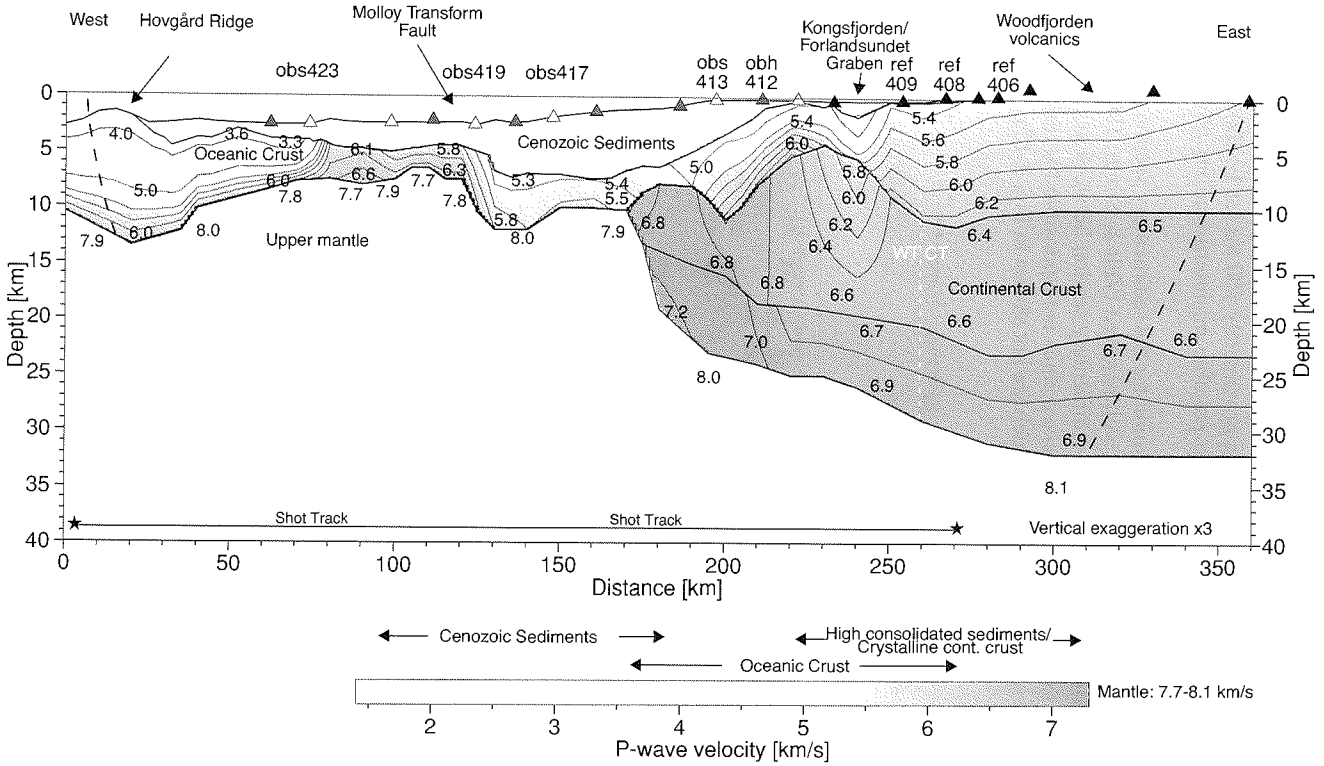

Figure 3-11: Final p-wave velocity model for profile AWI-99400.
The greyshade shows the seismic velocity field, as do the contour lines (4.0 and 5.0 km/s; 5.4-6.8 km/s, 0.2 km/s-interval). Triangles as for Fig. 3-1. The southern and northern maximum extents of penetrating rays are marked by dashed lines. The white dashed line marks the approximately boundary between the western and eastern terrane of Svalbard's Caledonian orogeny. Vertical exaggeration is x3.

and down until the calculated traveltime exceeded the assigned error of the pick. The assigned traveltime errors vary between ±100 and 200 ms, depending on the quality of the phase registration. Therefore this empirical test is strongly dependent on the assigned errors to the picks. Since the wavelength is approximately 100 ms (at 10 Hz) our chosen errors include at least one, but at most two possible misinterpretations of the correct phase location.

Fig. 3-12a summarises the resulting resolution for the sedimentary section. Generally, values greater than 0.5 are considered to be well resolved (Zelt & Smith, 1992). Due to the large number of diving waves the upper sedimentary section between km 100 to 200 is well resolved. To the west the lack of reversed shots is responsible for resolution values near zero for the sedimentary section, which are not shown in Fig. 3-12a.

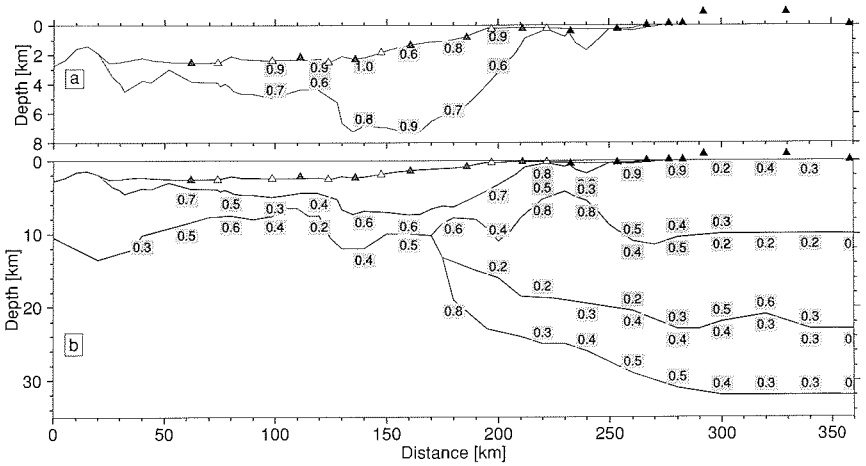

Figure 3-12: Resolution of the p-wave velocity field along profile AWI-99400.
Resolution was calculated according to Zelt & Smith (1992) and resampled to 20 km intervals. Triangles as for Fig. 3-1. The upper figure (a) shows values for the sedimentary section, the lower figure (b) for the residual crust.

The eastern continental section of the profile shows a very uneven lateral and vertical distribution of resolution values (Fig. 3-12b). Km 180-250 of the upper unit are well resolved showing values of 0.7 to 0.9. Downwards and towards the east resolution decreases to 0.2 to 0.4. The same is true for the middle unit (10 to 20 km depth), although the low-velocity zone between km 220 and 250 is well resolved. The lower levels are poorly constrained with values of 0.2 to 0.5. Modelled rays of wide-angle reflections increase the resolution to 0.6 in the middle unit further to the east (km 320). The lower unit above the crust-mantle boundary is better constrained, due to several wide-angle reflections providing good ray coverage. Upper mantle resolution values are approximately 0.8 below the eastern continental profile section but can only be determined west of km 250.

Resolutions for the oceanic crustal section and the upper mantle below are also variable (Fig. 3-12b). Values of 0.3 to 0.7 are calculated for the crustal parts, and are slightly lower in the upper mantle.

Using the empirical method for the determination of depth level uncertainties we found that depth determinations in the top 10 km of the crust have a maximum error of ±0.7 km, if the assigned traveltime errors do not exceed ±100 ms. This results in a maximum error of 10% of the absolute depth level. Downwards the depth uncertainty increases slightly to values of ±0.9 km independent of the assigned errors of ±150 to ±250 ms. Consequently, the mismatch is approximately 6% of the absolute depth levels of 10 to 32 km of the middle and lower crustal levels.

3.3.6 Gravity data acquisition and characteristics

Gravity data were acquired along the shot track by RV Polarstern with the shipboard gravity meter. Processing comprises integration to the International Gravity Standardization Net 1971 (IGSN71) using harbour links at Tromsø (Norway) and Bremerhaven (Germany). Further, an Eotvös correction was applied to obtain the free-air gravity anomaly. Data for the onshore section east of Kongsfjorden was extracted from the free-air anomaly grid of the Svalbard/Greenland region of Boebel (2000) and adjusted to the processed ships gravity.

The anomaly variation along the entire profile is approximately 145 mgal (Fig. 3-13; -65 mgal at km 334; 80 mgal at km 10). Gravity increases towards the west along the onshore section of the profile from -50 to 0 mgal, with some short-wavelength anomalies at km 300 to 360. At approximately km 200 a gravity maximum of 60 mgal is observed forming a 40 km wide anomaly. Gravity decreases continuously towards Molloy Transform Fault at km 140. The oceanic crustal section to the west is characterised by a plateau with gentle undulations. The Hovgård Ridge at the western edge of the profile terminates the gravity record by a strong, 75 mgal positive anomaly peak.

3.3.7 Gravity modelling

The p-wave velocity model presented above was gridded and transformed into an initial density model using the non-linear velocity-density regression of Christensen & Mooney (1995). This relation includes mantle rocks, such as dunite and pyroxenite and is therefore suitable for crust-mantle studies. Subsequently, blocks were digitised within an interval of 0.05 g/cm^3. Rock densities for the sedimentary cover were set to 2.10 and 2.40 g/cm^3, the mantle density is uniform 3.3 g/cm^3. The potential field data interpretation software LCT was used to model free-air gravity.

Initial model A

Fig. 3-13 shows the calculated density model as described above. It is obvious that the model does not fit the observed gravity field:

- (i) There is a -50 mgal misfit along the mostly unstretched continental section of the profile.
- (ii) There is a +50 mgal misfit at km 200 and

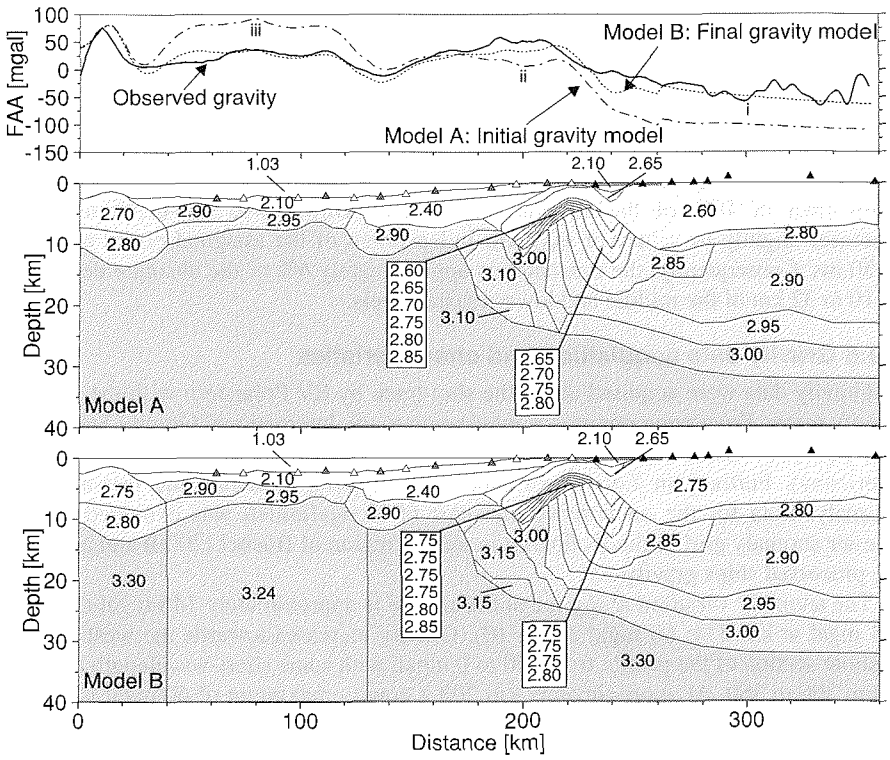

Figure 3-13: Initial (model A) and final (model B) density models for profile AWI-99400.
The observed free-air anomaly is marked by a thick solid line in the upper graph. The derived free-air anomaly from model A is marked by a dashed-dotted line, from model B by a dotted line. For calculation of densities and modelling parameters see text. Triangles as for Fig. 3-1.

- (iii) there is a 60 mgal misfit over the region between the Hovgård Ridge and Molloy Transform Fault.

Final model B

We applied the following modifications to the density model to eliminate these misfits (Fig. 3-13):

- (i) Raising density of the upper part of the eastern continental section to 2.75 g/cm^3. This is consistent with density measurements on field rock samples published by Kurinin (1970) and Howells et al. (1977). Kurinin (1970) report on mean group densities of 2.68 to 2.72 g/cm^3 for Devonian sedimentary and metamorphic rocks. Howells et al. (1977) defined formation densities of 2.72 to 2.76 g/cm^3 for Pre-Devonian to Devonian rocks of northern Svalbard.

- (ii) Further west, densities of the zone of slightly increased seismic velocities (Fig. 3-13; km 200) are raised to 3.15 g/cm^3.
- (iii) Between Hovgård Ridge and Molloy Transform Fault the mantle density of 3.30 g/cm^3 was decreased to 3.24 g/cm^3, to produce a downward shift of calculated gravity values by approximately 60 mgal. Low mantle densities of 3.26 g/cm^3 are also suggested for the Northern Atlantic Senja Margin (Fig. 3-2; Breivik et al., 1999) by modelling the thermal structure of the lithosphere. Below Hovgård Ridge the mantle density of 3.30 g/cm^3 remains unchanged since the gravity calculation using model A fits the observed field well.

3.3.8 The final density model

The final density model B (Fig. 3-13) gives further constraint to the modelled velocity structure. The crustal density variations of model B compared to the initial model A, imply velocities that are within the given uncertainties of the final velocity model and the non-linear regression of Christensen & Mooney (1995). The negative shift in mantle density of approximately 0.1 g/cm^3 below the oceanic crustal section is consistent with the relatively low observed seismic velocities of 7.7-7.8 km/s in the upper mantle. The high densities of 3.15 g/cm^3 within the middle crust at km 200 may point to an underestimation of the seismic velocity of 7.2 km/s at this location. The recalculation of the seismic velocity from the modelled density derives values of 7.4 km/s, which is slightly higher than the estimated velocity uncertainty for this depth level.

3.4 Interpretation and discussion

For further discussion and interpretation of the velocity- and density structure the profile AWI-99400 is split into four individual sections:

- (1) The Cenozoic sedimentary cover from km 20 to 245, which overlays continental, transitional and oceanic crust.
- (2) The eastern continental section east of km 200, which covers parts of the western and central terrane of the Svalbard Archipelago. It is mainly characterised by a 8 km thick Paleozoic sedimentary basin, known from geological record (Fig. 3-1).
- (3) The transition to the oceanic domain to the west, that features a steep Moho uplift of 15 km, a zone of slightly elevated seismic velocities and a pronounced density anomaly.
- (4) The oceanic section of the profile west of km 170, which is subdivided into two sub-regions by the Molloy Transform Fault at km 120. The interpretation of the different sections is summarised in Fig. 3-14.

3.4.1 The Cenozoic sedimentary cover east of Molloy Transform Fault

Seismic reflection data published by Eiken & Hinz (1993) and Eiken (1993) shows three sedimentary sequences (YP-1 to YP-3; Fig. 3-14) for northwestern Svalbard and the adjacent Yermak Plateau. Geissler (2001) attributed sonobuoy-derived seismic velocities to the individual sequences. The seismic velocities are defined as follows: 3.2 to

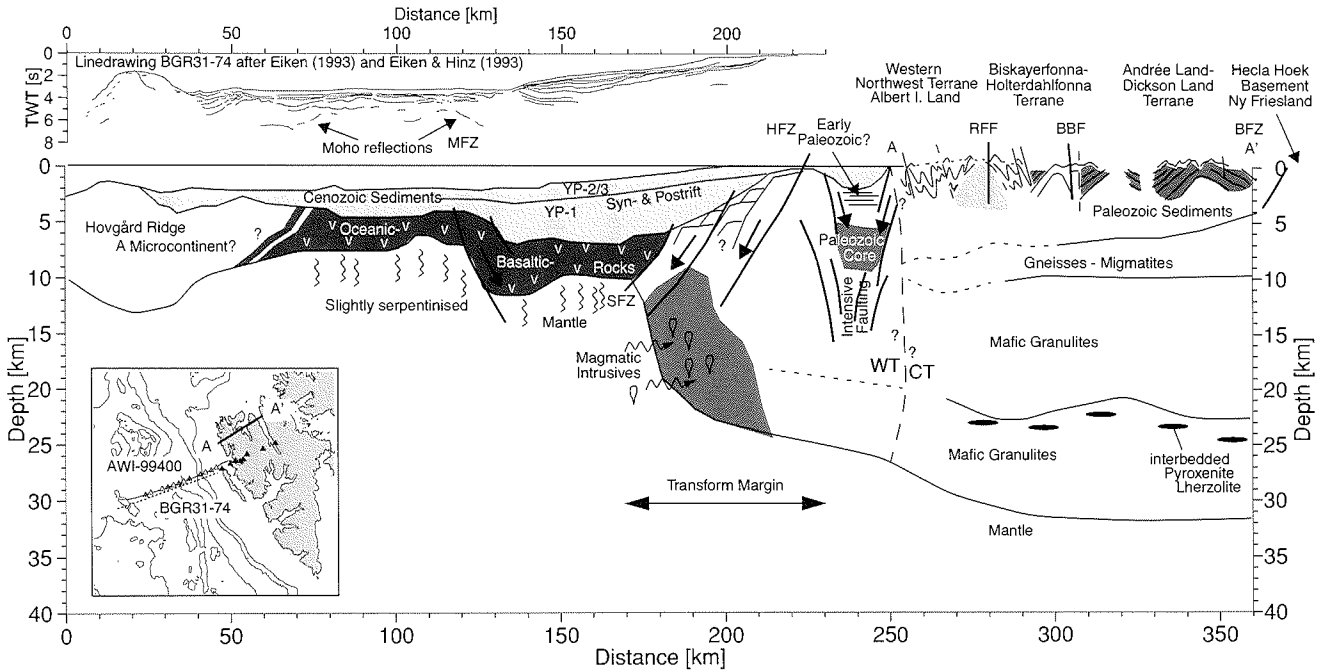

Figure 3-14: Geological interpretation of the velocity model along profile AWI-99400.
For the oceanic crustal section a line drawing of multichannel line BGR31-74 (Eiken, 1993; Eiken & Hinz, 1993) is shown. See insert map for location (dotted line). Note that the steep Moho topography at the Molloy Transform Fault was imaged on the multichannel transect. The eastern continental section also shows a geological cross section for northwestern Svalbard (A-A'; after Hjelle & Lauritzen, 1982). The geological profile is marked on the insert map by a thick black line. Generally, continental crust is coloured white, oceanic dark grey. The mid-grey colour indicates Paleozoic sedimentary rocks. The crosshatch pattern marks the zone along the sheared margin that is intruded, as characterised by higher seismic velocities (up to 7.2 km/s). The vertical dashed line at km 250 marks approximately the boundary between the western and central terrane of Svalbard (WT/CT). HFZ: Hornsund Lineament. RFF: Raudfjorden Fault. BBF: Breibogen Fault. BFZ: Billefjorden Fault. MFZ: Molloy Fracture Zone.

4.2 km/s for YP-1 (lower), 1.9 to 2.4 km/s for YP-2 (middle) and 1.7 to 1.8 km/s for YP-3 (upper). A comparable velocity structure is also found for the lower sequences in the northern Barents Sea (Myhre & Eldholm, 1988; ESP1-5; 3.2 to 4.3 km/s, 1.9 to 3.2 km/s), so that a regional trend can be deduced. The observed seismic velocities along profile AWI-99400 suggest that our data indicate the presence of sequences YP-1 and YP-2. Henceforward, we will take 2.4 km/s to mark the approximate boundary between YP-1 and YP-2. The applied low-frequency airgun source obviously limits only the vertical resolution for the shallowest and thin sequence, YP-3.

Eiken (1993) suggests a Late Oligocene (36 Ma) to Late Miocene (7 Ma) age for YP-1. The youngest strata of YP-2 are supposed to be Early Quarternary. Our data thus show more than 4 km of YP-1 strata west of the Molloy Transform Fault (Fig. 3-1). According to the estimated age, this sequence comprises syn- and post-rift sediments and sedimentary rocks. The work of Steel et al. (1985) indicates, that Early to Middle Paleocene clastics were deposited on either side of the uplifting West Spitsbergen Fold Belt during transtensional movements. Therefore, the lower parts of YP-1 may comprise Paleocene strata.

3.4.2 The eastern continental section

This profile section covers the western and the central terrane of Svalbard. Station ref409 (Fig. 3-1 and Fig. 3-3) is approximately located at the bounding Kongsfjorden-Hansbreen Fault Zone.

Central terrane (km 250 to 360)

Geological cross-sections of the central terrane cut through several basement provinces (or sub-terranes), i.e. the Western NW Terrane of Albert I. Land to the west of the Raudfjorden Fault Zone, the Biskayerfonna-Holterdahlfonna Terrane west of Breibogen Fault Zone and the Andrée Land-Dickson Land Terrane west of Billefjorden Fault Zone (Fig. 3-1 and Fig. 3-14; Hjelle & Lauritzen, 1982). Although the lithology of each terrane is extremely varied, this is not reflected in the observed velocity structure. The modelled seismic velocity is distributed uniformly in the upper crust, with only slight changes suggesting the presence of the metamorphic rocks of Albert I. Land and the Hecla Hoek province east of Billefjorden Fault Zone.

We suggest the lower sequences of the Devonian Basin (Fig. 3-1) are located at depths of 4 to 7 km following the 6.1 km/s-isocontour, the maximum seismic velocity observed for Paleozoic strata of the Svalbard-Greenland depositional realm (e.g. Jackson, 1990; Hajnal et al., 1990; Schlindwein & Jokat, 1999).

In petrological models of the deeper structure of Svalbard's central terrane (more precisely the basement province east of the Breibogen Fault Zone; Fig. 3-1; Amundsen et al., 1987), the crust is built up of three rock units, regionally overlain by Paleozoic sedimentary rocks. The proposed rock types are (i) gneisses, (ii) granulites and (iii) granulites with small amounts of interbedded pyroxenite/lherzolite. The latter unit is not associated to large igneous intrusives related to mantle plume activity, since new seismic refraction data from the Yermak Plateau indicate the probable non-existence of the Yermak Hot Spot (Ritzmann & Jokat, 2003; see chapter 2). The rock units (i) to (iii) were

related to velocities of (i) 6.1 to 6.3 km/s, (ii) 6.4 to 6.6 km/s and (iii) 6.7 to 6.8 km/s, respectively (Chan & Mitchell, 1982). Our results for the central terrane reinforce these models. Granulitic rocks are therefore supposed at depths between 10 and 22 km. Similar seismic velocities (6.1 km/s) for the upper crystalline layer are reported for the Isfjorden region 100 km further south (Sellevoll et al., 1991). The reflective horizon at 22 km depth indicates that lower crustal interbedded material possibly raise up to a certain depth level, probably defined by uniform p-T conditions or the brittle/ductile transition. A transitional crust-mantle boundary below Svalbard as suggested by Sellevoll et al. (1991) and Czuba et al. (1999) can not be confirmed for the northern region (velocities between 7.35 and 7.8 km/s). Instead our seismic model shows a first-order crust-mantle transition (Fig. 3-11 and Fig. 3-14).

Western terrane (km 210 to 250)

The western terrane (Fig. 3-1) is characterised by an abrupt decrease of seismic velocity and rock density to depths of 20 km directly below the Forlandsundet Graben (Fig. 3-11) within the Tertiary Western Spitsbergen Orogenic Belt (Fig. 3-2). The Caledonian geological suture between the central and western terranes at km 255 (Harland & Wright, 1979) is not obviously evident in our model. The Tertiary break-up of Svalbard and northern Greenland is supposed to have mainly involved strike-slip movements along the Hornsund Lineament since Oligocene times (Eldholm et al., 1987). This lineament is located to the west of the Prins Karls Forland and therefore west of the zone of altered seismic velocities within continental crust. Instead tectonic processes associated with the Forlandsundet Graben seem to have had a stronger effect on the seismic structure of the majority of the crust (Fig. 3-11).

The western Svalbard margin underwent compression and/or transpression during Paleocene and Eocene times, resulting in the Western Spitsbergen Orogenic Belt (e.g. Steel et al., 1985). Nevertheless there is evidence, that initial subsidence of the Forlandsundet Graben took place during the main interval of mainly transpressive movements. A strike-slip/pull-apart character for the Forlandsundet Graben is mentioned by several authors, although the specific dating of compressive and transtensional phases is still under debate (e.g. Lepvrier & Geyssant, 1985; Steel et al., 1985, Harland, 1997e). A further tectonic model for the graben formation suggests extension in the lee of a wrench fault curvature controlled by resistant landmasses in northeastern Svalbard (Steel et al., 1985). A general model for the entire West Spitsbergen Fold Belt was proposed by Lowell (1972). Within a convergent strike-slip zone crustal sheets were thrusted up to result in a typical "flower structure". Later, the Forlandsundet Graben developed possibly as a collapse graben along the axis of the main fold belt (Steel et al., 1985). This kind of tectonic requires an intensively faulted, deep axial root zone along the graben location with possible deep seated mylonitic rocks. Whatever model is suggested, deep penetrating faults can be supposed to extend below the Forlandsundet, due to the general strike-slip character. Hence, the low seismic velocities might result from extensively fractured formations in deep reaching faults on either side of the graben and below. Since the total crustal thickness wanes by approximately 4 km along this section (km 220 to 250), it

seems that this brittle zone was extended during later transtensional movements, further decreasing the seismic velocity. Moreover it seems that tectonic processes related to the location of Forlandsundet Graben result in the general decoupling of western from the central Svalbard, leaving behind a stable interior of Svalbard. The deeper roots of the Western Spitsbergen Orogenic Belt are lying in close proximity to the Caledonian suture (i.e. Kongsfjorden-Hansbreen Fault Zone) which leads to the assumption that possibly Tertiary movements reactivated older shear zones.

In addition to a tectonic cause, the anomalous low seismic velocities below 6.0 km/s might represent Paleozoic sedimentary rocks as in the upper crust of the central terrane. Accordingly, any narrow sedimentary trough would be downfaulted approximately 4 km, i.e. the throw of the Forlandsundet Graben (Eiken & Austegard, 1987). Deeper seated Paleozoic rocks were also found below the Oligocene Danskøya Basin (Fig. 3-1; Eiken, 1993) approximately 120 km further north (Ritzmann & Jokat, 2003; see section 2.6.2). In a similar way, at the Forlandsundet Graben a 5 km Tertiary sequences might cover deeper Paleozoic rocks, within a probable transtensional graben setting. The preservation of Devonian sedimentary rocks within the Tertiary Fold Belt is also observed onshore in the region of the Hornsund (Fig. 3-1; e.g. Steel et al., 1985).

In summary, we interpret the upper/middle crust below Forlandsundet Graben to consist of both downfaulted Paleozoic sedimentary strata and deeper brittle-fractured crystalline rocks due to intensive fault tectonics.

Further west, off Prins Karls Forland, the profile crosses the Hornsund Lineament (Eiken, 1993). Like the Caledonian suture (at km 255) the deeper trend of the Hornsund Lineament is not clearly visible. It may follow the isovelocity contour of the upper crystalline layer, in a westward dipping (listric?) manner. Published seismic reflection data (Eiken & Austegard, 1987; Eiken, 1993) show that the lineament consists of two separate blocks at Sjubrebanken north of Prins Karls Forland. Our deep seismic data off Kongsfjorden do not define the internal structure of the lineament. The absence of stepwise deepening of the upper basement below the shelf sedimentary rocks may point to a more uniform structure here. The striking manifestation of the Forlandsundet Graben compared to the absence of striking features for the Hornsund Lineament suggests that the two structures have separate, and rather different tectonic histories.

3.4.3 The continent-ocean transition

The continent-ocean transition along profile AWI-99400 is characterised by a rapid change in Moho depth on the eastern continental section which gives way to thin oceanic crust at km 170. This transition is characterised by the highest seismic velocities found for continental crust along the profile (7.2 km/s). This observation is further constrained by the seismic structure of the margin 100 km further north (profile AWI-99200; Czuba et al., in prep.). Here, the most westerly continental section exhibits seismic velocities of 7.3 to 7.35 km/s within a broad continent-ocean transition[1]. The maximum steepness of the Moho along profile AWI-99400 is achieved directly east of the transition, where the Moho dips at high angles of 45° from 10 to 20 km depth. The rapid decrease of Moho

depth at the continent-ocean transition may be characteristic of sheared or transform continental margins. At such margins, complex rifting occurs along a continental transform fault, followed by the development of an active transform boundary separating oceanic from continental crust. Later the ridge passes the continental section and the transform becomes inactive apart from differential subsidence (Lorenzo, 1997). It was supposed that oblique shear controlled the evolution of the western Svalbard margin prior to chron 13 (Oligocene) and changed to oblique extension afterwards during the rifting process (Faleide et al., 1991). The new seismic velocity model indicates that the western margin of Svalbard is segmented on this basis, with both sheared and obliquely-extended crustal sections alternating along the margin.

The continent-ocean transform off northern Prins Karls Forland formed due to the action of the Spitsbergen Fracture Zone north of the Molloy Ridge (Fig. 3-1 and Fig. 3-2). The southeasterly trend of the fracture zone towards Prins Karls Forland dictates therefore the orientation of the continent ocean-transition off northwestern Svalbard (Fig. 3-15).

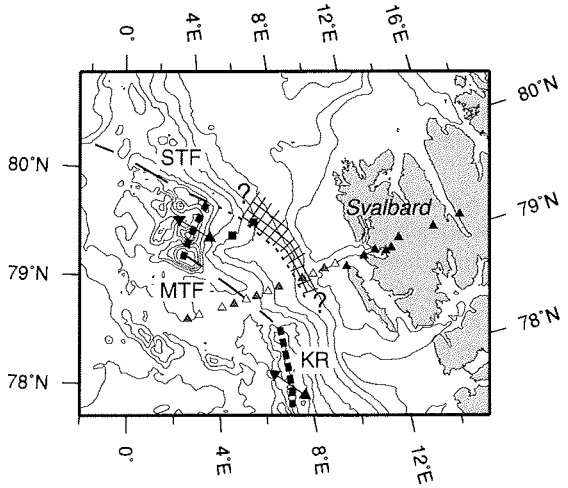

Figure 3-15: Map of the proposed southeastern extension of the Spitsbergen Transform Fault/Fracture Zone.
The cross-hatch pattern marks the location of higher seismic velocities within observed continental crust (derived from this study and Czuba et al., in prep.). Thick dotted lines are spreading ridges, and long dashed lines are the respective transform faults between. KR: Knipovich Ridge. MTF: Molloy Transform Fault. STF: Spitsbergen Transform Fault. Triangles as for Fig. 3-1. Bathymetry: IBCAO (Jakobsson et al., 2000).

[1]Note, that these high seismic velocities were modelled by the cooperating working group of the Polish Academy of Science (Czuba et al., in prep.). Chapter 5 of this thesis gives a secondary, independent interpretation of profile AWI-99200. Here, the broad continent-ocean transition is confirmed, whereas seismic velocities within the lower crust do not exceed 7.0 km/s.

The crustal structure of sheared margins constrained by seismic refraction experiments is well known from the Côte d'Ivoire-Ghana margin (Edwards et al., 1997) and the eastern Canada margins (Reid, 1988; Todd et al., 1988; Reid & Jackson, 1997), off Queen Charlotte Island (Horn et al., 1984), the Exmouth Plateau (Lorenzo et al., 1991) and the nearby Senja-Barents Sea margin (Faleide et al., 1991).

The Côte d'Ivoire-Ghana margin shows a similar extreme topography of the Moho to that observed along profile AWI-99400. The other margins are characterised by a broader, 30-60 km wide transition zone. Comparing the velocity structure of these margins, high seismic velocities are common directly at the continent-ocean transition. In the case of the Côte d'Ivoire-Ghana margin, oceanic and continental crust are separated by a high seismic velocity unit (5.8 to 7.3 km/s). The cause of these velocities is ambiguous, the interfacing body is either interpreted as tectonically emplaced lower crustal/mantle rocks or heavily intruded basic igneous rocks (Edwards et al., 1997). Intrusions might occur in the presence of a slight transtensional stress component making the ancient transform slightly leaky. The nearby Senja margin (Eldholm et al., 1987) exhibits such leaky behaviour since volcanic activity and similar high seismic velocities are found within the crust (7.1 km/s).

Horn et al. (1984) modelled a 20 km wide body (5.5 to 7.4 km/s) at the transition of Queen Charlotte margin as sheared basalts and gabbros. This body extends down to depths of 17 km, shows a deepening lower edge towards the continent, and is similar to that found along our profile. Unfortunately, it is uncertain whether the Queen Charlotte Margin body has a continental or oceanic character (Horn et al., 1984).

In summary, we deduce that the sheared margin off Prins Karls Forland differs from those reported above, since an altered high velocity section of continental crust is observed (Fig. 3-11; km 170-300). A significant amount of mantle derived melts may contaminate the lower and middle crust at the transition, raising the velocity here. According to Lorenzo et al. (1991) the large temperature contrast over juvenile transform margins might result in convection-induced secondary melting of the upper mantle (referring to Mutter et al., 1988). This may lead to intrusions during the passage of the ridge segment and/or hot oceanic crust. Further, the melt supply might occur by a simple ridge-continental crust interaction during transit of the hot Molloy Ridge along sheared continental crust. The melt fraction distribution with depth can be lowered at slow spreading ridges (White et al., 1992; White et al., 2001) compared to normal spreading rates, which might force the emplacement of melts into the lower parts of the crust below 10 km.

3.4.4 The western oceanic section and Hovgård Ridge

Oceanic crust (km 45 to 170)

The profile covers two ancient oceanic crustal sections, on each side of the Molloy Transform Fault (Fig. 3-1). The section to the east was formed at the Molloy Ridge spreading segment, while that to the west is formed at the Knipovich Ridge. An age prediction of the surveyed crustal sections is difficult, since detailed magnetic data are missing. Recently published magnetic data of Oakey et al. (1998) reveals no regular

spreading anomalies for the northern Knipovich Ridge and Molloy Ridge. Using the synthetic flowlines of Eldholm et al. (1990) chron 5 (~9.5 Ma) should occur ~70 km off the Knipovich Ridge at 77°N (based on Talwani & Eldholm, 1977). Our profile AWI-99400 obliquely intersects the Molloy Transform Fault (130 km length; Crane et al., 2001) roughly half way between the two ridge-transform intersections. The surveyed crustal sections are 70 to 100 km off the axes of the spreading centres. We therefore conclude that the age ranges roughly between 10 and 15 Ma (Middle Miocene), keeping in mind that Crane et al. (1991) mentioned the possibility of extremely asymmetric spreading rates at the Knipovich Ridge.

The absence of seismic velocities higher than 6.6 km/s is very prominent and reflects the absence of oceanic layer 3 along the profile. Further, this excludes a serpentinisation front to the Moho (Minshull et al., 1998). Velocities vary between 5.3 and 6.6 km/s on either side of the Molloy Transform Fault and total thicknesses of the igneous portion range between 2 and 4.5 km. This is thin compared to the global mean of approximately 7.1 km, based on seismic experiments (White et al., 1992).

After White et al. (2001) crustal thicknesses of mid-ocean ridges decrease sharply for spreading rates below 20 mm/a. They conclude that conductive heat loss is the most important factor inhibiting melt production. According to the observations of Bown & White (1994) crustal thinning is dedicated to the thinning of oceanic layer 3. Since the Knipovich and Molloy Ridges are characterised by slow spreading rates of ~8 mm/a (Eldholm et al., 1990) the correlation between spreading rate and layer 3-thickness (or absence) is confirmed by our study. The observed crustal thicknesses are in good agreement with those derived by rare earth element inversion (for the Knipovich Ridge) of 2.77 to 4.9 km of White et al. (2001). Further, our derived crustal structure is comparable to that of Klingelhöfer et al. (2000) parallel to the Mohns Ridge at 72°N (Fig. 3-2). Thicknesses vary around 4 km and the absence, or at least the thinning of layer 3 is supposed to be the reason. It should be noted that the upper basement velocities of layer 2 at the Mohns Ridge are lower than observed along profile AWI-99400 (2.5 to 3.0 km/s).

The formation of thin oceanic crust is not restricted to slow spreading ridge processes. It is reported that thinned oceanic crust adjacent to the continent-ocean transition is a common feature of non-volcanic rifted margins which developed over tens of millions of years and are sometimes characterised by a 100 to 200 km wide extensional zone (e.g. western Iberia margin; Whitmarsh et al., 1993; Whitmarsh et al., 2001). Long-lived extension and in direct vicinity of cooler crust are supposed to enhance conductive cooling of the ascending mantle. As a consequence, less melt is generated compared to simple adiabatic decompression. Additional new seismic refraction lines in northwestern Svalbard show conditions which promote conductive cooling:

- (i) A rifted-volcanic margin history for the western Svalbard/Greenland break-up and a hotter asthenosphere (Jackson et al., 1984; Vågnes & Amundsen, 1993) can be excluded (Ritzmann & Jokat, 2003; see chapter 2).

- (ii) Relatively cool continental crust extents up to 7°E off northern Svalbard and builds therefore a shielding block around oceanic crust (Fig. 11; Czuba et al., in prep.; see also chapter 5).
- (iii) Earliest movements between Svalbard and Greenland started probably in the Earliest Paleocene (Håkansson & Stemmerik, 1984) while actual seafloor spreading took place ~30 Ma later (s.a.).

It seems therefore plausible that both the slow spreading regime and long-lived rifting of cool continental margins enhance heat loss of the ascending mantle, resulting in the very thin crust and the absence of layer 3.

The differing seismic velocities for the oceanic layer 2 on either sides of the Molloy Transform Fault remains problematic. One explanation could be that this is simply the result of different ages of the crust. However, the difference in age is estimated as just 1 Ma at maximum. If this difference accounts enough to induce this strong velocity variation remains very doubtful. The seismic structure of the oceanic crust may also be a function of tectonics or thermal diffusion effects related to the proximity of the Molloy Transform Fault. The possibility of a different petrology may be a further point of discussion, which will not further debated here.

Molloy Transform Fault (km 130)

The Molloy Transform Fault is characterised by an unusual steep asymmetric topography of the crust-mantle boundary and by an increase of seismic velocity from east to west. Oceanic layer 3 is absent. According to studies of transform faults in the North Atlantic (Detrick et al., 1993; note that the authors commonly use the term *fracture zones* for transform faults **and** fracture zones) the lack of layer 3-velocities (or higher) within the crust is typical for transform faults with a large offset (> 100 km; here: Knipovich to Molloy Ridge: ~130 km).

A common feature of transform faults in the North Atlantic (Detrick et al., 1993; Charlie-Gibbs, Vema) is the broad symmetrical upwarping of the Moho below the valley and accompanying transverse ridges on both sides. In contrast, the Molloy Transform Fault exhibits a pronounced asymmetric structure. A comparison with seismic reflection data of Eiken & Hinz (1993) and Eiken (1993) shows that the steep topography of the sub-sedimentary crust was already known (Fig. 3-14; linedrawing). But arrivals were interpreted as intra-basement reflections assuming a deeper crust-mantle boundary. This study shows that crust at the Molloy Transform Fault is thinner than previously expected. Regarding the basement topography across the transform it seems likely that the transform itself acts as a hinge for differential subsidence of the flanking oceanic sections. This may be have been enhanced by the different sedimentary load. On the eastern side accumulated sediments and sedimentary rocks may amplify the subsidence of the oceanic crust, probably due to the vicinity of continental Svalbard. Normal faulting of the region between the Molloy Transform Fault and the Hovgård Ridge is evidenced by Eiken's (1993; including Baturin, 1990) compilation of seismic lines off western Svalbard, which was attributed to moderate extension after formation of igneous crust. Crane et al. (2001) suggest that fault traces imaged north of the Molloy Transform Fault are due

to rifting of the Knipovich Ridge that has propagated north beyond the rift-transform intersection in geologically recent times. For the location of Molloy Transform Fault both interpretations have to be upgraded and basement subsidence has to be considered to play a substantial role in fault development. A sedimentary sequence of more than 4 km thickness is observed at the transform fault, which is supposed to thicken towards north (Vestnesa; Eiken, 1993; Fig. 3-1). Therefore we suppose basement subsidence along the entire transform fault.

Further constraint on an northeastward dipping normal fault complex might be given by the work of Okay & Crane (1993). They propose a dipping detachment from the Spitsbergen Transform Fault underneath the Yermak Plateau, which was initiated by simple shear tectonic break-up and later asymmetric spreading. Hence, the trend of the normal faulting at Molloy Transform Fault might be a stress relict from the initial break-up.

Hovgård Ridge (km 0 to 45)

Due to the limited data background the structure and interpretation of Hovgård Ridge is speculative. The relatively low seismic velocities at the upper crustal level give rise to the assumption that the shallow ridge is built up of thickened oceanic crust or higher consolidated sedimentary rocks are present. But a thick layer 3 (as is typical for thickened plateau-like oceanic crust) with higher seismic velocities (> 7.2 km/s) cannot be confirmed. Myhre et al. (1982) supposed the ridge to be a microcontinent rifted off Svalbard since 36 Ma. The reconstruction of Eldholm et al. (1987) indicates a stepwise opening of the Greenland Sea and shows the separation of the continental Hovgård Ridge fragment from Svalbard-Greenland prior to actual spreading at the northern Knipovich Ridge and Molloy Ridge. Low velocities of the deeper ridge result possibly from a strong tectonised structure due to the extreme extension during the detachment from Svalbard-Greenland. Our seismic refraction data are strongly ambiguous, therefore the nature of the Hovgård Ridge remains unexplored.

Upper mantle

Upper mantle velocities along the oceanic section of the profile are lower than along the continental section of Svalbard (8.0 to 8.1 km/s; see also Ritzmann & Jokat, 2003), which possibly points to a change in petrology. This is further supported by lower densities, at least for the region to the west of Molloy Transform Fault. The lowering of mantle seismic velocities may result from a slight serpentinisation of upper mantle peridotites. After Minshull et al. (1998) thin oceanic crust, slow spreading ridges and fracture zones all favour serpentinisation by providing faulted pathways for seawater to penetrate the upper mantle. And in the fact lowest seismic velocities are found below the Molloy Transform Fault. Further fractures and faults associated with the Hovgård Ridge, the Hovgård Fracture Zone (Myhre et al., 1982) and the transform margin might provide additional pathways to mantle levels. According to Christensen (1966) ~20% serpentinisation is required to reduce seismic velocity to 7.1-7.6 km/s, whereas the latter is the lowest velocity observed. As the velocity distribution is not homogeneous we expect different degrees of serpentinisation. Observed seismic velocities for the upper mantle at the Mohns Ridge are similarly low and attributed to serpentinisation as reported by Klingelhöfer et al. (2000).

3.5 The development of the continental margin off Kongsfjorden: A regional view

Our seismic refraction profile crosses the continental margin of Svalbard at 79°N. Here, we summarise the discussion given above, by reference to a schematic model of the Tertiary evolution of the Kongsfjorden margin (Fig. 3-16a-c):

During the Paleocene West Spitsbergen Orogeny intensive transpressive shear affected most of the crust (Fig. 3-16a). From our modelled velocity structure it is not possible to distinguish between multiple suggested models concerning its details. However, it is widely accepted that a first phase of subsidence took place prior to the Post-Oligocene transtensional configuration (e.g. Steel et al., 1985). The intensive transpressive shear led most probable to the weakening of the brittle upper crust. Interestingly, the West Spitsbergen Orogeny was located east of the Hornsund Lineament, although other major faults, such as the Trolle Land Fracture Zone and the Hornsund Lineament were present early in the Paleocene (Fig. 3-16a; Eldholm et al., 1987). The deeper roots of the orogeny are located adjacent to the Caledonian suture between Svalbard's western and central terranes, although our velocity model can not show the suture. (Fig. 3-11). Probably, it is not possible to distinguish between the Caledonian suture and the Tertiary orogen since both structures are located close together (Fig. 3-1 and Fig. 3-2). Possibly the old Caledonian suture was reactivated for the Tertiary orogenic movements.

Since Oligocene times the stress pattern changed to transtension, and major crustal thinning occurred west of the Forlandsundet Graben region (mostly within Svalbard's western terrane). Extension was mostly decoupled from inner Svalbard (i.e. the central terrane; Fig. 3-16b), possibly due to the proximity of the weak Caledonian suture and the deeper Forlandsundet Graben (relax phase). The Forlandsundet Graben subsided by about 5 km, burying Devonian sedimentary rocks beneath the Tertiary cover. Seismic reflection surveys show that the Hornsund Lineament off northwestern Svalbard is characterised by two crustal blocks, which indicate transtensional rift movement. As northeastern Greenland and Svalbard separated from each other, the juvenile Spitsbergen Transform Fault developed within the rift as an intracontinental transform. We suppose a slight oblique strike of the young transform to the Hornsund Lineament (Fig. 3-16b). The wedge-shaped continental fragment to the northeast was intensively stretched, so that a zone of crustal thinning is observed off Svalbard's most northern margin (Czuba et al., in prep.; see also chapter 5).

Spreading at mid-ocean ridges migrated successively towards the north during the Miocene (Crane et al., 1991; Fig. 3-16c). Disregarding the exact onset of spreading at the Knipovich and Molloy Ridges, Svalbard's northern margin off Kongsfjorden was an active transform fault bordering a narrow oceanic basin. Since the sedimentary thickness in the Molloy Ridge basin is a multiple compared to that in the southerly Knipovich Ridge basin, a higher sedimentation rate is expected in the north. Possibly the narrow Molloy Ridge basin was bordered to the east and west by a sheared continental margin, assuming that the northern continuation of the Molloy Transform Fault plays a similar role as the Spitsbergen Transform Fault did on the Svalbard margin (Fig. 3-16c). It seems

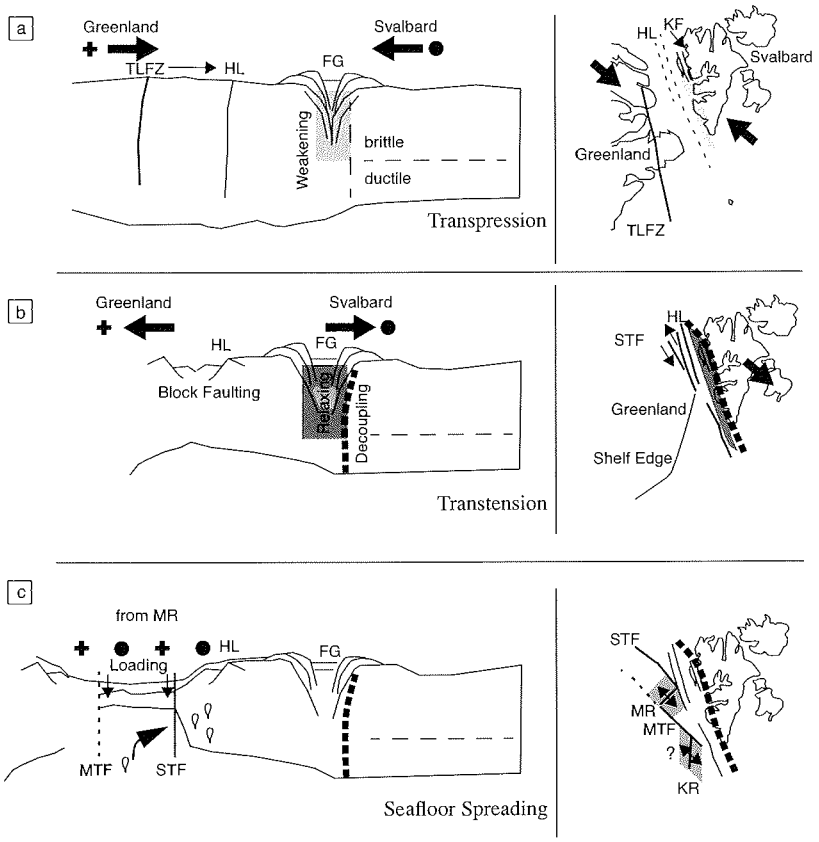

Figure 3-16: Schematic evolution of the continental margin off Kongsfjorden derived from the interpretation of seismic refraction profile AWI-99400.

(a) Early Paleocene: The Trolle Land Fracture Zone (TLFZ) was an active transform between Svalbard and Greenland. A transpressional regime dominated (grey) and resulted in the West Spitsbergen Fold Belt. Nevertheless first subsidence of the Forlandsundet Graben (FG) is achieved. Intensive shearing weakened the upper brittle part of the crust. Until the Oligocene the major transform migrated further east. Note that Crane et al. (1991) term this broad shear region the Spitsbergen Shear Zone, including the present-day Hornsund Fault and Bjørnøya-Sørkapp Fault. The vertical dotted line indicates approximately the boundary between the central and the western terrane. (b) Oligocene: Transpression was replaced by transtension, and the major fault system was located at the Hornsund Lineament (HL). Stress was taken off the Forlandsundet region, and thinning occurred to the west, decoupled from central Svalbard. At the HL oblique rifting and block faulting led to further thinning. The Spitsbergen Transform Fault (STF) developed as an intracontinental transform sub-parallel to the HL. (c) Miocene: Spreading started at the Molloy Ridge (MR), and the continental margin was sheared off the parts of the oceanic province on the Greenland plate. Sedimentation from central Svalbard increased loading on the Molloy Ridge crustal segment, and therefore subsidence. The sedimentation rate in the juvenile Molloy Ridge oceanic basin was higher than at the northern Knipovich Ridge (KR). As a consequence, the Molloy transform (MTF) started to act in a hinge-like fashion. Note that the onset of spreading at Knipovich Ridge probably occurred earlier than at Molloy Ridge. Kongsfjorden (KF).

possible, that this transform developed parallel to the Spitsbergen intracontinental transform fault forming a mirrored Greenland conjugate margin.

3.6 Conclusions

The seismic refraction profile off Kongsfjorden (Svalbard) provides a detailed seismic velocity structure of a sheared continental margin. It also gives new information concerning the geology of central Svalbard and the development and evolution of the northwestern continental margin of Eurasia. The sheared margin off Kongsfjorden is further slightly influenced by magmatic activity. Svalbard's western continental margin seems to be higher segmented as expected. Between Prins Karls Forland and the northern coast of Svalbard, the margin is part of the Spitsbergen Fracture Zone.

Our main results are:

- (1) The seismic velocity structure does not resolve Caledonian crustal blocks. Late Paleozoic sedimentary rocks are modelled with a thickness of up to 7 km and additional Paleozoic sedimentary rocks occur below the Forlandsundet Graben. These rock units can be associated with those of Svalbard's central terrane and the lithology found by Amundsen et al. (1987).
- (2) The crustal structure of the upper 20 km below Forlandsundet Graben exhibits low seismic velocities, interpreted as due to intensive brittle faulting during the Early Paleocene transpressional movements between Svalbard and Greenland. Later, this weak zone may have decoupled central Svalbard from the western parts, restricting crustal thinning to the western terrane. Since this structure is located adjacent to the (sinistral) Caledonian suture between the western and central terrane, (dextral) Tertiary movements may reactivated the Paleozoic shear zone.
- (3) The continent-ocean transition can be classified as a sheared margin, with the Spitsbergen Transform Fault/Spitsbergen Fracture Zone as the trace of the fault. A steep increase (45°) in Moho depth of more than 10 km is observed at the transition Seismic velocities at the transition are the highest observed (7.2 km/s) along the entire continental section. We attribute this to magmatic intrusions during the early break-up process in the Fram Strait.
- (4) The oceanic crust adjacent to the continent-ocean transition is thin, ranging between 2 and 4 km. The observed seismic velocities indicate the absence of oceanic layer 3. We attribute the thinning to decreased partial melting due to conductive heat loss at the Molloy- and Knipovich Ridges. The proximity of cool continental crust might have further enhanced conductive cooling. More than 4 km thick sedimentary sequences are observed at the Molloy Ridge crustal segment, compared with only 2 km in the Knipovich Ridge segment. We suggest differential loading leads to a hinge-like behaviour and normal faulting at of the Molloy Transform Fault.
- (5) The occurrence of a transform margin off Kongsfjorden directly adjacent to a rifted segment ~100 km further north (Czuba et al., in prep.) leads to the assumption that the western margin of Svalbard and the Yermak Plateau is more segmented than previously expected.

CHAPTER 4:
CRUSTAL STRUCTURE BETWEEN THE KNIPOVICH RIDGE AND THE VAN MIJENFJORDEN (SVALBARD)

Oliver Ritzmann[1], Wilfried Jokat[1], Rolf Mjelde[2] & Hideki Shimamura[3]

[1] Alfred Wegener Institute for Polar and Marine Research, Bremerhaven, Germany
[2] Institute of Solid Earth Physics, University of Bergen, Bergen, Norway
[3] Institute of Seismology and Volcanology, Hokkaido University, Sapporo, Japan

Submitted to Marine Geophysical Researches, Kluwer Academic Publishers Netherlands, January 2003

4.1 Abstract

The Alfred Wegener Institute of Polar and Marine Research, the University of Bergen and the Hokkaido University acquired new seismic refraction data along a transect from the Knipovich Ridge to the inner Van Mijenfjorden in southern Svalbard. A close spacing of on- and offshore receivers and a dense marine shot pattern provide the data for a high resolution p-wave velocity model for geological interpretation. Additional new seismic reflection data (University of Bergen) yield structural information for a more reliable analysis.

Crustal thickness along the Van Mijenfjorden is 33 to 34 km. Seismic velocities of 5.0 km/s are observed within the upper crustal section of the Tertiary Central Spitsbergen Basin. A Paleozoic sedimentary basin with a depth of 8 to 10 km is associated with the Nordfjorden Block. The seismic velocities are up to 6.0 km/s. Paleozoic sedimentary rocks are expected further to the west of the Hornsund Lineament since seismic velocities reveal a similar range here. West of the Bellsund the continental crust thins gradually over a 90 km wide rifted zone. The velocity structure within this section is very complex and comprises zones of decreased velocities below the West Spitsbergen Fold Belt (down to 20 km depth) and slightly elevated velocities (7.2 km/s) at the crust-mantle transition. The first structure is interpreted as intensively fractured rocks linked to Post-Late Paleocene transpressive orogenic activity and subsequently affected by transtension during break-up from Greenland. The faster deep crustal velocities are supposed to express intrusions formed by magmatic interaction of the northern Knipovich Ridge with the neighbouring young rifted crust during the Miocene.

Oceanic crust on each side of the Knipovich Ridge is thin (~3.5 km) and is characterised by the absence of oceanic layer 3 (3.5/4.1 to 4.7 km/s). The oceanic section exhibits zones of very thin crust (~1 km) that are interpreted as fracture zones. Beneath these we observed decreased mantle velocities (~7.3 km/s) indicating probable serpentinisation of peridotites along these fracture zones. Thickness variations further provide information about the segmentation and magma supply along the northern Knipovich Ridge.

4.2 Introduction

The crustal structure of the interior of the Svalbard Archipelago, its western continental margin, the neighbouring oceanic province and the Knipovich Ridge have been investigated by e.g. Guterch et al. (1978), Sellevoll et al. (1991), Myhre & Eldholm (1988) and Faleide et al. (1991). In these studies the lateral resolution of velocities in the seismic refraction data is too limited to provide a detailed image across the continental margin of western Svalbard. Due to this, detailed knowledge about Svalbard's crustal structure and evolution is rather limited.

In 1997 the Alfred Wegener Institute of Polar- and Marine Research (Germany) carried out a seismic refraction experiment in the region of the Knipovich Ridge, Bellsund and Van Mijenfjorden (AWI-97260; Jokat et al., 1998). A close spacing of on- and offshore receivers and a dense shot pattern yield the detailed velocity structure of Svalbard's Caledonian terrane configuration (Harland & Wright, 1979), the West Spitsbergen Fold Belt (Steel et al., 1985) and the continent-ocean boundary along the Hornsund Lineament (Myhre & Eldholm, 1988; Eiken & Austegard, 1987).

During the OBS98 survey by the University of Bergen (Norway) and Hokkaido University (Japan) profile AWI-97260 was extended along the Knipovich Ridge in order to provide a complete transect for further analysis of possible interaction between the mid-ocean ridge and young rifted crust during break-up (profile 9, Mjelde et al., 1998). The data base was completed by the acquisition of seismic reflection data by the University of Bergen in 1999 on a parallel line across the oceanic crustal section and the outer continent-ocean transition (profile 7; Mjelde & Johansen, 1999). Airborne gravity data of (Boebel, 2000) is used to further constrain the interpretation of newly derived seismic data.

4.2.1 Geological and geophysical setting

The Svalbard Archipelago is situated at the northwestern corner of the Eurasian continent and is separated from northeastern Greenland by the Fram Strait (Fig. 4-1). Svalbard itself has been suggested to consist of three basement terranes that amalgamated in the Devonian. These terranes are bounded by sinistral transform faults, the Kongsfjorden-Hansbreen Fault Zone and Billefjorden Fault Zone (Harland & Wright, 1979; Fig. 4-1). A rival interpretation insists that Svalbard is built up of a unique basement province (Manby & Lyberis, 1992). Northern Svalbard is widely covered by Devonian sedimentary rocks (Fig. 4-1) that dip below the Late Paleozoic/Mesozoic and Cenozoic cover in southern Svalbard (Nordfjorden Block, Isfjorden; Johannessen & Steel, 1992; Nøttvedt et al., 1993). The western coastal province south of Kongsfjorden mainly comprises the West Spitsbergen Fold Belt which formed during Late Paleocene to Mid-Eocene transpression (Steel et al., 1985; Harland, 1997e). Sediments derived from the orogen accumulated on either side of the belt and are preserved onshore in the Tertiary Central Spitsbergen Basin (Harland, 1997e) and offshore as shown by seismic reflection surveys (Schlüter & Hinz, 1978). During the early, mainly transpressive movements of the orogeny elongated basins such as the Forlandsundet Graben (Gabrielsen et al., 1992) and the Bellsund Graben (Eiken & Austegard, 1987) subsided in the centre of the belt. Both

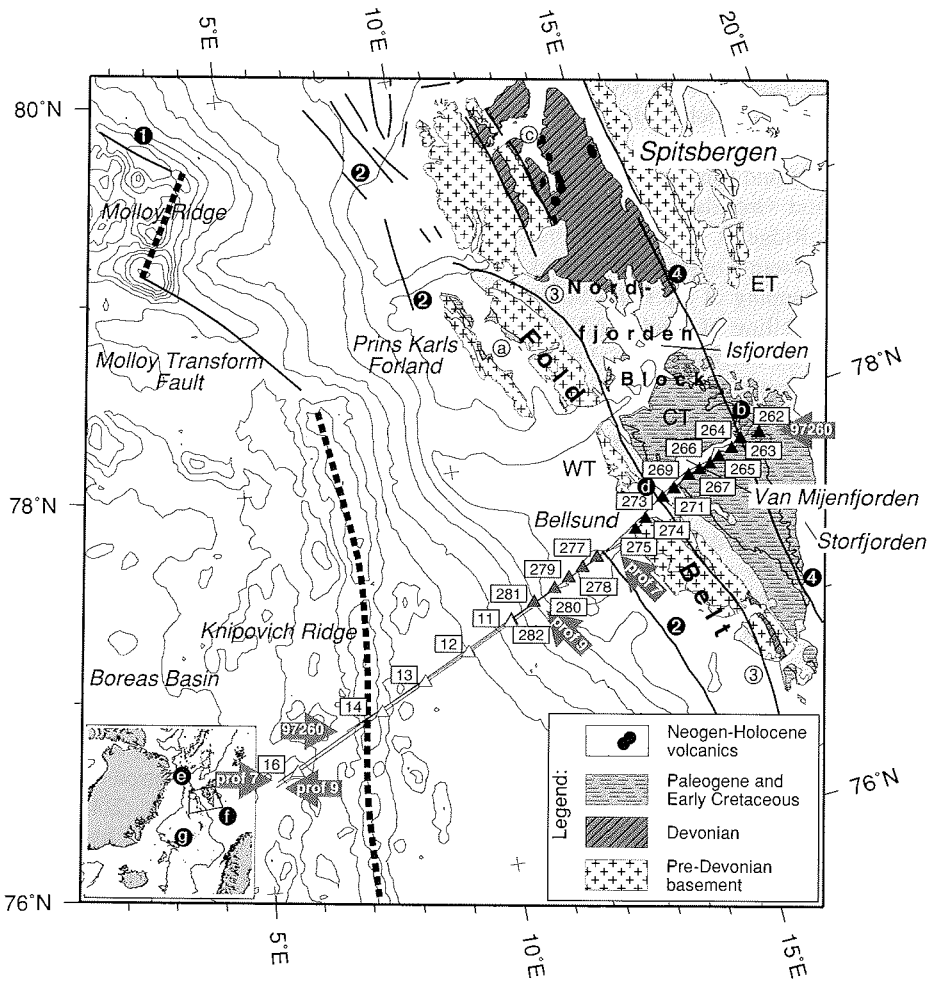

Figure 4-1: Location of seismic refraction profiles AWI-97260 and profile 9 and seismic reflection profile 7.

Grey thick arrows mark the western and eastern start and end of the profiles. The profile tracks are marked by thin black lines, RefTek-stations (black), obh-stations (grey) and obs-stations (white) by triangles with the respective station numbers in squares. Simplified geology after Harland (1997a). Thick black lines are major faults: (1) Spitsbergen Transform Fault, (2) Hornsund Lineament, (3) Kongsfjorden-Hansbreen Fault Zone, (4) Billefjorden Fault Zone. Spreading ridges are marked by a thick dotted line. Geographic locations used in the text: (a) Forlandsundet, (b) Heer Land, (c) Woodfjorden, (d) Akseløya, (e) Fram Strait, (f) Barents Sea, (g) Mohns Ridge. Western-, central- and eastern terranes (WT, CT and ET). Plate boundary after Boebel (2000). Bathymetry: IBCAO (500 m-contour interval + 200 m-contour; Jakobsson et al., 2000).

resemble pull-apart structures, but their exact geological history is still under debate (Steel et al., 1985; Harland, 1997e).

After the initial opening of the Norwegian-Greenland Sea in the Early Paleocene the mid-oceanic ridge system propagated northward along the Spitsbergen Shear Zone, forming the Knipovich Ridge (Eldholm et al., 1987; Crane et al., 1991). Since the Mid-Oligocene transpressive movements dominated along the western Svalbard margin and the Hornsund Lineament is supposed to have been the active fault system between Svalbard and Greenland (Eldholm et al., 1987; Eiken, 1993). Spreading along the Knipovich Ridge is slow (0.8 cm/a, half rate) and possibly extremely asymmetric: favouring accretion to the eastern flank (Eldholm et al., 1990; Crane et al., 1991). Recent structural mapping of the Fram Strait using airborne gravity data and subsequent plate tectonic modelling of Boebel (2000) assume the onset of spreading at Molloy Ridge occurred in the Early Miocene. Further north within the Fram Strait spreading started in the Early Pliocene.

4.2.2 Previous deep seismic investigations

Deep seismic investigations of the Svalbard Archipelago started in 1976 (Guterch, 1978; Sellevoll et al., 1991). All experiments are characterised by few onshore seismic receivers and a widely spaced (~10 km) offshore shot pattern. Unfortunately, these experiments were not able to resolve a detailed lateral velocity structure. Similar data were acquired on later surveys (Sellevoll et al., 1991; Czuba et al., 1999) and further expanding spread profiles were carried out (Myhre & Eldholm, 1988; Faleide et al., 1991).

A crustal thickness of ~36 km is expected below central Svalbard (Sellevoll et al., 1991). A seismic transect from Storfjorden and Van Mijenfjorden to Isfjorden (Fig. 4-1) indicates a ~3 km thick transitional layer above the Moho (7.8 km/s). Crustal thickness decreases towards the outer fjords to 26-27 km (Forlandsundet) where stretched continental crust is supposed. This was recently confirmed by Ritzmann & Jokat (2003; chapter 2). The continent-ocean boundary off western Svalbard is determined by seismic reflection profiles only (Hornsund Lineament; Myhre & Eldholm, 1988; Eiken, 1994). Additional constraints on the crustal structure off Isfjorden are given by gravity modelling (Myhre & Eldholm, 1988; Sundvor & Austegard, 1990) which generally confirms the continental crustal character of western Svalbard.

Petrological constraints on the crustal composition of Svalbard come from mantle derived xenoliths found in the Woodfjorden (Amundsen et al., 1987; Fig. 4-1) that reveal a good correlation to the simple velocity structure published by Chan & Mitchell (1982). The northern central terrane (Harland & Wright, 1979) consists of a gneissic structure (~6.2 km/s) down to 16 km depth that is partly overlaid by Paleozoic/Mesozoic sedimentary/metasedimentary rocks. The mafic granulites below (~6.4 km/s) are supposed to be intruded by mantle derived lherzolites within the lower 5 km (6.8 km/s; Amundsen et al., 1987).

4.3 New geophysical data

The data along the deep seismic transect off Van Mijenfjorden were collected during three cruises of the research vessels *RV Polarstern* (Germany) and *RV Håkon Mosby* (Norway) in 1997, 1998 and 1999 (Jokat et al., 1998; Mjelde et al., 1998; Mjelde & Johansen, 1999).

4.3.1 Seismic refraction data - Acquisition

Seismic refraction data was acquired during the cruise leg ARK13/3 of *RV Polarstern* (profile AWI-97260) using 7 offshore ocean-bottom hydrophone systems (one failed; 13.3°E-10.8°E) and 15 onshore RefTek seismometer stations (14.0°E-17.3°E). Each of the onshore receivers was equipped with an array of at least 18 geophones (vertical component registrations). Eight of the RefTek seismometer stations were connected to a geophone array ~500 m away from the main station. Thus, in total 23 record sections from the onshore stations were achieved. A total number of 1595 shots used an array of three large-volume airguns with a total charge of 152 l (Fig. 4-1; 6.8°E-16.7°E). The shot track extends from the valley of the Knipovich Ridge to the eastern part of the Van Mijenfjorden. Velocity modelling for this study was performed using data from all offshore stations and a selection of 11 stations onshore, so that the receiver spacing varies from 10-16 km (offshore) and from 6-15 km (onshore).

Profile AWI-97260 was extended in 1998 during cruise OBS-98 of *RV Håkon Mosby* (profile 9; Fig. 4-1) using 6 ocean-bottom seismometer devices (one failed; 3-component; 5.5°E-10.7°E). Profile 9 comprises 873 shots fired from 5.2°E-11.3°E using a four-airgun array with a total charge of ~79 l. The receiver spacing is ~30 km along profile 9 with one larger gap of 50 km.

The overall length of seismic refraction transects AWI-97260 and profile 9 is about 340 km extending from the southeastern Boreas Basin to western Heer Land in southern Svalbard (Fig. 4-1). Elevation varies along the profiles from -3250 m to 700 m.

4.3.2 Seismic refraction data - Processing and Characteristics

Prior to analysis seismic refraction data was processed with a bandpass filter passing frequencies of 5 to 17 Hz. A better amplitude equalisation of large offset arrivals was reached using a 1 s-automatic gain control (agc). Generally, onshore seismic data within the Van Mijenfjorden is characterised by strong amplitude reverberations, most likely due to short-wavelength water column multiples on a glacial compacted seafloor (Fig. 4-2a and b). Noise is further expected from strong side-reflections within the fjord and peg-leg type travelpaths within the sedimentary section (bottom simulating reflectors; Posewang & Mienert, 1999). Along profile 9 signal enhancement by predictive deconvolution of obs-data was performed. Here, the wave train is also characterised by strong multiples/reverberations running parallel to the first arrivals (Fig. 4-3a). The operator length was set to 170 ms, and a gap length of 10 ms was determined to give best results. The filter operation was applied to the entire trace lengths. Fig. 4-3b clearly indicates the

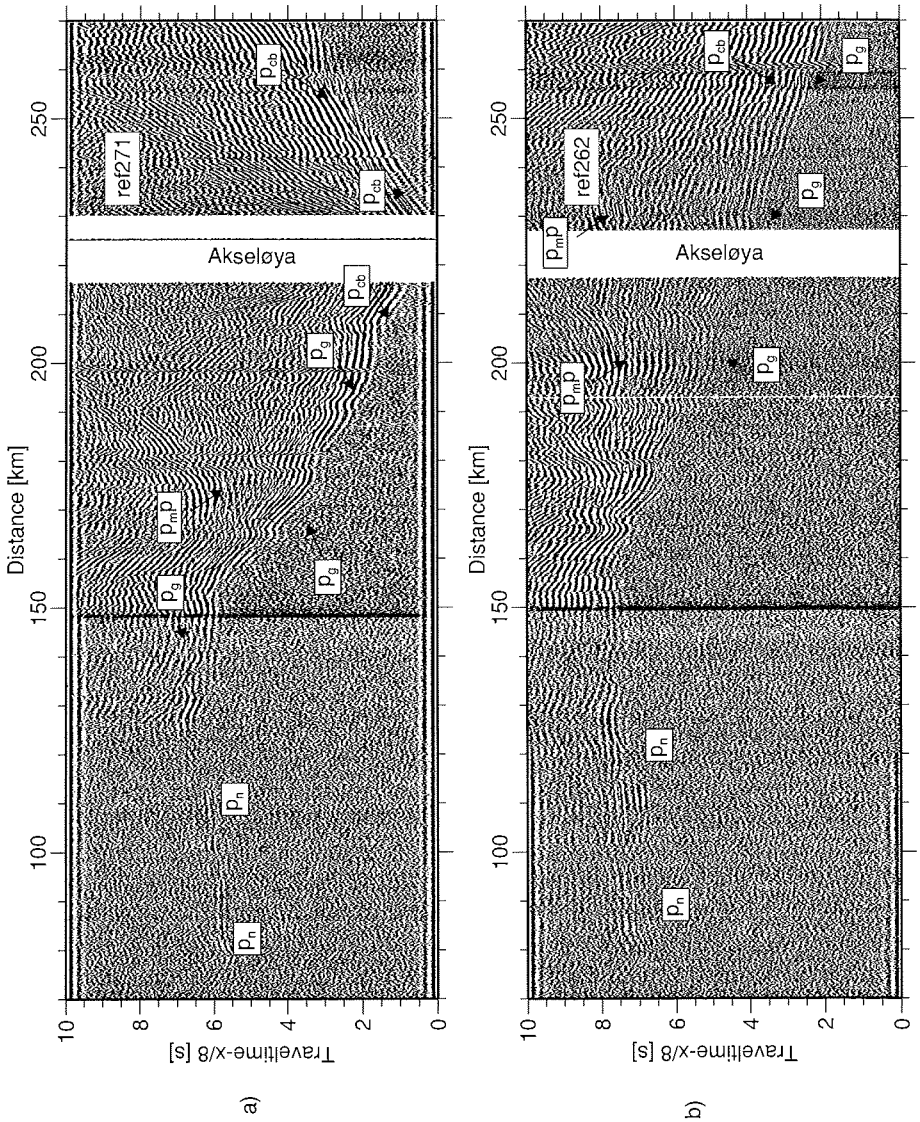

Figure 4-2: Record sections of station ref271, ref262, obh277 and obs14.
A bandpass filter passing frequencies from 5-17 Hz was applied to the data and a 1 s-automatic gain control. Stations obs14 is further processed by predictive deconvolution (see text).

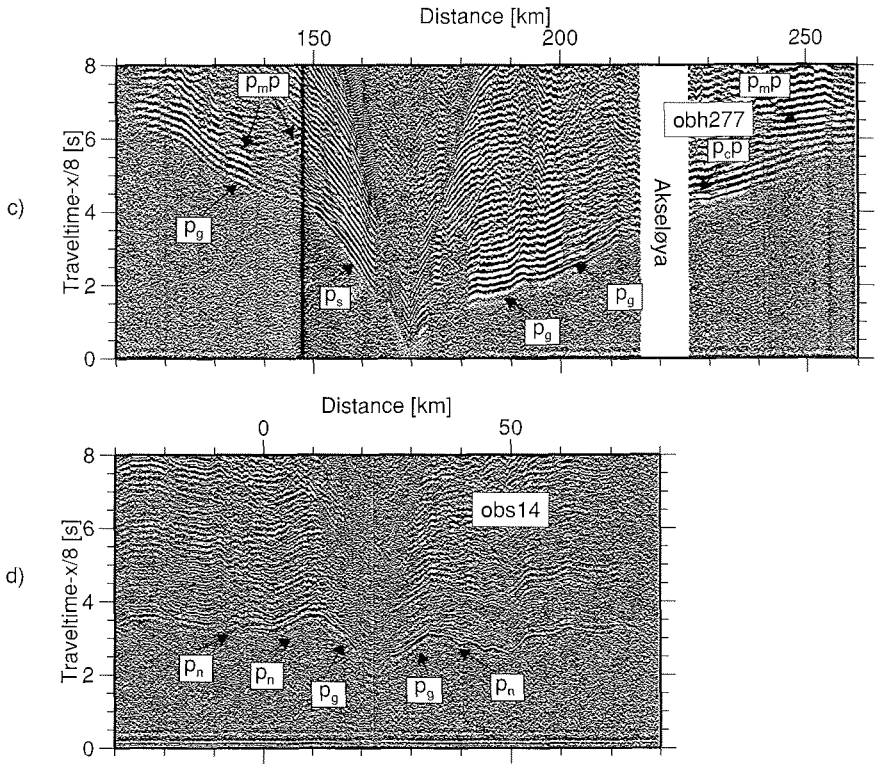

Figure 4-2: Continued.

advantage of the applied deconvolution, i.e. later secondary arrivals are better seen on the seismic sections. Hence, velocity gradients are calculated more precisely.

Figs. 2a and b show the recordings of the stations ref271 and ref262 (located approximately 16 km east of Akseløya and at the eastern end of the profile). These sections are representative of the continental profile section along the Van Mijenfjorden. At near offsets the first arrivals are diving p-waves through the Cretaceous to Cenozoic cover of Svalbard's Central Basin (Fig. 4-2a; p_{cb}). Further east these become secondary arrivals (Fig. 4-2b). West of Akseløya at km 200 seismic velocities increase apparently at the Kongsfjorden-Hansbreen Fault Zone (p_g). Seismic velocities of p_g-phases decrease again in the westerly direction, where traveltimes are delayed due to the thickening of the Cenozoic sedimentary cover of the shelf region (Fig. 4-2a and b). At km 150 a further increase in the seismic velocity of p_g-phases occurs on the seismic recordings. This is due to higher velocities of ~7.2 km/s at 15 to 20 km depth along the continent-ocean transition. Moho reflections (p_mp) occur consistently at 6 to 7 s all along the eastern pro-

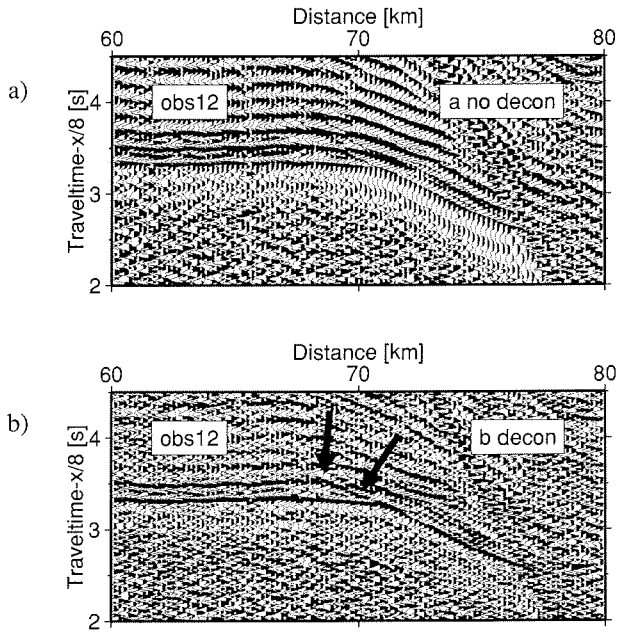

Figure 4-3: Predictive deconvolution example (station obs12). *The upper figure (a) shows an enlargement of the recording of obs12 (20 km to the east of the station). Data are filtered with a bandpass filter (5-17 Hz) and scaled by automatic gain control (1 s). The lower data set (b) shows the results of deconvolution after filtering and subsequent filtering as discussed in the text. Note, that the strong reverberation pattern in the upper figure at km 70 is suppressed after applying deconvolution (black arrows).*

file section. Later arrivals are often observed in the vicinity of p_mp-reflections and exhibit very large apparent seismic velocities. Subsequent raytracing of the data shows that these phases can not be consistently explained by a single steep dipping boundary. Instead, we attribute them to large lateral variations along the continental margin and possibly 3D-effects. P_n-phases, for determination of upper mantle seismic velocities were recorded on various stations and are characterised by strong amplitude variations (Fig. 4-2a). This might be ascribed to scattering of seismic energy due to a strong basement- and Moho topography along the oceanic section. The data of obh277 (Fig. 4-2c), located directly above the Horsund Lineament, allows us to observe the characteristics of the continent-ocean transition. Here, first arrivals at near offsets (< 20 km) indicate seismic velocities of 1.7 to 3.5 km/s for the sedimentary cover on the shelf. As observed on example ref277 the p_g-phase, penetrating the middle crust, shows strongly variable seismic velocities between km 110 and 160. This is mainly due to the bathymetry, a varying

thickness of the sedimentary cover and the lateral inhomogeneous sub-sedimentary crustal construction.

The crust-mantle boundary is defined by p_mp-reflections that are located within a strong reverberation pattern (Fig. 4-2c). The velocity structure of oceanic crust is demonstrated by the recording of station obs14 (Fig. 4-2d; see also Fig. 4-3b for station obs12). At near offsets first arrivals are crustal p_g-phases that are ascribed to oceanic layer 2 (3.5-4.5 km/s). At near critical distances of 10 to 15 km first arrivals exhibit velocities of ~7.9 km/s (and higher) which we interpret as p_n-arrivals. Due to the position of station obs14 in the median valley of the Knipovich Ridge proximal p_n-phases show anomalous high apparent velocities (large bathymetric differences). Phase undulations and amplitude variations of p_n-phases are due to a strong basement and Moho topography commonly found.

4.3.3 Seismic reflection data - Acquisition

Seismic reflection data between the Knipovich Ridge and the Bellsund (Fig. 4-1) was collected on cruise leg III of *RV Håkon Mosby* in 1999 (profile 7/AWI-99530; 5.2°E-13.5°E). This survey was carried out in cooperation with the Norwegian Petroleum Directorate and Norsk Hydro. The hydrophone cable (3000 m) comprised 120 channels with a group spacing of 25 m. A 7 airgun array with a total charge of 47 l was used to produce the acoustic energy. The resulting length of the profile is 233 km (~5000 shots) parallel to the seismic refraction lines.

4.3.4 Seismic reflection data - Processing and Characteristics

Stacking was done using a CDP-distance of 50 m (fold=30). The following processing sequence comprehends prestack-filtering in the f-k-domain, to reduce strong water bottom multiples from the upper shelf to the deep sea environment east of Knipovich Ridge (CDPs 6400-9400). CDP-gathers are (i) nmo-corrected and (ii) overcorrected, to separate primary and multiple reflections according to their apparent velocities within the f-k domain. Subsequent filtering eliminates seismic energy in the quadrant $k>0$. Finally, the applied overcorrection was removed and the data were stacked. To display the section, data were bandpass filtered within the upper 3 s passing frequencies of 18 to 75 Hz and with reduced high-cut frequencies thereafter to reduce high-frequency noise in the region of basement and sub-basement reflections (<55 Hz between 3 and 4 s; <45 Hz below 4 s). Seismic traces were scaled using a 200 ms automatic gain control.

Fig. 4-4 shows the seismic reflection data for the oceanic crustal section east of Knipovich Ridge (CDPs 4000-6800). The upper parts are characterised by continuous reflections with a thickness of 0.5 to 2 s (twt). Beneath this a diffractive event at 3 to 3.5 s (twt) caps a mostly transparent part of the data, with continuous reflections occurring only east of CDP 5600 between 3 and 3.5 s (twt). Reflections below 4 s (twt) show a discontinuous wavy pattern in a 0.5 s (twt) thick band. Along the profile section this sub-sedimentary reflective band describes two antiforms with their summits located at CDP ~4200 and ~5600.

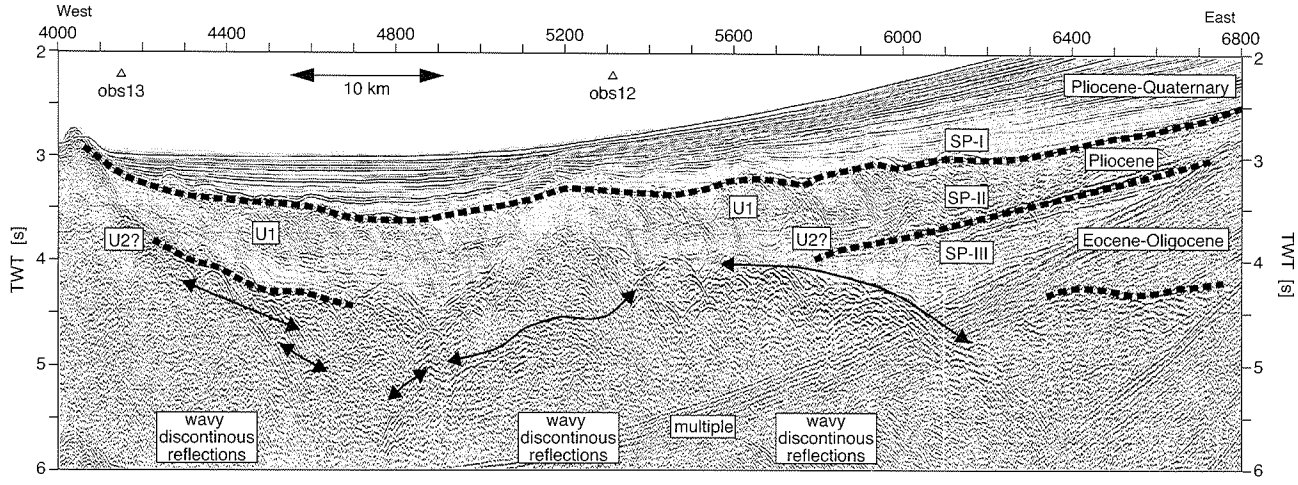

Figure 4-4: Record section of profile 7 from CDP 4000 to 6800.
Stratigraphy and age determination after Schlüter & Hinz (1978). Thick black dotted lines indicate the U1- and U2 unconformities and a deeper seated reflection that probably marks the boundary between Late Paleozoic sedimentary rocks and crystalline basement (CDP 6300-6800). Thin black arrows follow the upper outline of sub-sedimentary reflective bands that are interpreted as thin oceanic crust and the Moho. White triangles locate the stations obs12 and obs13.

4.3.5 Gravity data

Gravity data along the seismic refraction transects AWI-97260 and profile 9 was extracted from the free-air anomaly grid of Boebel (2000). This grid is mainly based on airborne gravity measurements and secondary shipborne data. The grid cells measure 20'x5'. It provides a continuous free-air anomaly profile along both seismic profiles and the landward extension in Heer Land.

4.4 Modelling of refraction data

4.4.1 Technique

Seismic refraction data gathered along profiles AWI-97260 and profile 9 comprise 22 stations that are used for raytracing. We performed the modelling with the software package *rayinvr* of Zelt & Smith (1992). After picking of clear high-amplitude arrivals, which were mostly first arrivals and Moho-reflections, 1D models for each station were calculated. These 22 single 1D profiles were gathered to a final 340 km long 2D transect (-50 to 290 km; Knipovich Ridge is located at km 0). Generally, a forward modelling technique was applied, in which the modelling took place layer by layer. Velocity-depth nodes were held fixed when the next, deeper layer was modelled. Improved traveltime fits come with the addition of nodes in the model, especially along the oceanic section. We put more emphasis on matching the slope and shape of the observed traveltimes branches than on minimizing the traveltime residual provided by the program *rayinvr*. We interpret first arrivals commonly as diving waves, since gradients are mostly observed. An exception is the mantle layer, whose velocity structure was modelled using head-waves.

Using this initial model, we calculated traveltimes for phases at stations where the S/N-ratio had caused problems. These data were inspected a second time in order to search for additional low amplitude arrivals. Of the 5500 picks in the final set, about 40% are p_n-phases or p_mp-reflections. Approximately two thirds are located east of km 120 along the continental profile section. This reflects the close receiver spacing there. The final fit of observed traveltimes was derived from two runs of the inversion method of *rayinvr* to the velocity model. Raytracing examples for the different crustal sections (oceanic crust, continent-ocean transition, continental crust) are shown in Fig. 4-5a-f. This figure further shows example raypaths for three stations (obs14, obs16, obh279, ref275, ref273 and ref263) which cover different crustal sections along the entire transect. All the important modelled structures are densely sampled by rays, with the exception of the deeper continental crust east of km 180. This is only constrained by wide-angle reflections (Fig. 4-5e and f).

4.4.2 Resolution and uncertainty of the modelled velocity structure

The reliability of the final velocity structure is expressed in the resolution calculated by the inversion algorithm of *rayinvr* (Zelt & Smith, 1992). This quantitative approach of *rayinvr* is based on the relative number of rays which determine or assign the parametrisation, i.e. the velocity nodes. According to Zelt & Smith (1992) resolution values of 0.5

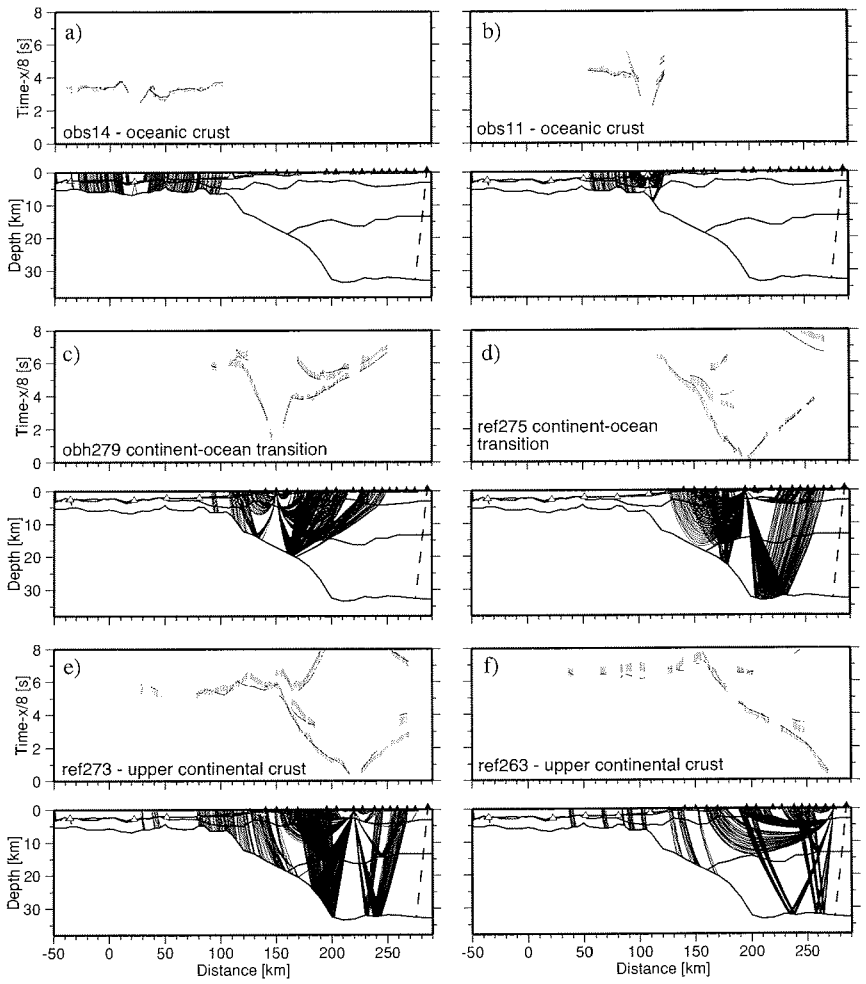

Figure 4-5: Raytracing examples along profile AWI-97260.
Stations (a) obs14, (b) obs11, (c) obh279, (d) ref275, (e) ref273 and (f) ref263. The six examples cover different parts of the refraction transect. The upper parts of a-f show the observed and calculated p-wave arrivals. Grey errors bars indicate the assigned error to the picked traveltimes. Black lines show the traveltimes calculated using the final velocity model shown in Fig. 4-7. The lower figures of a-f are the respective paths for rays calculated by rayinvr (Zelt & Smith, 1992).

or greater are considered to be well resolved. A resolution is calculated for each velocity node in our final model, and these are interpolated onto a 0.5x1.0 km grid. The resulting calculated resolution is shown in Fig. 4-6.

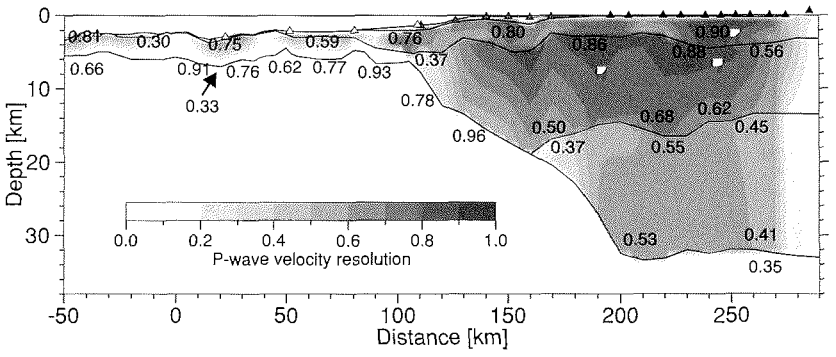

Figure 4-6: Resolution of the p-wave velocity field along profile AWI-97260.
Resolution was calculated by rayinvr (Zelt & Smith, 1992) and resampled to 20 km intervals. The greyshade shows the resolution, as well as the single shown values. Triangles as for Fig. 4-1.

Continental crust east of km 120 and the Cenozoic sedimentary section are in general well resolved, exhibiting values between 0.5 and 0.9. Exceptions occur at the outer sides of the middle and upper layers, where resolution decreases to 0.4 and below. Along the oceanic crustal section the resolution is satisfying in the vicinity of the deployed receivers (0.3 to 0.8) but decreases below 0.2 at the positions between. The mantle layer is generally well resolved west of km 150 due to the large number of p_n-phases on most seismic recordings (0.6 to 0.9). To the east mantle resolution decreases rapidly (~0.3) since critical distances of p_n-phases are too large to penetrate the upper mantle in depths of >30 km.

4.5 Results and interpretation

The final velocity model along the profiles AWI-97260 and profile 9 is shown in Fig. 4-7. A line drawing interpretation of profile 7 is superimposed. The following section contains detailed descriptions of the velocity model as well as our favoured interpretation of the observed structures. Fig. 4-8 shows the final geological interpretation of the Knipovich Ridge-Bellsund-Van Mijenfjorden seismic transect.

4.5.1 Sedimentary cover

Sediments and sedimentary rocks east of Akseløya (km 190 to 290)

Between Akseløya at km 190 and the eastern end of the profile in Heer Land (Fig. 4-1) the seismic velocities of the upper layer of the velocity model range from 4.5 (4.6) to 5.4 km/s (Fig. 4-7). The middle layer exhibits low seismic velocities between 5.6 and 6.0 km/s in a trough-like structure down to depths of 15 km.

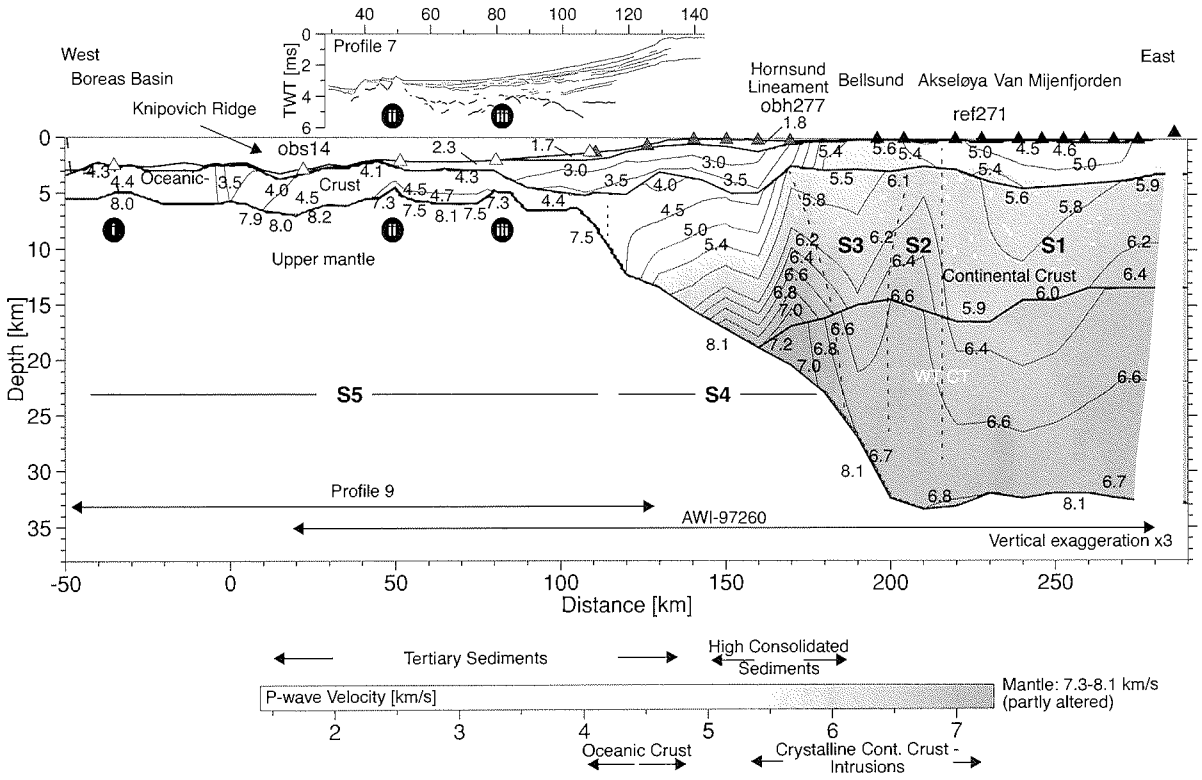

Figure 4-7: Final p-wave velocity model for profile AWI-97260 and profile 9.
The greyshade shows the seismic velocity field as do the annotated contour lines. Triangles as for Fig. 4-1. Thin dashed lines indicate the approximate boundary of the segments S1 to S5 as used in the text. Vertical exaggeration is x3. A line drawing of profile 7 (km 28-143) is shown in the upper part. The annotated greyscale below gives a rough interpretation of seismic velocities.

After Harland (1997f) the estimated thickness of Paleocene-Eocene strata of the Central Spitsbergen Basin amounts to 2.5 to 3.5 km. This thickness coincides with the 5.0 km/s-velocity contour. Velocities greater than 5.0 km/s are interpreted therefore as older (Carboniferous/Permian to Cretaceous) sedimentary rocks below. Where these crop out between Akseløya and station ref270 (Fig. 4-1) the velocity model shows seismic velocities of 5.4 km/s at the surface (Fig. 4-7). Similar velocities are observed for Late Paleozoic to Mesozoic sedimentary rocks of northern Greenland and Svalbard (Jackson, 1990; Hajnal et al., 1990; Eiken, 1994). Devonian sedimentary rocks of the Nordfjorden Block (km 220 to 270) are suggested to be present below the Central Spitsbergen Basin (Johannessen & Steel, 1992; Nøttvedt et al., 1993). Based on velocities for Devonian sedimentary rocks of up to 6.0 km/s found in northern Svalbard (Ritzmann et al., subm. to Marine Geophys. Res., see chapter 3), we propose that the reflective horizon at depths of 12 to 15 km marks the base of Devonian deposits. The eastern termination of the Nordfjorden Block is marked by the Billefjorden Fault Zone at km 275 (Fig. 4-1; ref263). Here seismic velocities increase within the middle crust to 5.9-6.4 km/s. Crystalline basement is supposed to have been thrusted over Devonian sedimentary strata along the westward verging Billefjorden Fault. In the Late Carboniferous this uplifted basement section experienced downfaulting further east in Heer Land, so that deep sedimentary basins developed (Nøttvedt et al., 1993). The observed velocity structure does not illustrate these events (Fig. 4-7). We attribute that to the limited extension of our profile east of the fault (~15 km), although the western flank of the basement high is well resolved. In contrast the western flank of the Nordfjorden Block is clearly evidenced by the increase of seismic velocities at km 200-220 (6.1-6.6 km/s). This zone coincides with the surface trace of the Kongsfjorden-Hansbreen Fault Zone (the proposed boundary between Svalbard's central and western terranes).

Sediments and sedimentary rocks of the western shelf and deep sea environment (km 50 to 180)

Off Van Mijenfjorden (km 70 to 160) the upper layer of the velocity model exhibits seismic velocities ranging from 1.7-1.8 km/s at the top to 3.5-3.9 km/s at the bottom. This layer comprises Cenozoic sedimentary strata. The thickness of this model layer varies between 2 and 5 km. Seismic velocities for the sedimentary sequences off Van Mijenfjorden found by Schlüter & Hinz (1978) and Myhre & Eldholm (1988) range between 1.7-3.8 km/s and 1.9-3.7 km/s, respectively. Schlüter & Hinz (1978) observed two sedimentary unconformities U1 (Pliocene, 3.5 Ma) and U2 (Eocene-Oligocene, ~36 Ma) subdividing the offshore sedimentary record off Van Mijenfjorden into three sequences (SP-I, SP-II and SP-III; see also Fig. 4-4). They suggest the absence of Oligocene-Miocene sedimentary strata above U2 due to a major drop in sea-level in Oligocene times. South of 76°N Myhre & Eldholm (1988) observed the gradual extinction of U2, giving way to a continuous Post-Eocene sequence.

The lower boundary of the modelled upper sedimentary layer at km 120 (5 km depth; Fig. 4-7) shows a ridge, that is inferred from early p-wave arrivals on station obh281, with velocity of >4.0 km/s. We interpret this phase to be derived from sedimentary units. The nature of the deeper seated refractors within SP-III (Fig. 4-4) with seismic velocities

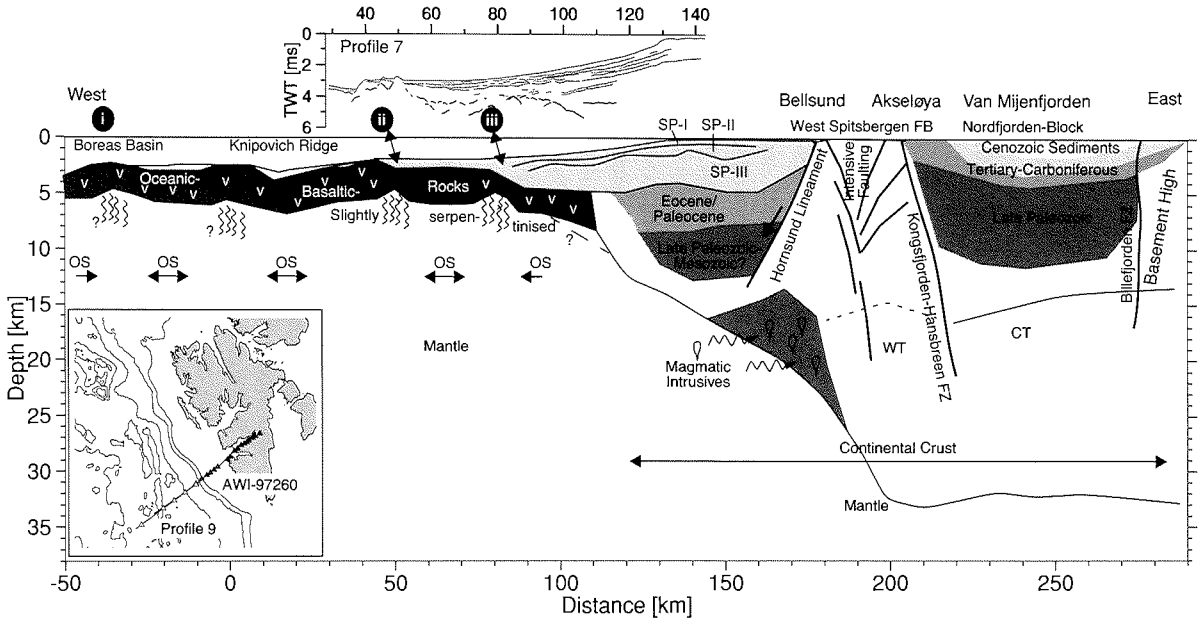

Figure 4-8: Geological interpretation of the velocity model of the profiles AWI-97260 and profile 9.
In additional the line drawing of profile 7 (km 28-143) is shown. Generally, crystalline continental crust is coloured white, oceanic dark grey. Stratigraphy (SP-I, II, III) of the offshore sedimentary wedge east of Akseløya after Schlüter & Hinz (1978). The crosshatch pattern marks the trapezoidal zone along the rifted continental margin that is intruded, as characterised by higher seismic velocities (up to 7.2 km/s). Zones i to iii are characterised by thinned oceanic crust and correspond to the sub-sedimentary (crustal) topography (black vertical arrows). OS: Oceanic segments following the observed crustal thicknesses. WT: western terrane. CT: central terrane of Svalbard.

of 4.5-5.5 km/s is uncertain (Myhre & Eldholm, 1988). Comparing these velocities found with those in the Tertiary Central Spitsbergen Basin (4.5-5.0 km/s; km 220-270) it is plausible that lower SP-III comprises Early Tertiary (Paleocene/Eocene) or even older sequences. The inferred depth of the base of the Paleocene is with respect to the 5.0 km/s-isovelocity contour, at 9 to 10 km depth. After Harland (1997f) the thickness of Paleogene sedimentary rocks in the Central Spitsbergen Basin is 2.5 to 3.5 km, which is comparable to that observed to the west of the orogenic belt.

Mann & Townsend (1989) and Townsend & Mann (1989) suggest still older (Carboniferous) sedimentary deposits below the Bellsund in the Bellsundbanken Graben. It is uncertain if this graben extends further west across the Hornsund Lineament. In the case of occurrence of Late Paleozoic sedimentary rocks the 5.5 km/s-contour might mark the sediment-basement boundary (10.5 to 12 km depth), analog to velocities found elsewhere (Jackson, 1990; Hajnal et al., 1990; Eiken, 1994). This would therefore imply a total offshore sedimentary thickness of about 10 km, from a crustal thickness of 13 to 20 km (km 120-160; Fig. 4-7). A strong reflective horizon (4.5 s twt) in the seismic reflection data of profile 7 might be additional evidence for a deeper seated sediment-basement boundary (Fig. 4-4 and Fig. 4-7, line drawing; CDP 6300-6700; also observed by Schlüter & Hinz (1978), line 25 at ~5 s twt).

Between km -50 and 60 the thickness of the sedimentary cover on oceanic crust decreases to a maximum of 1.5 km. Locally only 100 to 200 m are observed, and some oceanic basement ridges feature no modelled sedimentary cover (e.g. km 45). Seismic velocities at the top of the sedimentary section are ~1.7 km/s, at the base velocities do not exceed 2.3 km/s.

Tertiary sedimentary strata are further expected east of the Hornsund Lineament within a 28 km wide graben centred on km 180 that is most probably a similar feature to the Forlandsundet Graben north of Isfjorden (Eiken & Austegard, 1987; Eiken, 1994). About 4 km of sedimentary deposits (2 s twt) are observed (Eiken, 1994). Due to the failure of obh276 at km 183 on top of this graben no sedimentary (low velocity-) phases were detected. Therefore the seismic velocity structure of the graben remains unexplored. Only the bounding basement-flanks are constrained.

4.5.2 Continental crust

The eastern continental profile section along km 190 to 290 comprises Svalbard's western and central basement terranes (Harland & Wright, 1979; Harland, 1997b). The Caledonian docking of these terranes, the Tertiary Spitsbergen Orogeny (Steel et al., 1985; Harland, 1997e) and Post-Oligocene rifting are the major tectonic events that affected the continental crustal structure.

Caledonian terranes (Segments S1-S2)

The Caledonian suture is supposed to be located at the sinistral Kongsfjorden-Hansbreen Fault Zone (Harland & Wright, 1979) which is located at km ~215. Here, the upper and lower units of the crust show a striking change in seismic velocities (Fig. 4-7; S1-S2). The lateral change in velocity at depths above 12 km is attributed to the boundary of the Devonian sedimentary rocks (Nordfjorden Block). Nevertheless, within the

middle and lower crust the western terrane exhibits higher velocities of 6.6 km/s, compared to 6.2 km/s in the central terrane (Fig. 4-7). Only a narrow section of the western terrane at km ~220, can be classified as unaffected by the Tertiary Spitsbergen Orogeny, as the Tertiary Spitsbergen Fold Belt adjoins this section. The total range of seismic velocities of continental crust along segments S1 and S2 can be compared to the work of Chan & Mitchell (1982) and Amundsen et al. (1987) who determine velocities of 6.1-6.3 km/s, 6.4-6.6 km/s and 6.7-6.8 km/s for northwestern Svalbard (Woodfjorden; Fig. 4-1). This three layer structure and related mid-crustal reflections (Ritzmann & Jokat, 2003; see chapter 2; Ritzmann et al., subm. to Marine Geophys. Res., see chapter 3) are not seen in southern Svalbard. The depth to the Moho is about 34 km below the Van Mijenfjorden, and in good agreement to depths published by Sellevoll et al. (1991) and Faleide et al. (1991). Sellevoll et al. (1991) suppose a crust-mantle transitional layer (7.8 km/s), but in contrast our data indicate a first-order discontinuity at the Moho (Fig. 4-7). High lower crustal seismic velocities (Czuba et al., 1999; 7.2 to 7.3 km/s) are further not confirmed by our transect.

West Spitsbergen Fold Belt (Segment S3)

The West Spitsbergen Fold Belt extends approximately from the position of obh277 to Akseløya (km 170-210; Fig. 4-1) along Svalbard's western terrane. The deeper seismic velocity structure exhibits a 20 to 30 km wide trough-like structure. In the centre at km 190 low velocities of 5.5 and 6.2 km/s and 6.4 to 6.8 km/s are observed for the middle and lower crust, respectively. In contrast the flanks have higher velocities, e.g. 6.2 km/s at 5 to 10 km (Fig. 4-7). Due to the failure of obh276 the upper 5 km, which feature the Tertiary graben below the Bellsund (Eiken & Austegard, 1987; Eiken, 1994) is not well resolved.

Models for the evolution of the West Spitsbergen Fold Belt are generally based on the transpressive movements between Svalbard and Greenland during the Late Paleocene to Eocene (Lowell, 1972; Steel et al., 1985; Müller & Spielhagen, 1990; Harland, 1997e). Thrust faults of the fold belt steepen with depth and towards the centre of the belt. Further, geological mapping shows that local strike-slip faults pass over into thrusts (Kellog, 1975; Steel et al., 1985). This leads to the assumption of a large flower structure model for the fold belt (Lowell, 1972; Myhre et al., 1982; Nøttvedt et al., 1993). A principal problem is the subsidence of the graben system along Svalbard's west coast within this mostly transpressive regime (e.g. Forlandsundet Graben, Tertiary graben below the Bellsund; Steel et al., 1985; Eiken, 1993; Eiken, 1994). Steel et al. (1985) supposed local extension adjacent to a curved strike-slip zone or a collapse scenario in the central part of the uplifted and arched orogenic belt. Gabrielsen et al. (1992) show that the Forlandsundet Graben is bounded by steep marginal faults with a dip-slip character.

From the observed velocity structure we favour kinematic models with steep, vertical (strike-slip) faults that penetrate much of the crust (e.g Lowell et al.'s (1972) flower structure). We assume convergent motion along these faults to fracture extensively the brittle rock construction of the upper and middle crust (and result in possible deep seated mylonitic rocks). After the transpressive orogenic phase (Late Paleocene to Eocene), the stress field changed along western Svalbard to transtension from Oligocene onwards

(Eldholm et al., 1987). Henceforward, tensional release occurred at the centre of the fold belt leaving behind an intensively brittle-fractured rock formation.

This model is similar to that on a parallel refraction transect at Kongsfjorden (Ritzmann et al., subm. to Marine Geophys. Res., see chapter 3), where the velocity structure below northern Forlandsundet Graben (Fig. 4-7) is similar. Another similarity to the Kongsfjorden transect is the confinement of continental thinning to the region west of the fold belt (the western terrane). It seems that the strike-slip dominated orogeny led to the decoupling of western from inner Svalbard (Ritzmann, et al., subm. to Marine Geophys. Res., see chapter 3).

The continent-ocean transition (Segment S4)

The continent-ocean transition is marked by a gradual decrease of crustal thickness within a broad zone of approximately 80 km (Fig. 4-7). The Moho depth shallows from ~34 km along the central terrane to ~8 km at the transition to the oceanic crust. Two steep sections with an eastward dip of ~30° occur at km 120 and 190. Seismic velocities in the segment S4 lower than 5.5 km/s are interpreted as Late Paleozoic to Mesozoic sedimentary rocks (see above). The isovelocity contourlines describe a steep lateral decrease of seismic velocity towards the west between km 160 and 180 (5 to 15 km depth). Here, a lateral velocity gradient of ~0.1 1/s is observed (Fig. 4-7). The occurrence of the large lateral velocity gradients in the upper and middle crust coincides with the position of the Hornsund Lineament (Myhre & Eldholm, 1988; Eiken, 1993). Eiken & Austegard (1987) interpret the Hornsund Lineament off Van Mijenfjorden as two east-verging faults bounding a rotated crustal block. The westward dip (listric?) of the velocity contours might support this interpretation, keeping in mind that highly consolidated sedimentary rocks might build up the top of this block.

The velocity structure at the crust-mantle transition features high seismic velocities of 7.2 km/s (km 150 to 170): the highest seismic velocity within continental crust along the entire profile. This zone of elevated velocities is interpreted as altered crust. A 40x8 km wide trapezoidal body of higher velocities is observed at 15 to 25 km depth. Elevated seismic velocities in the deeper crust at continental margins are associated with mantle derived mafic/ultramafic melts and are a common phenomenon at rifted volcanic margins and emplaced by underplating and intrusions (White & McKenzie, 1989). A rifted volcanic margin history for the western Svalbard margin is excluded, since seismic refraction data in proximity to the proposed Yermak Hot Spot (Feden et al., 1979; Jackson et al., 1984) reveals no indications for a volcanic evolution (Ritzmann & Jokat, 2003; see chapter 2). Oceanic crust adjacent to rifted volcanic margins exhibits enhanced thicknesses (White & McKenzie, 1992) which is not observed off Van Mijenfjorden (Fig. 4-7; km 70-110). Mutter et al. (1988) propose convection induced secondary melting in the mantle when the lithosphere exhibits large horizontal thermal gradients, i.e. cool continental crust lies adjacent to a relatively hot ascending mantle diapir. Such a process is supposed to induce intrusive magmatism at sheared continental margins (Lorenzo et al., 1991) and is the likely origin of high seismic velocities at the Kongsfjorden Margin (~7.2 km/s; Ritzmann et al., subm. to Marine Geophys. Res., see chapter 3). The striking difference off Van Mijenfjorden is that the body of slightly elevated velocities is

enframed by stretched continental crust (and probably rotated blocks) instead of marking the sheared continent-ocean transition. We suppose the northward propagating Knipovich Ridge (Crane et al., 1991; Boebel, 2000) to be the source of mantle derived melts. Tectonic reconstructions of Crane et al. (1991) and Boebel (2000) place the northernmost Knipovich Ridge in close proximity to the Hornsund Lineament at the continental margin of western Svalbard (20 to 9.5 Ma). Hence magmatic contamination (mafic/ultramafic intrusions), probably induced by convection partial melting (Mutter et al., 1988), seems possible. At extreme slow-spreading ridges such as Knipovich Ridge (0.8 cm/a, half rate; Eldholm et al., 1990), the melt fraction distribution can be lowered with depth (White et al., 2001). This might promote melt injection into the lower parts of the crust (15-25 km depth) off Van Mijenfjorden).

4.5.3 Oceanic crust

The western oceanic section (Segment S5)

Oceanic crust is surveyed along a 170 km long section on the seismic refraction profile. Despite a large receiver spacing the seismic structure and the thickness variations along that section are, due to numerous p_n-phases, well constrained at least for the section east of Knipovich Ridge. The thickness of igneous crust varies between 1.5 and 4.0 km. Lower thicknesses are associated with three 8-12 km wide crustal sections at km (i) -35, (ii) 50 and (iii) 85. Seismic reflection data of profile 7 (Fig. 4-4 and Fig. 4-7, line drawing) supports the trend in Moho-topography between ii and iii. Sub-sedimentary reflections occur deeper (5 s twt) between the thinned crustal sections. The deeper reflections between CDP 5600 and 6000 (~km 90-100; Fig. 4-4) exhibit a thickness of up 0.5 s twt. The seismic velocities derived from wide-angle data within the oceanic crust off Knipovich Ridge range from 4.1 (4.3) to 4.7 km/s. Hence, for a crustal thickness of 1.5 km a respective twt of ~0.5 s is calculated. This implies that the lower reflections shown in Fig. 4-4 are probably reflected off the Moho.

At the ridge seismic velocities are decreased to 2.5 to 3.5 km/s. Application of the inversion method of Zelt & Smith (1992) also derives low seismic velocities for mantle rocks underneath the thinned crustal sections at km 50 and 85 (ii, iii). At minimum, velocities 7.3 km/s are calculated, compared to 8.2 km/s below oceanic crust with a thickness of 3.5 to 4 km. Due to the marginal position of obs16 (km -35) seismic velocities below section i are less constrained (8.0 km/s).

At km 100 reflection data (Fig. 4-4) reveals a deepening crust-mantle boundary that might reflect a mismatch in our determination from velocity modelling.

The observed seismic velocities in oceanic crust indicate only the presence of oceanic layer 2. P-wave velocities of layer 3 above the oceanic Moho are typically greater than 6.5 km/s, and rarely exceed 7.2 km/s (White et al., 1992). The absence of oceanic layer 3 is typical for slow-spreading ridges with a half spreading rate below 2 cm/a (White et al., 2001). According to Eldholm et al. (1990) a rate of 0.8 cm/a is expected for the northern Knipovich Ridge. Conductive cooling of the slowly ascending mantle (White et al., 2001) is therefore supposed to decrease the melt fraction at Knipovich Ridge leading to lower magma supply for the creation of layer 3. As proposed above the proximity of cool

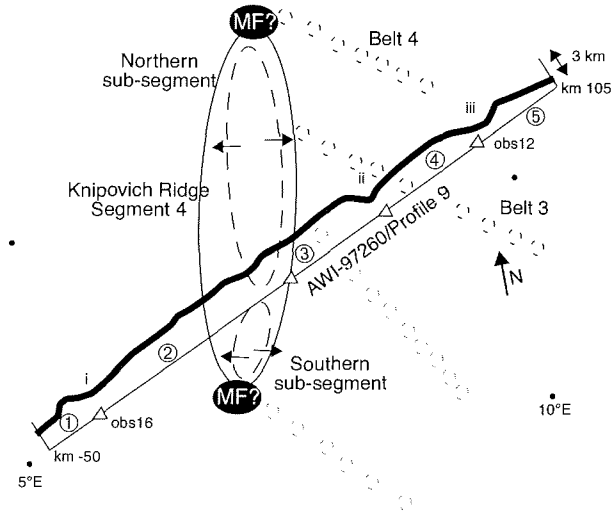

Figure 4-9: Oceanic crustal thickness along the seismic refraction transect. *Oceanic crustal thickness (thick line in graph) along the seismic refraction transect (thin straight line) and Knipovich Ridge second order segment 4 (solid oval with two (third order) sub-segments, dashed ovals; after Crane et al., 2001). Sections i, ii and iii are the respective zones of thinned oceanic crust as used in the text. Thin black arrows indicate the spreading direction of the third order segments as inferred from fault orientation at the ridge. The chains of open circles show the track of observed seamount belts (grey: belt 1 and 2; black: belt 3 and 4; Crane et al., 2001). Magma focus points (MF) at the boundaries of the segment after Crane et al. (2001). White triangles indicate the positions of deployed obs receivers. Note, that the seamount belts 3 and 4 intersect the refraction transects at profile sections ii and iii.*

continental crust might further enhance conductive heat loss at the ridge (after Lorenzo et al., 1991).

Following Crane et al.'s (2001) segmentation model of the Knipovich Ridge, the oceanic crust explored east of the ridge was formed at the second order segment 4 (76°38'N to 77°25'N). The authors conclude that magma supply is focused at the segment ends (Fig.) and argue therefore against models for magma accretion of e.g. Lin et al. (1990) in which buoyancy-driven mantle flow feeds the central positions of high order segments where maximum crustal thickness is achieved. Assuming the bounding discontinuities were always stationary, the segment boundaries project onto km ~-10 and ~85 (iii) on our profile, using the spreading direction vectors of Crane et al. (2001) based on DeMets et al. (1990). At these projection points the thickness of oceanic crust is not enhanced and magma supply is therefore probably not focused at the segment boundaries. Further it seems that the northern third-order sub-segment of segment 4 is itself segmented since we interpret the thinned crustal sections at km 50 and 85 (ii, iii) as fracture zones. The projection paths of these fracture zones correspond with observed seamount belts 3 and 4

(Crane et al., 2001). Low mantle velocities of 7.3 km/s below these zones of thinned crust may represent serpentinised peridotites, such as found on North Atlantic fracture zones (Detrick et al., 1993). We suppose roughly 20% serpentinisation according to Christensen (1966) who determined seismic velocities of 7.2 to 7.3 km/s on such partially serpentinised peridotites. Summarising the discussion above we propose a different kind of magma distribution along Knipovich Ridge, since 5 crustal segments are observed along the transect (separated by i, ii, iii and the northern tip of the southern sub-segment see Fig. ; km ~0). The observed seamount belts (Crane et al., 2001) are supposed to have developed adjacent to the thin crust along the fracture zones, although it has to be considered that these belts may be outcrops of a fracture-parallel transverse ridge.

4.5.4 Modelling of the free-air anomaly

As a further element for interpretation and discussion of the observed crustal structure we modelled free-air gravity anomaly data. The deduced density structure along the profiles is intended to constrain the observed velocity structure using common velocity/density relationships. The modelled densities further provide additional rheologic properties.

Observed free-air anomaly

The observed free-air anomaly shows an overall variation of ~105 mGal (Fig. 4-10). The most pronounced negative anomalies are observed at the Knipovich Ridge (i; -55 mGal; Fig. 4-10) and at the continent-ocean boundary (ii; -100 mGal). The continental profile section along the Tertiary Central Spitsbergen Basin shows a mean level of ~42 mGal with an increasing trend east of km 250 (~0 mGal). The oceanic crust and the western continent-ocean transition (west of km 190) show a common level of approximately +50 mGal with some negative anomalies superimposed (-5 to -20 mGal amplitude) between (iii-vi) exhibiting a wavelength of 20 to 50 km.

The initial density model

The observed velocity structure was transformed into an initial density model A (Fig. 4-10): Over the continental crust the velocity model was digitised and converted to density bodies in 0.05 g/cm^3-increments using the non-linear velocity-density relationship of Christensen & Mooney (1995). The density for offshore sedimentary cover was set to 2.10 (uppermost) and 2.40 g/cm^3. We chose a density of 2.90 g/cm^3 for oceanic crust after Christensen & Mooney (1995). In zones of decreased seismic velocities below thinned oceanic crust, we assign a decreased density of 3.15 g/cm^3, according to density determinations of Christensen (1966) on partially serpentinised peridotites (22%). The residual mantle density was set to 3.3 g/cm^3.

The long-wavelength variation of the calculated free-air anomaly of model A is about 350 mGal (Fig. 4-10). This is more than three times higher than observed. A positive deviation along the oceanic profile (up to 150 mGal west of km 140) and a negative deviation on the transitional and continental section (70 to 100 mGal east of km 140) is achieved. Nevertheless short wavelength anomalies (such as i, ii or vi) are well matched.

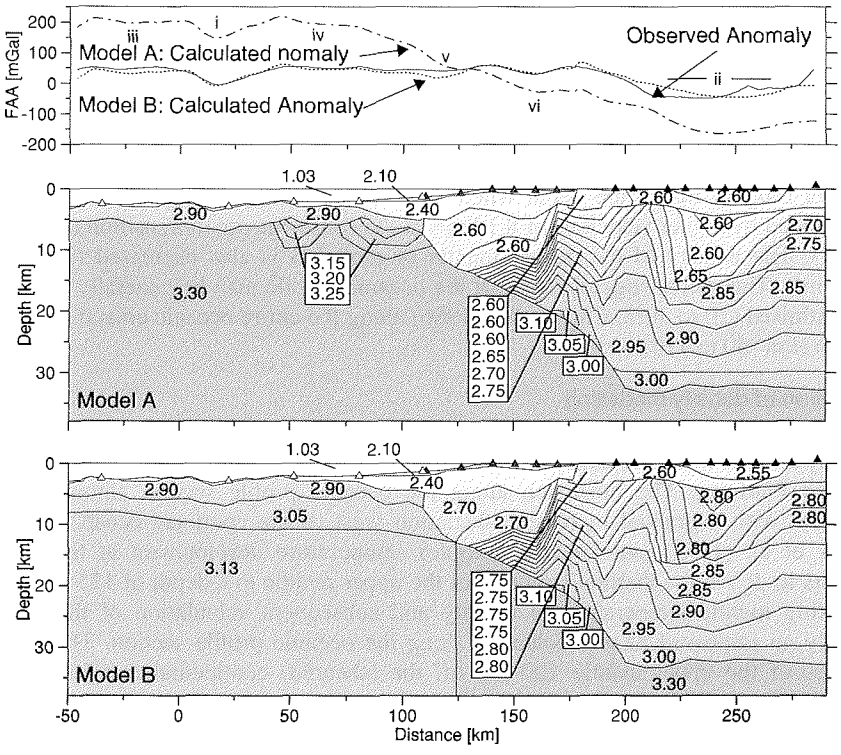

Figure 4-10: Initial (model A) and final (model B) density models for profile AWI-97260 and profile 9.
The observed free-air anomaly is marked by a thick solid line in the upper graph. The calculated free-air anomaly from model A is marked by a dashed-dotted line, from model B by a dotted line. For calculation of densities and modelling parameters see text. Triangles as for Fig. 4-1.

The final density model

The following changes were applied to provide a better fitting free-air anomaly model (model B, Fig. 4-10):

- (1) In order to increase the anomaly on the eastern continental section the densities within the upper and middle crust had to be increased by about 0.05 to 0.2 g/cm^3. Densities for the Tertiary Central Spitsbergen Basin were lowered to more reasonable values (2.55 g/cm^3). The high densities within the upper crystalline crust are consistent with densities up to 2.8 g/cm^3 measured on Svalbard rock samples by Kurinin (1970) and Howells et al. (1977) and with observations in northern Svalbard published by Ritzmann et al. (subm. to Marine Geo-

phys. Res., see chapter 3). Densities of 2.70 g/cm^3 are inferred for depths of 5 to 15 km west of the Hornsund Lineament where Paleozoic or Mesozoic sedimentary rocks are expected from the velocity structure. Kurinin (1970) and Howells et al. (1977) measured similar group densities on rock samples of such sedimentary rocks.

- (2) To match the free-air anomaly on the oceanic crustal section, the mantle density was generally decreased to 3.05 g/cm^3 down to depths of ~10 km. This level roughly marks the depth where low mantle velocities of 7.5 km/s are replaced by higher velocities of 8.1 km/s at the continent-ocean transition (Fig. 4-7). The density of the deeper mantle of model B is also decreased (3.13 g/cm^3). The model suggest thus that the oceanic mantle may be generally serpentinised (20 to 30%; Christensen, 1966) along the entire oceanic crustal section (km -50 to 110).

Evaluation of density modelling

Breivik et al. (1999) report a similar extreme mismatch between the observed free-air anomaly and the inferred anomaly from seismic crustal models off Senja Margin and the Svalbard Platform. The mismatch along the oceanic profile section amounts up to 200 mGal with a gradual increasing deviation west of the continent-ocean boundary. Breivik et al. (1999) simulate the complex temperature development at the margin transects to derive the thermal structure of the upper mantle to a depth of 125 km. After converting mantle temperature to density and subsequent calculation of the free-air anomaly an improved fit was achieved along the oceanic profile section. The derived densities of the upper mantle 100 km off the (sheared) continental margin are 3.16 (sub-crustal) to ~3.26 g/cm^3 (125 km depth).

With reference to this we conclude that our gravity modelling only provides a reasonable structure along the eastern continental section. For the oceanic section model B (Fig. 4-10) can be merely regarded as a simple approximation, since a detailed mantle structure is missing. Further research has to be carried out, the solution may be given by simple thermal modelling of the upper mantle as done by Breivik et al. (1999).

4.6 The development of the continental margin off Van Mijenfjorden

The velocity structure of the continental margin off Van Mijenfjorden can be used for a simple schematic Cenozoic evolution model, since it reveals information about the West Spitsbergen Orogeny as well as the rifting procedure in Oligocene.

The Spitsbergen Orogeny was a Late Paleocene transpressive event (Steel et al., 1985; Eldholm et al., 1987). According to our observations along the seismic refraction profile we characterise the deeper roots of the fold belt as intensively faulted rocks, that are most probably related to oblique convergent wrenching. This gave way to transtension since the Oligocene (Eldholm et al., 1987) and the intensively faulted rock units entered a relaxing phase (Fig. 4-11a). Crustal thinning occurred but is limited to the Caledonian western terrane of Svalbard. These observations are similar to those made along the seismic refraction transect off Kongsfjorden (Ritzmann et al., subm to Marine Geophys.

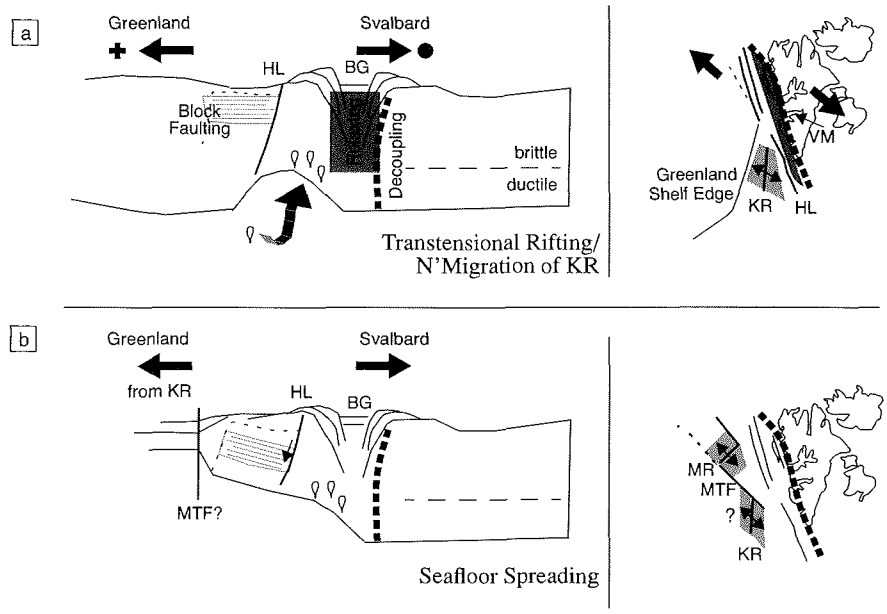

Figure 4-11: Schematic evolution of the continental margin off Van Mijenfjorden derived from the interpretation of seismic refraction profiles AWI-97260 and profile 9.
During the Paleocene a transpressional regime dominated between Svalbard and Greenland and resulted in the West Spitsbergen Fold Belt (cross hatch pattern). Since first subsidence of the Forlandsundet Graben is achieved during this phase we propose a similar history for the Bellsund Graben (BG) off Van Mijenfjorden (VM). Intensive shearing weakened the upper brittle part of the crust. The vertical dotted line indicates approximately the boundary between the central and the western terrane. (a) Since Oligocene transtension occurred and the Hornsund Lineament (HL) was the active fault system between Svalbard and Greenland. Stress was taken off the Fold Belt (Bellsund region), and thinning of the western terrane occurred decoupled from central Svalbard. West of the HL block faulting took place. Note that the upper crust is supposed to comprise Paleozoic to Mesozoic consolidated sedimentary rocks (grey box). The northern segment of the Knipovich Ridge (KR) was situated directly adjacent to the slightly thinned crust off Van Mijenfjorden. Mantle derived melts from the deeper Knipovich Ridge were injected into the lower crust at the central rift. Later (b) the mid-ocean ridge system migrated further north. Rifted crustal sections were tilted and buried below younger sediments.

Res., see chapter 3). Both profiles reveal that crustal thinning is decoupled from inner Svalbard (the central terrane), probably the consequence of the former transpressive suture of the West Spitsbergen Fold Belt, that itself is located in close proximity to the Caledonian suture.

The main fault zone between Svalbard and Greenland was most probably the Hornsund Lineament (Eiken, 1993) that is supposed to bound a Paleozoic (Carboniferous?) or Mesozoic sedimentary basin to the east (e.g. Mann & Townsend, 1989; Townsend & Mann, 1989). The Knipovich Ridge is supposed to have been located adjacent to Van Mijenfjorden during the Miocene (Crane et al., 1991; Boebel, 2000). Elevated lower crustal velocities are found at the continent-ocean transition and we suppose magmatic interaction between the deeper mid-oceanic ridge and the continental crust, keeping in mind that a rifted-volcanic evolution can be excluded (Ritzmann & Jokat, 2003; see chapter 2). As the mid-ocean ridge system migrated further north of the Knipovich Ridge (Fig. 4-11b) opening of the Fram Strait, continental crust off Van Mijenfjorden was further thinned, rifted and probably block-faulted (Eiken & Austegard, 1987). The Hornsund Lineament developed. It remains unclear if the Molloy Transform Fault developed prior to the northern Knipovich Ridge leading to a sheared margin in the outer zone of the continent-ocean transition (km 110).

4.7 Conclusions

The main results of our study are:

- (1) Cenozoic sediments and sedimentary rocks on- and offshore exhibit seismic velocities from 4.5 to 5.4 km/s (Spitsbergen Tertiary Basin, onshore) and 1.7 and 3.9 km/s (offshore) with maximum thicknesses of 3.5 and 5 km, respectively. Below the Cenozoic cover onshore are up to 8 km of Devonian rocks associated with the Nordfjorden Block. West of the Hornsund Lineament the velocity structure gives rise to the suspicion that Paleozoic (Carboniferous) sedimentary strata occur below the Cenozoic cover.
- (2) The western and central Caledonian terranes can be differentiated, the boundary occurs at the western termination of the Devonian deposits on the Nordfjorden Block. Seismic velocities range from 5.4 km/s at the top (W'Akseløya) to 6.8 km/s at the Moho. The upper and middle crust at the West Spitsbergen Fold Belt reveals decreased seismic velocities that are interpreted as an intensively faulted rock construction due to transpressive movements during the West Spitsbergen Orogeny. The lower parts of the rifted crust show a small zone of slightly elevated velocities (7.2 km/s). These are interpreted as mantle derived mafic or ultramafic rocks, intruded while the northern Knipovich Ridge was adjacent to the young rift off Van Mijenfjorden.
- (3) The oceanic crust related to the Knipovich Ridge shows maximum thicknesses of 4.0 km. The seismic velocities observed within oceanic crust indicate the absence of layer 3 (3.5/4.1 to 4.7 km/s). Minimum thicknesses of 1 to 2 km are achieved in narrow zones, interpreted as fracture zones. Below these fractures the seismic velocity of the upper mantle is low (7.3 km/s) leading to the assumption that the mantle is partly serpentinised. The distribution of fracture zones and thicker crustal sections (30 to 50 km/spacing) give new constraints on the segmentation of the northern Knipovich Ridge.
- (4) Density modelling along the seismic refraction transect confirms the observed velocity structure for the continental and transitional crustal sections.

We assume an extreme mismatch of up to 150 mGal along the oceanic profile section is due to a more complex density (i.e. thermal) structure of the upper mantle.

- The deep structure formed during the Cenozoic evolution of the West Spitsbergen Fold Belt off Van Mijenfjorden are similar to those observed off Kongsfjorden (Ritzmann et al., subm. to Marine Geophys. Res., see chapter 3). But the evolution of the continental margin differs since a rifted margin (instead of sheared) is observed off Van Mijenfjorden. Both margins reveal probable contamination by mantle derived ultramafic melts resulting in slightly elevated seismic velocities. In both cases the close proximity of the young plate boundary to the continental crust is considered to be responsible.

Additional Work

CHAPTER 5:
ADDITIONAL SEISMIC REFRACTION DATA ACQUIRED IN 1997: PROFILE AWI-99200

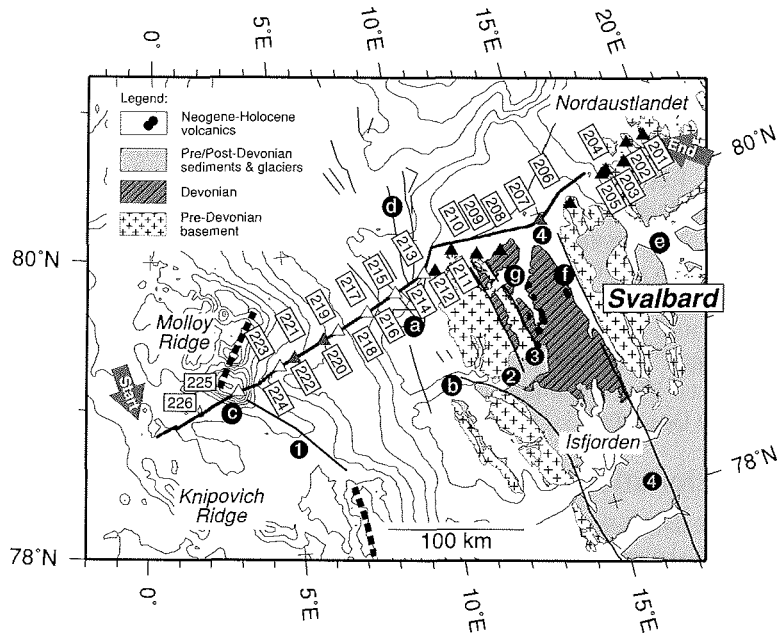

Figure 5-1: Location of seismic refraction profile AWI-99200.
The profile is marked by a thick black line, RefTek- and OBS- and OBH stations by black, grey and white triangles, respectively. Geology: Harland (1997a). Black lines are major faults onshore and offshore, numbered circles mark the following structures: (1) Molloy Transform Fault, (2) Raudfjorden Fault Zone, (3) Breibogen Fault Zone, (4) Billefjorden Fault Zone. Letters indicate the following locations: (a) Sjubrebanken, (b) Kongsfjorden/Forlandsundet, (c) Molloy Deep (d) Danskøya Basin, (e) Hinlopen Streetet, (f) Wijdefjorden, (g) Woodfjorden. Bathymetry: Jakobsson et al. (2000).

5.1 Aim of this chapter

The seismic refraction profiles discussed in the chapters 2 to 4 were gathered during expeditions ARK13/2 and ARK15/2 of *RV Polarstern*. During the latter expedition additional seismic refraction data were gathered by the Alfred Wegener Institute on a profile along the northern coast of Svalbard extending from western Nordaustlandet to the Molloy Deep (Jokat et al., 2000; Fig. 5-1). In order to complete the presentation of the deep

seismic data off Svalbard this chapter deals with profile AWI-99200. The profile completes a sequence of W-E striking seismic refraction profiles across Svalbard's western continental margin. Thus, a dense pattern of new seismic lines constrains local differences along the margin and provides spatial information about margin segmentation that was mentioned earlier in this thesis (section 3.6 (5)).

Profile AWI-99200 was first modelled by Czuba et al. (in prep). The following discussion of the profile is a second, independent interpretation.

5.2 Data acquisition

Seismic signals were generated by two large volume airguns with a total charge of 92 l. In total 2214 shots were fired. The approximate shot spacing is 175 m along the 430 km long seismic transect (Fig. 5-1; 0°E-17.2°E). The seismic energy was recorded by 11 onshore RefTek seismometer stations located between 10.7°E and 19.8°E (ref201-ref206 and ref208-ref212; one failed). A gap in the RefTek receiver spacing was occupied by an ocean-bottom hydrophone system (obh207; Fig. 5-1). The spacing of seismic stations east of 10.7°E varies between 10 and 37 km. Off the western coastline 14 ocean-bottom seismometer and hydrophone systems were deployed. Due to failures and some poor data quality, only 9 stations are usable for subsequent processing and velocity modelling. Therefore, the station spacing west of 10.7°E varies between 13 and 45 km (Fig. 5-1). The maximum deployment depth of offshore seismic receivers is 5500 m (Molloy Deep; Fig. 5-1) while onshore deployment altitudes do not exceed 30 m.

5.3 Characteristics of seismic refraction data

Generally the data quality of the 19 successful stations is very good. 4 representative data sections are shown in Fig. 5-2 and Fig. 5-3. These sections reveal the basic velocity structure along the northern Svalbard margin. The applied processing sequence and general data characteristics (e.g. phase appearance, correlation) are similar to those discussed in section 2.3.2.

P-phases at near offsets (<10 km) represent low seismic velocities of ~3.8 km/s on either side of station obh207 (p_{cb}; Fig. 5-2a). Beyond, seismic velocities increase to 6.0 km/s in the east, while slightly lower velocities of 5.6 km/s indicate a different lithology in the west. P_g-phases are observed up to distances of 170 km (Fig. 5-2a and b) providing a velocity gradient determination down to depths of 20-25 km. Seismic velocities along the eastern profile section east of km 200, range between 5.8 and 6.9 km/s. Locally, slightly higher seismic velocities of 7.2 km/s are observed (Fig. 5-2a; p_g at km 150-180). P_g-phases exhibit local undulations of traveltime. Four very prominent traveltime undulations are observed at km 190 (u_1), 210 (u_2), 230-240 (u_3) and 280 (u_4) along all data sections. These are associated with basement depth variations below the Cenozoic sedimentary cover. A first-order Moho discontinuity along the entire profile is inferred by deep crustal and mantle phases (Fig. 5-2a). Traveltimes of p_mp-reflections recorded on the western side of obs215 occur only 1 s earlier than to the east of it (at 8 km/s reduced traveltime) pointing to only smooth variations in Moho-depth between km 180 and 300.

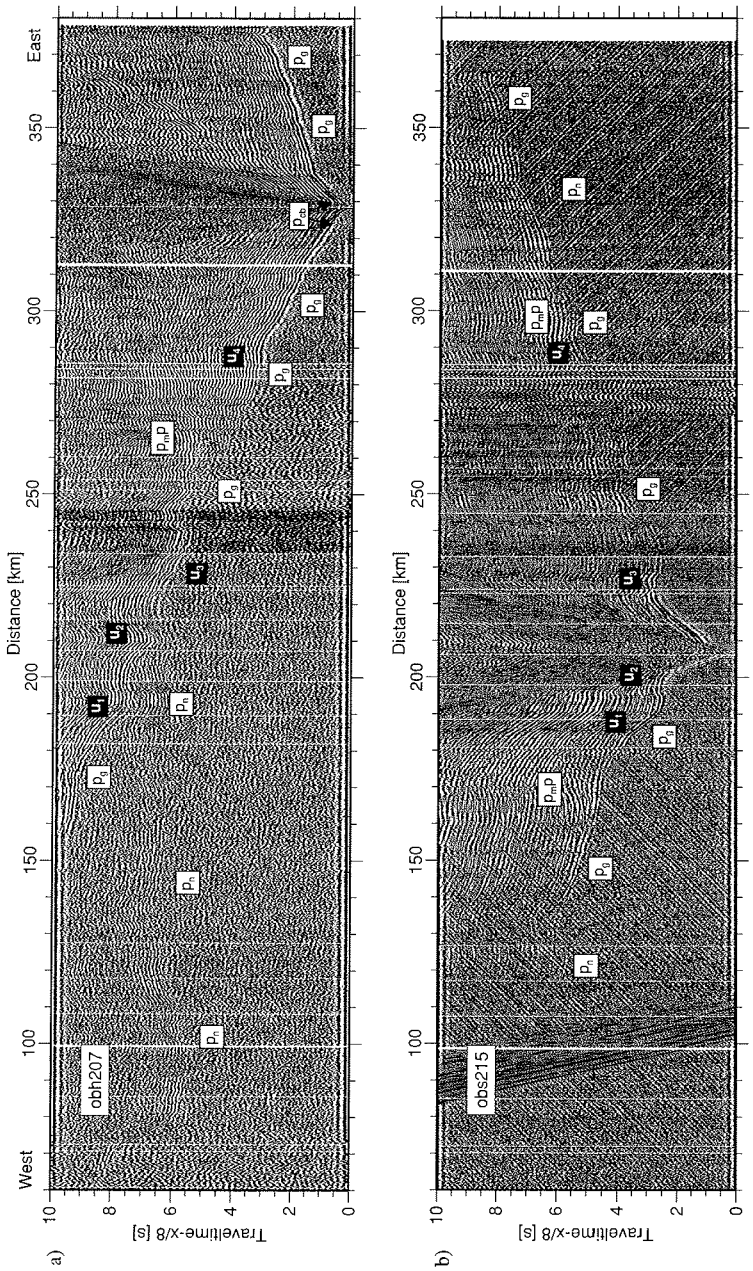

Figure 5-2: Record sections of stations (a) obh207 and (b) obs215.
A bandpass filter, passing frequencies from 5-17 Hz, and a 1 s-automatic gain control, were applied to the data.

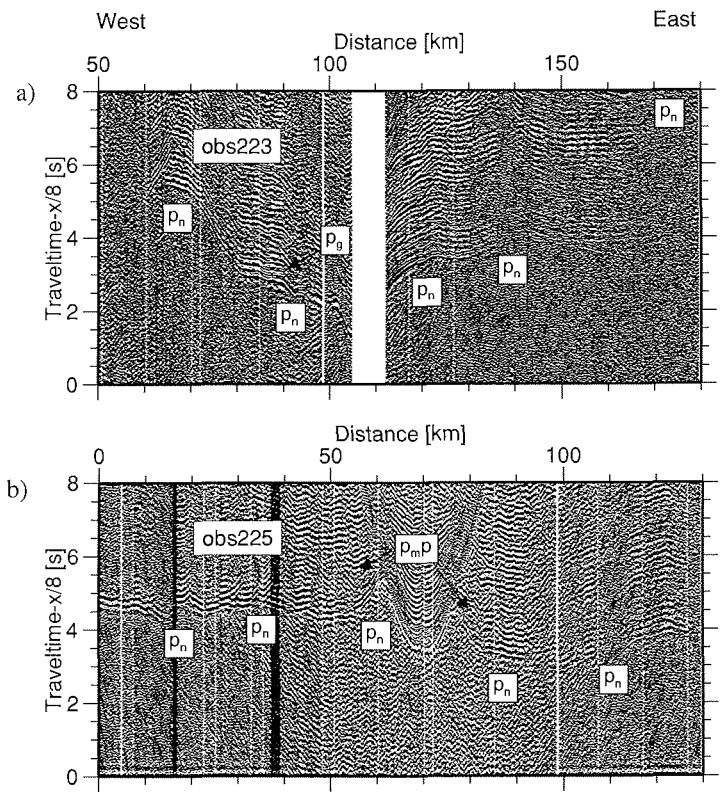

Figure 5-3: Record sections of stations (a) obs223 and (b) obs225.
A bandpass filter, passing frequencies from 5-17 Hz, and a 1 s-automatic gain control were applied to the data.

High velocity phases (>7.6 km/s) dominate sections recorded along the oceanic profile west of km 100 (Fig. 5-3a and b; obs223 and obs225). These appear very early at 3 to 4 s and in close proximity of the receiver. This suggests an extremely thin crustal layer at these locations (Fig. 5-1). Due to a very steep bathymetric slope in the vicinity of the Molloy Deep p_n-phases receive traveltime shifts of 1.5 to 2 s. The failure of the receiver station west of Molloy Deep provides only non-reversed shots west of km 70. Therefore, the velocity structure of the adjacent Hovgård Ridge remains profoundly unconstrained and is not further debated in this study.

5.4 Modelling of seismic data

5.4.1 Modelling procedure

Modelling of seismic refraction data of profile AWI-99200 was performed using the raytracing software *rayinvr* (Zelt & Smith, 1992). The general modelling strategy is similar to that described in section 2.4.

In total ~6300 travel time picks were taken from the seismic sections. About 2900 picks constrain the crust-mantle boundary (Moho-reflections or refracted at the Moho). Due to the large number of traveltime picks the velocity model is densely covered by rays. A selection of 8 examples covering different sections along the profile are shown in Fig. 5-4a-h.

5.4.2 Resolution and uncertainty of the final model

The numerical resolution of the final velocity model was calculated using the inversion method of Zelt & Smith (1992; for methodical details see section 2.4.3). According to the authors, velocity nodes with a resolution greater than 0.5 are considered to be well resolved.

The Cenozoic sedimentary cover between km 100 and 250 is well resolved (Fig. 5-5). Resolutions of 0.6 to 0.9 is calculated. The upper and middle crust of the eastern continental crustal section shows values mostly above 0.6. At deeper levels the resolution decreases rapidly to 0.2-0.4. This is mainly due to sparse diving-wave information penetrating deeper than 20 km. Two zones of slightly higher resolution occur at km 200 and 350 (Fig. 5-5; 0.4-0.8; lower crust). The oceanic crustal section east of km 100 is not well resolved due to the lack of stations and the absence of p_g-phases penetrating the extremely thin oceanic crust. Mantle seismic velocities are well resolved, showing values from 0.3 to 0.9. This is mainly due to the large number of picked p_n-phases.

Uncertainties in depth of the individual layer boundaries are derived by varying nodes of the velocity model up and down until the calculated traveltime no longer fits the assigned error. The assigned errors vary between ±100 ms (mainly upper crust) to ±250 ms (mainly lower crust) and are similar to those chosen for data of profile AWI-99300. The errors of depth level for the current model AWI-99200 can therefore be taken from Table 1 (section 2.4.3), which concludes a maximum depth uncertainty of ~10% of the determined depth level for the upper crust and ~5% for the lower crust.

5.5 The final velocity model and geological interpretation

Fig. 5-6a shows the final velocity structure along profile AWI-99200. It can be subdivided into three sections: East of km 300 an unstretched section of continental crust is present. Between km 110 and 300 a large extended transitional crustal section is observed, while the proximity of Molloy Ridge (km 50 to 110) is made up of very thin oceanic crust.

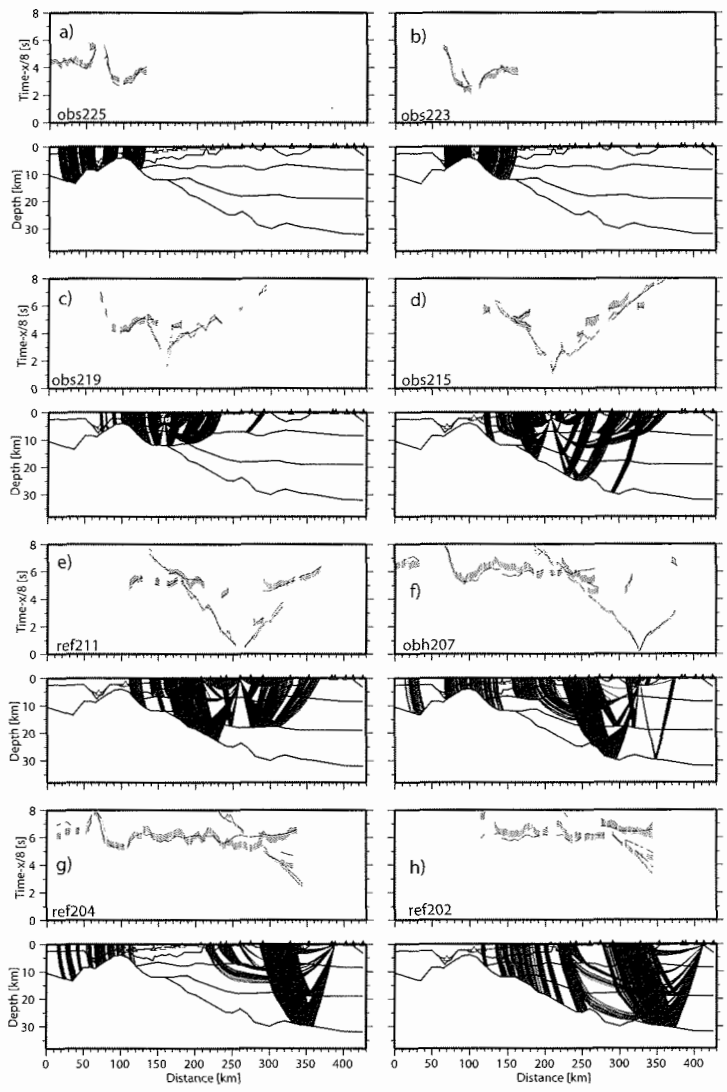

Figure 5-4: Examples of raytracing of data from profile AWI-99200.
The eight examples cover different parts of the refraction transect. The upper parts of a-h show the observed and calculated p-wave arrivals. Grey errors bars indicate the assigned error to the picked traveltimes. Black lines show the traveltimes calculated using the final velocity model shown in Fig. 5-6a. The lower figures a-h are the respective paths for rays calculated by rayinvr (Zelt & Smith, 1992).

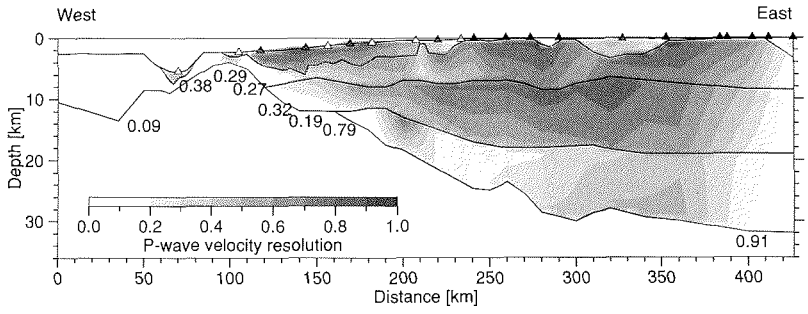

Figure 5-5: Resolution of the final p-wave velocity model along profile AWI-99200. Resolution was calculated according to Zelt & Smith (1992). The greyshade shows the resolution as do point data. Triangles as for Fig. 5-1.

5.5.1 Continental crust

The crustal thickness along this segment varies between 28 and 32 km. It comprises the central and eastern Caledonian terranes which docked along the Billefjorden Fault Zone (Fig. 5-1 and Fig. 5-6).

The onshore geology exhibits a Late Silurian-Devonian Basin (Harland, 1997a) between km 270 and 320, that is characterised by seismic velocities of 5.3 (5.6) to 5.8 km/s (cf. Jackson, 1990; Hajnal et al., 1990; and section 3.4.2). East of km 320 (obh207) metamorphic rocks of the Hecla Hoek province are present (Harland, 1997a). The seismic velocities are slightly higher at the top of the crust and exhibit values up to 5.9 km/s. Three shallow sedimentary basins with low seismic velocities of 2.4-5.2 km/s (CB1, CB2 and CB3) are observed within the uppermost crust and are interpreted to be Mesozoic to Cenozoic in age (Fig. 5-6).

The deeper crust shows seismic velocities between 6.0 and 6.9 km/s. Both Caledonian terranes exhibit a deep crustal reflector at ~20 km depth. Amundsen et al. (1987) proposed layered pyroxenites/lherzolites at this depth. At km 310 seismic velocities at the crust-mantle boundary increase slightly to about 7.2 km/s. The seismic velocity distribution mirrors observations made along the profiles AWI-99300 and AWI-99400, therefore a similar composition of the deeper crust is suggested (i.e. granulites/mafic granulites; see sections 2.6.1 and 3.4.2).

5.5.2 Extended continental crust

The continent-ocean transition along profile AWI-99200 is characterised by a broad zone of continental thinning (~190 km; Fig. 5-6). The total crustal thickness wanes from ~30 km to 10 km. The overlying 8 km thick Late Paleozoic sedimentary basin is also observed along this section. Offshore, a 4 to 5 km thick sedimentary wedge is present, showing velocities of 2.4-3.2 km/s. These sediments and sedimentary rocks are interpreted to be Cenozoic in age (Eiken & Austegard, 1987; Eiken, 1993). Below the Cenozoic cover seismic velocities of 5.2 to 5.6 km/s are observed. In the discussion of section

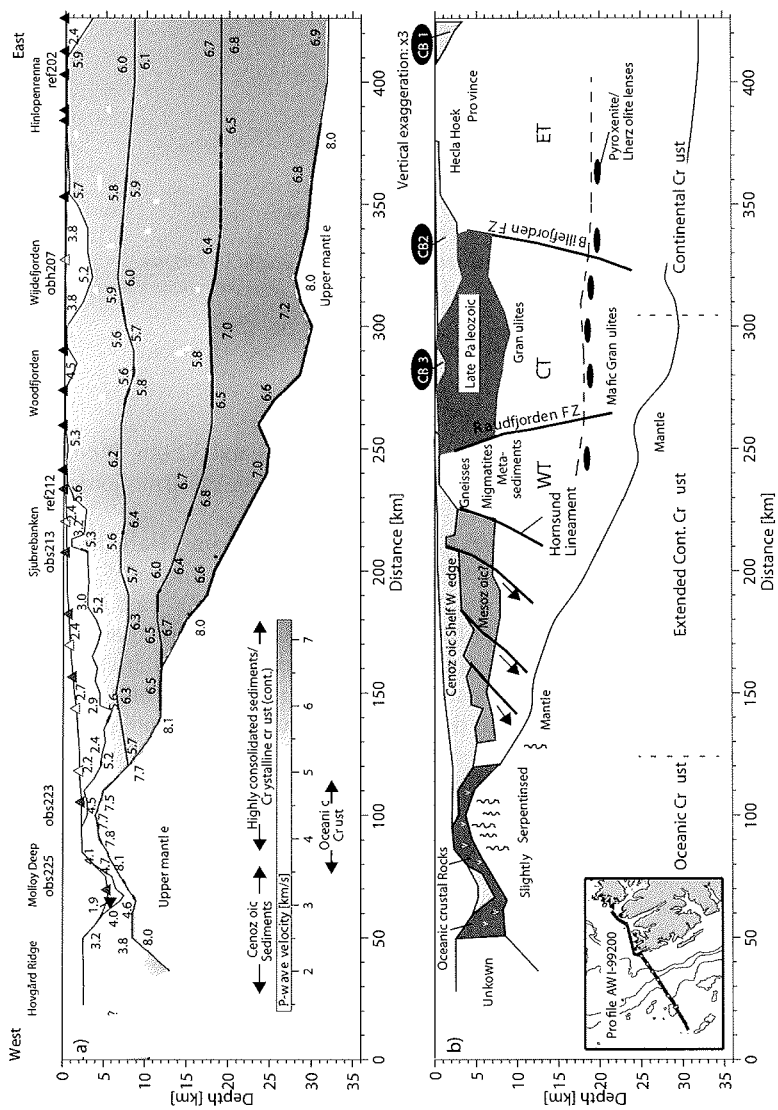

Figure 5-6: Final p-wave velocity model for profile AWI-99200 (a) and geological interpretation (b). *The greyshade shows the seismic velocity field as do the annotated contour lines. Triangles as for Fig. 5-1. The annotated greyscale below gives a rough interpretation of seismic velocities. Geological interpretation of the velocity model: Generally, crystalline continental crust is coloured white, oceanic dark grey. CB: Cenozoic sedimentary basins. WT: western terrane, CT: central terrane, ET*

3.4.1 (off Van Mijenfjorden) a similar crustal layer is interpreted as consolidated Mesozoic sedimentary rocks (Mann & Townsend, 1989). The boundary between Cenozoic and older sedimentary rocks shows varying depth between km 120 and 230. Seismic reflection profiling of Eiken (1994) shows at least two east-tilted continental blocks at the northern Hornsund Lineament (Fig. 5-1). According to the basement topography of the Pre-Cenozoic sedimentary rocks, further block-bounding faults are assumed west of the Hornsund Lineament leading to a rotated fault block-construction between km 120 and 230 (Fig. 5-6b).

Gneisses, migmatites and metasedimentary rocks are known from onshore geological mapping in the northwestern onshore basement province (Hjelle, 1979; Harland, 1997b) and are thus expected for the region between the sedimentary basins (Fig. 5-6b).

5.5.3 Oceanic crust

Crustal seismic velocities along the oceanic section range from 3.2 to 4.1 km/s at the top to 4.6-4.7 km/s at the base (Fig. 5-6a). The entire thickness varies between 1.5 and 4 km. Seismic velocities reflect the absence of layer 3, a general feature of oceanic crust adjacent to Svalbard's western continental margin (cf. sections 3.4.4 and 4.5.3). The profile is unreversed west of obs225 (km 70) so that the velocity structure of the adjacent Hovgård Ridge remains ambiguous. Low seismic velocities of 3.2 km/s for the upper oceanic basement are similar to those found along profile AWI-99400 (section 3.4.4).

Seismic velocities in the upper mantle are not homogeneously distributed. Between km 80 and 130 a total range of 7.5 to 8.1 km/s is modelled. But low velocities are restricted to the areas below the thin oceanic crust and the continent-ocean transition, where serpentinised mantle peridotites are expected (Detrick et al., 1993). Similar seismic velocities are found along profiles AWI-99400 and AWI-97260 (sections 3.4.4 and 4.5.3) where 20% serpentinisation of upper mantle peridotites is expected (according to Christensen, 1966 and Minshull et al., 1998).

5.6 Brief discussion of Profile AWI-99200 with respect to the continental margin

Profile AWI-99200 is located 100-150 km north of profile AWI-99400. The continental margin observed along the latter profile is interpreted as a sheared margin, since the transition from continental to oceanic crust is marked by an abrupt decrease in Moho-depth (chapter 3). In contrast, the structural style of the margin along profile AWI-99200 exhibits an extremely broad zone of crustal thinning (~190 km). A further difference is the absence of seismic velocities greater than 7.2 km/s that are interpreted as intrusions (a rival interpretation is given by Czuba et al. (in prep.), cf. section 3.4.3). The continental margin surveyed off northern Svalbard can instead be classified as a non-volcanic rifted margin since no significant amount of melt is modelled in the lowermost crust.

The profile over the oceanic lithosphere west of km 110 crosses obliquely the region between the Molloy Transform Fault, Spitsbergen Fracture Zone and Molloy Ridge (Fig. 5-1). The generally sparse magmatism is also represented in the very thin oceanic crust.

As observed along the transects off Kongsfjorden and Van Mijenfjorden it lacks a gabbroic layer 3 and is therefore thinned compared to the global mean.

CHAPTER 6:
A CONCLUDING TECTONIC BREAK-UP MODEL FOR WESTERN SVALBARD AND THE FRAM STRAIT

Within this chapter the newly derived structural information along the seismic refraction transects (Table 3) is used to improve and upgrade the most recent plate tectonic reconstruction of Boebel (2000). The schematic evolution models discussed for the Svalbard margin off Kongsfjorden (section 3.5) and off Van Mijenfjorden (section 4.6) focused on the local continental margin and the West Spitsbergen Orogen. On the basis of the magnetic anomaly field observations of Verhoef et al. (1996) these models will be extended to the western Yermak Plateau. The spatial magnetic field observations offer a good prospect to refine the break-up model of Svalbard and northeast Greenland.

6.1 Evaluation of the reconstruction of Boebel (2000)

The proposed plate boundary between northern Greenland (North American Plate) and Svalbard/Yermak Plateau (Eurasian Plate; Fig. 6-1) is defined using structural interpretation of density models based on airborne gravity data over the Fram Strait (Boebel, 2000). In detail, crustal models of Boebel (2000) exhibit large differences to those using the high-resolution seismic refraction transects discussed in this thesis. Nevertheless, the gross classification of crustal types agrees reasonably well with those discussed. The geographic locations of plate bounding elements (mid-ocean ridges and transform faults) fit well to the information derived from velocity modelling.

6.2 Magnetic anomalies along the western Svalbard/Yermak Plateau continental margin

Fig. 6-1 shows the magnetic anomaly along Svalbard's western continental margin and the Yermak Plateau (after Verhoef et al., 1996). The most prominent (positive) anomalies of 700 to 900 nT are observed on the northeastern Yermak Plateau. Feden et al. (1979) and Jackson et al. (1984) supposed a mantle plume magmatic origin for these anomalies, but a rifted volcanic history is excluded by the analysis of profile AWI-99300 (chapter 2). Further anomalies occur en echelon along the western Svalbard and Yermak Plateau continental margin (WSYA, Western Svalbard/Yermak Plateau Anomalies; Fig. 6-1):

- WSYA1 extends ~90 km from the southern Bellsund to the Hornsund (see also Fig. 3-1) and has an extension of ~80 km perpendicular to the coastline. The peak-to-peak amplitude of WSYA1 is ~700 nT.
- Off Prins Karls Forland and Kongsfjorden two peaks of ~65 and ~85 nT make up WSYA2. This anomaly has a higher aspect-ratio of ~110 km along and

Table 3: Crustal features along the new seismic refraction profiles.

Profile	Type of margin	Magmatism	Adjacent Oceanic Crust and underlying mantle	Prominent Magnetic Anomalies (see. Fig. 6-1)
AWI-99300 Yermak Plateau	non-volcanic	N-S Simple Shear extension, decompressive melting at 17-22 km depth	-	10°E/80°N Southern Danskøya Basin/ Sjubrebanken, ~150 nT
AWI-99400 Kongsfjorden	sheared non-volcanic	slight intrusions into the lower/middle crust at the shear at 9-22 km depth	layer 3 absent	9°E/78.8°N off Prins Karls Forland 180-200 nT, WSYA2
97260 & profile 9 Van Mijenfjorden	rifted non-volcanic	slight intrusions into the lower/middle crust near the cont.-ocean transition at 14-23 km depth	layer 3 absent	12°E/77°N Southern Bellsund, ~700 nT, WSYA1

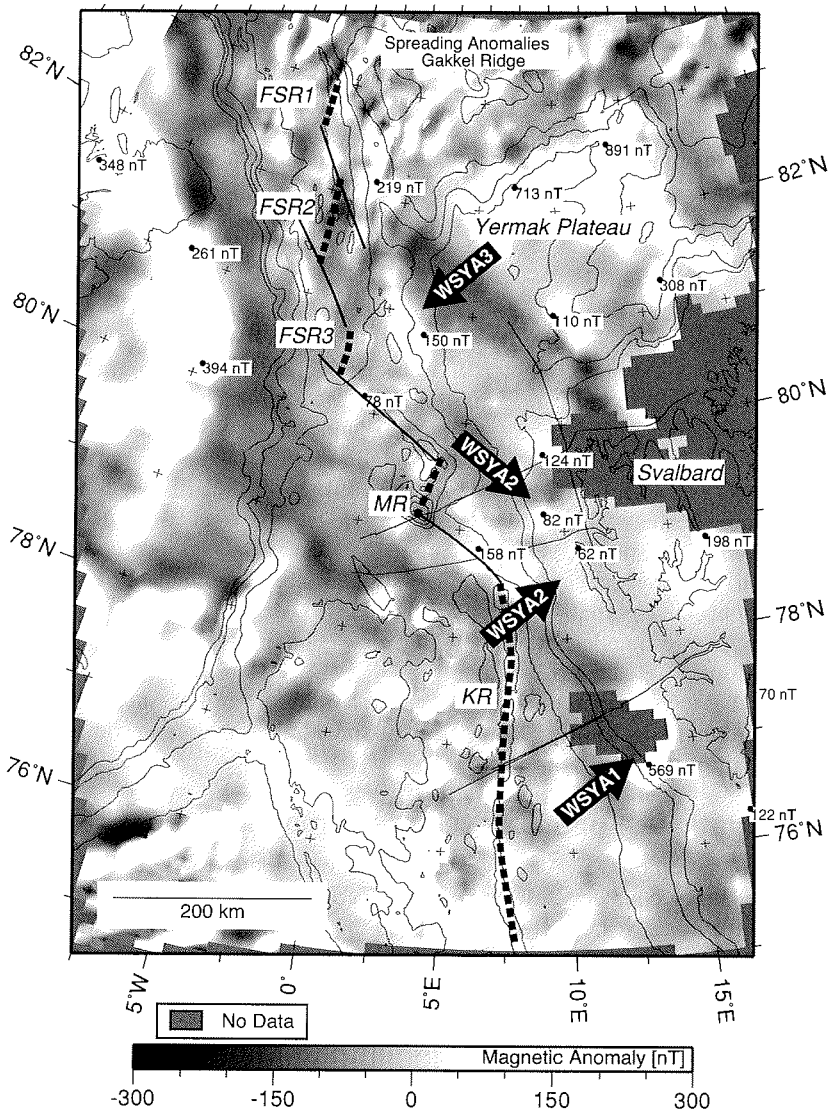

Figure 6-1: Magnetic anomaly after Verhoef et al. (1996).
Data were re-gridded at 0.5°x1°. Thick black arrows (WSYA1, 2 and 3) point to the locations of positive magnetic anomalies along the western margins of Svalbard and the Yermak Plateau. Plate boundary after Boebel (2000; thick dashed lines: ridges; solid lines transform faults and fracture zones). Also plotted as black lines are the locations of the seismic refraction profiles discussed in this thesis. Bathymetry after Jakobsson et al. (2000). KR: Knipovich Ridge, MR: Molloy Ridge, FSR1 to 3: Fram Strait (mid-oceanic) ridge segments.

~50 km across the margin compared to WSYA1. The total peak-to-peak amplitude is approximately 180 to 200 nT.

- The western rim of the central Yermak Plateau shows a similar elongated but slightly stronger anomaly WSYA3 (~320 nT peak-to-peak). According to profile AWI-99300 (section 2.7.1; Fig. 2-16) this anomaly is expected to be located on the margin of a segment of stretched continental crust.
- A further small anomaly is observed at 81.5°N/2.5°W. It is associated with the seafloor spreading anomaly pattern north of 82°N (~400 nT peak-to-peak; Fig. 6-1).

The locations of WSYA1 and WSYA2 coincide with the locations of slightly elevated seismic velocities along the profiles AWI-97260 and AWI-99400 (Fig. 6-1; Table 3). Both margin sections are interpreted to have been affected by slight magmatic intrusions, associated with the proximity of a mid-ocean ridge segment (Knipovich and Molloy Ridges) to the continental margins (section 3.4.3 and 4.5.2). WSYA3 occurs similarly to WSYA1 and 2 at the southeastern extremity of a Fram Strait spreading corridor, here the segments FSR2 and FSR3 (Fig. 6-1). Therefore, a likely tectonic history is suggested for central western Yermak Plateau that entails a similar geophysical observation: minor mantle derived magmatic intrusions contaminate the adjacent stretched continental crust and create a thermo-remanent magnetic field. Possibly, the magmatic activity was induced by convective partial melting due to the close proximity of cool continental crust and the hot oceanic mantle below the new ridge (Mutter et al., 1988; Lorenzo et al., 1991; see section 3.4.3 and 4.5.2).

It seems, that the segmentation of the Western Svalbard-Yermak Anomalies (WSYAs) is on the same basis as the recent and ancient spreading corridors in the neighbouring mid-oceanic ridges in the Fram Strait.

6.3 Evaluation of possible remanent magnetisation

The interpretation of WSYA1 to WSYA3 as the expression of thermo-remanent magnetisation of intrusive materials depends on the Curie temperature not being trespassed in the depth of the intrusives. After Fowler (1995) the maximum temperature for maintaining remanent magnetisation is about 580°C for magnetite and 680°C for haematite. According to the observations along the seismic refraction profiles, magmatic intrusives occur between 9 and 22 km depth along the western continental margin (Table 3). A standard geotherm for extended continental crust reveals a temperature level of ~400 to 600°C for this depth range (Fowler, 1995). Based on petrological analysis of xenoliths from northwestern Svalbard the constructed geotherm exhibits high temperatures of 780°C for a depth of ~15 km (5 kbar). Amundsen et al. (1987) ascribe the elevated geotherm to the high heat flow observed on the south-central Yermak Plateau (Crane et al., 1991) and estimate the Curie-"depth" of magnetite is only 6-8 km.

An opposing geotherm estimation is of only 450°C within the upper mantle at depths of 25 km off the western Barents Sea margin (Breivik et al., 1999). This geotherm comes from thermal modelling of the lithosphere considering conductive cooling across a sheared continental margin.

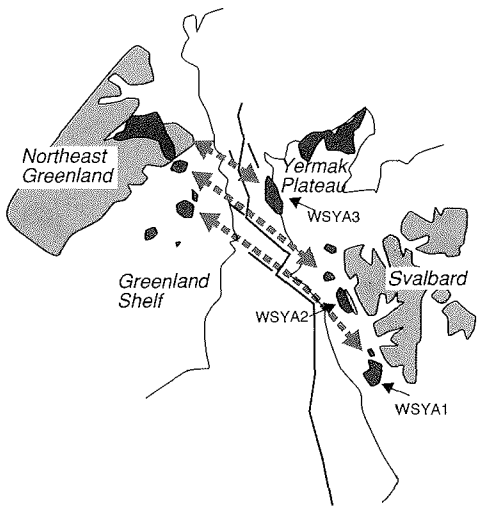

Figure 6-2: Magnetic anomalies on either side of the Fram Strait.
Grey thick arrows point to the possible counterparts of WSYA1 to WSYA3. The positive anomalies of Greenland are stronger and more homogeneous, which might result from a cooler geotherm due to a larger distance to the Fram Strait spreading system.

The effect of non-volcanic rifted crust and the oceanic rift axis adjacent to the continental margin on the geothermal gradient is debatable. Schlindwein & Jokat (1999) conclude that probably only the upper parts of intrusives along the East Greenland margin are lying above the Curie temperature. As the observed positive magnetic anomalies WSYA1 to WSYA2 coincide very well with the locations of the lower crustal volcanic bodies, and these are likely to be below the Curie depth, a remaining source within the upper sections is expected.

Along the conjugate margin of northern Greenland similar en echelon positive magnetic anomalies may be the counterparts to WSYA1-3 (Fig. 6-2). Schlindwein (1998) emphasizes that these anomalies interrupt the magnetic fabric of Greenland's N-S striking Caledonian fold belt, and that they are thus probably intrusive-sourced. The stronger and more homogenous appearance of the northern Greenland anomalies may result from a more distant location from the mid-oceanic ridges (a decreased geotherm) or from shallower source depths.

6.4 A recurring scenario during the entire break-up?

6.4.1 A hypothesis

Table 3 summarises the observed nature and style of continental margin off western Svalbard. The 400 km long continental margin is more segmented than previously

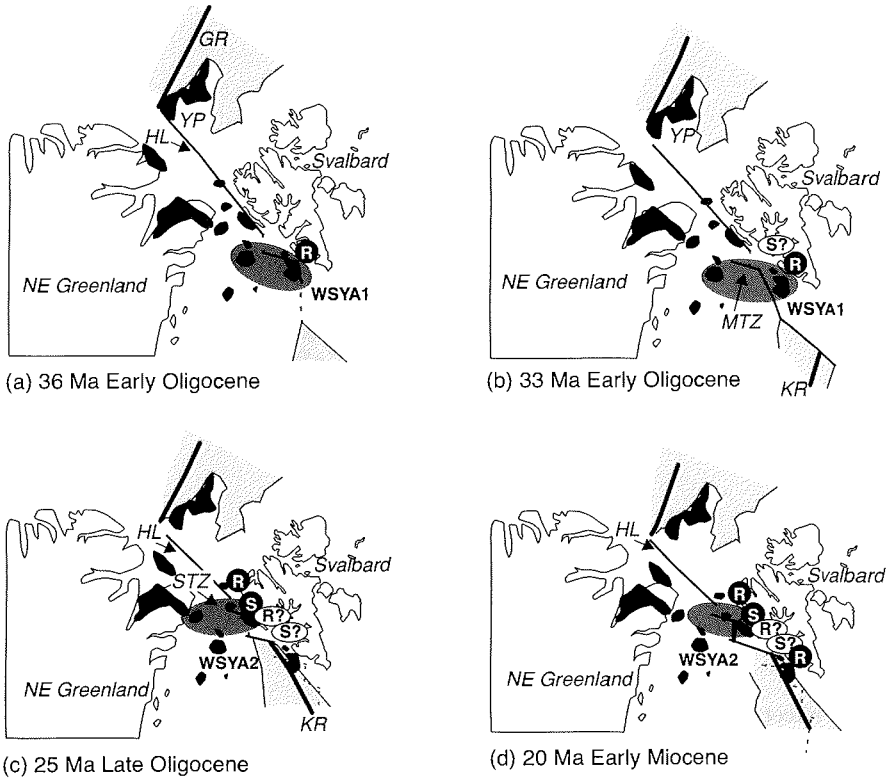

Figure 6-3: Schematic plate tectonic reconstruction based on Boebel (2000).
(YP) Yermak Plateau, (STF) Spitsbergen Transform Fault, (MTF) Molloy Transform Fault, (HL) Hornsund Lineament, (KR) Knipovich Ridge, (GR) Gakkel Ridge, (FSR) Fram Strait Ridge, (MJR) Morris Jesup Rise. White: continental crust; Black: Magnetic Anomalies (see Fig. 6-2); light grey: oceanic crust; dark grey: zone of magmatic exchange. R: Rifted. S: Sheared.

thought. The segmentation is achieved on the basis of fracture zones which are connected to active transform at the recent ridge crests in the Fram Strait. As a consequence, a rifted margin (AWI-97260), a sheared margin (AWI-99400) and a further very broad rifted margin (AWI-99200) are observed off western Svalbard (Table 3). This margin segmentation, the magnetic signature of the margin and the construction of the spreading ridge system in the Fram Strait give rise to the assumption that a recurring scenario took place during the break-up of Svalbard and Greenland that comprises the following steps:

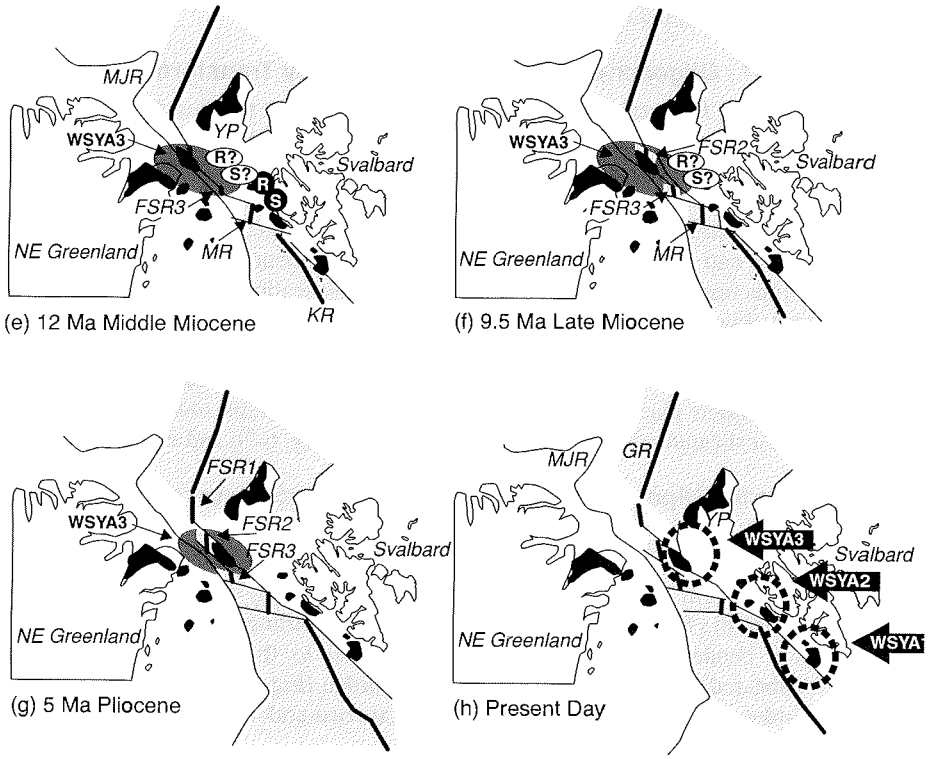

Fig. 6-3: Continued.

➥ Northward propagation of the spreading system and development of a new transform fault at its tip

N' ➥ Shearing of the continental margin

● Magmatic intrusions

S' ➥ Rifting of the continental margin adjacent to the young rift

➥ Northward migration of the spreading system through the rifted continental margin and development of a transform fault at its tip

Fig. 6-3a-h summarises this evolution schematically using the break-up model and suggested timing of Boebel (2000).

6.4.2 Episode I - Oligocene: Knipovich Ridge/Molloy Transform Fault

In the Oligocene the northward migrating Knipovich Ridge reached the southern tip of Svalbard (Boebel, 2000; Fig. 6-3a and b). This region was undergoing crustal thinning due to the transtensional tectonic regime (Müller & Spielhagen, 1990). Melt was injected into the young rifted crust (profile AWI-97260; WSYA1). Injection may have occurred along the Late Paleozoic Spitsbergen Shear Zone (Crane et al., 1991; the main suture between Eurasia and Greenland) and the Hornsund Lineament (Eldholm et al., 1987). Possibly the injection took place coincident with the first seafloor spreading adjacent to the rifted crust (Fig. 6-3c). The southernmost transform fault of the Fram Strait system (the Molloy Transform Fault) developed during the latest stage of the Oligocene. The Molloy Transform Fault strikes parallel to the Spitsbergen Transform fault and runs towards the Isfjorden like the Spitsbergen Transform Fault runs towards the Kongsfjorden. Hence a sheared margin off Isfjorden is formed (Fig. 6-3b and c)

6.4.3 Episode II - Oligocene/Miocene: Molloy Ridge/Spitsbergen Transform Fault

In the Late Oligocene/Early Miocene a new intracontinental transform evolved: the Spitsbergen Transform Fault. Earliest spreading at the Molloy Ridge is not expected prior to 20 Ma in the Early Miocene (Boebel, 2000). According to the results of profile AWI-99400, a bended southward progression parallel to the continental margin is observed. A sheared margin developed off Kongsfjorden (Fig. 6-3c-e). As observed off Van Mijenfjorden, melt was injected into continental crust under these conditions.

6.4.4 Episode III - Miocene: Fram Strait Ridges/Fram Strait Transform Faults

Transtensional tectonics and crustal thinning persisted longest off the northern rifted margin, where the broadest transition between unstretched continental and oceanic crust is observed (chapter 5). Also, oblique directed extensional movements thinned the northwesternmost crust of Svalbard (see chapter 2; simple shear tectonics). During the Middle and Latest Miocene (12 to 9.5 Ma) the northernmost section of the Hornsund Lineament (the rifting boundary) was gradually replaced by a mid-oceanic ridge plate boundary (Boebel, 2000; Fig. 6-3e and f). The Fram Strait Ridge segments are separated by large offsets of approximately 100 km. The strike of the separating transform faults is oblique to those further south. Their trends are parallel to the present day 2000 m-bathymetric contour, that roughly follows the continental margin here (Fig. 6-3f). Hence, a sheared margin evolution is also likely for the stretched continental Yermak Plateau (eastern terrane of Svalbard; section 2.7.1). Since the spreading system is in the same close proximity to the margin as further south, and the magnetic field shows a pronounced anomaly, intrusion of magma seems likely under similar conditions as within episodes I and II (Fig. 6-3e-h).

6.4.5 Discussion

The available geophysical information suggest that a simple evolution scenario recurred along the western margin of Svalbard and the Yermak Plateau. The magnetic anomalies WSYA1 and WSYA3 are entirely positive indicating a (short?) period of melt injection confined to a normal polarity interval. In contrast, WSYA2 exhibits a smooth central low at 79°N that may indicate injection during a geomagnetic reversal. Despite the central low on anomaly WSYA2 the majority of the anomaly exhibits positive values. There is no reason why melts should be intruded only in normal polarity chrons. The reversal process is random, and it may occurred during any given margin building episode.

But this hypothesis may give constraints on the prediction for the age of the actual break-up of the Fram Strait. Spreading anomalies are not observed within the northernmost Atlantic off western Svalbard (Fig. 6-1), and a detailed reconstruction using spreading anomaly ages is not possible. The suggested model should provide a new contribution for the discussion of possible ages for the break-up of Svalbard and Greenland. Certainly, this suggestion has to be tested and refined by plate tectonic modelling incorporating the reconstruction of Boebel (2000).

CHAPTER 7: SUMMARY AND PROSPECT

This chapter itemises the main results discussed in the previous chapters. Further, It summarises the main outstanding problems following the research activities discussed in this thesis. It also provides possible guidelines for future projects.

7.1 Summary

With respect to the aims of this thesis given in section 1.1 the main results are:

- Svalbard is supposed to be a composite of three allochthonous Caledonian terranes separated by major sinistral strike-slip faults (Fig. 1-1; Harland & Wright, 1979). The different lithologies across the terranes cannot be told apart by the seismic velocity structure, but the bounding suture between the western and central terranes coincides with the position of the West Spitsbergen Fold Belt and exhibits low seismic velocities. This may be the result of reactivation of the old sutures during Cenozoic transpressive movements, and led probably to the decoupling of the western terrane from central Svalbard, since crustal thinning is seen only in the western terrane.
- A rifted volcanic evolution for the Yermak Plateau associated with a mantle plume (Yermak Hot Spot; Feden et al., 1979; Jackson et al., 1984) can be excluded since the crust shows no large-scale volcanic features, although old and weak shear zones in the lithosphere are suggested to have provided ideal pathways for channelling and distribution of small amounts of magma (Spitsbergen Shear Zone; Crane et al., 1991). The southern Yermak Plateau shows a mid-crustal detachment originated by extensional movements in the Oligocene. Slight amounts of intrusions are associated with decompressive melting during crustal thinning. The Cenozoic detachment tectonics and subsequent basin subsidence are similar to the tectonic milieu proposed for the Late Paleozoic (Friend et al., 1997), but exhibit an opposite sense of movement (sinistral-dextral).
- The Late Paleocene/Eocene Spitsbergen Orogeny affects an extremely narrow belt along the western Svalbard margin. It is characterised by low seismic velocities that suggest the complete shearing and faulting of the brittle rock construction. With regard to these observations, the flower structure model of Lowell (1972) during the transpressive movement between Svalbard (Eurasia) and Greenland (North America) seems plausible.
- The continental margin off western Svalbard and the Yermak Plateau is more segmented than previously thought. Sheared and rifted segments are observed along the margin off western Svalbard. In the case of the margin off Kongsfjorden the sheared evolution is associated with the Spitsbergen Transform Fault in the southern Fram Strait. A common feature of the continental margin

off western Svalbard is the presence of slight amounts of mantle derived melt in the deeper crust. Since a hot spot related evolution is excluded for the western margin, the close proximity of the oceanic spreading centre is the suggested source. Due to the large thermal contrast between cool rifted crust and hot ascending mantle at the ridge convective partial melting may be initiated (Mutter et al., 1988). The zones of slight magmatic intrusion coincide with magnetic anomalies observed along the entire Fram Strait margin. A combined inspection of the most recent plate tectonic reconstruction of the Fram Strait (Boebel, 2000), the observed margin segmentation and intruded zones, shows that the segmentation probably continues adjacent to the Yermak Plateau.

- The slow spreading mid-oceanic ridge system off western Svalbard generates thin oceanic crust that shows no gabbroic layer 3. The underlying upper mantle exhibits low seismic velocities and is therefore most probably serpentinised.

7.2 Outstanding problems

7.2.1 Oceanic crust generated along the northern Knipovich Ridge

A concurrent analysis of seismic refraction data by the University of Bergen (Norway) between the Hornsund and the Knipovich Ridge (southern Svalbard margin; Fig. 4-1) reveals a different interpretation of first arrivals that constrain the velocity structure of oceanic crust (Ljones et al., subm.). The crustal section covered by the seismic transect is located ~100 km south of the Van Mijenfjorden transect (AWI-97260/profile 9; chapter 4). Ljones' et al. (subm.) interpret refracted phases beyond 10 km offset as arrivals from the middle and lower crust (p_g-phases). This leads to a three-layer model with the presence of a ~4 km thick oceanic layer 3 with velocities ranging from 6.6 to 7.2 km/s. A comparison of the data sections and the proposed interpretation of Ljones et al. (subm.) with those off Van Mijenfjorden (this study; section 4.3.2, see Fig. 4-3) exhibits a different inferred crustal structure at nearly similar data sections, since the absence of oceanic layer 3 is proposed in this thesis (i.e. a two-layer case; p_g-phases are interpreted as p_n-phases).

Whether or not the sub-sedimentary first arrivals represent crustal (Ljones et al., subm.) or mantle phases (this thesis) may be the basis of an enhanced comparative amplitude modelling. The velocity gradients within both proposed models differ greatly so that a comparative study of the real observed amplitudes can clarify the controversy of ambiguous phases.

7.2.2 Oceanic mantle construction

The structural interpretation of the oceanic upper mantle off western Svalbard is based on a p-wave velocity model. Observed s-wave phases are of poor quality. The observed oceanic mantle is mainly built up of partial serpentinised peridotites, since the seismic velocity is lower than usually expected for mantle type rocks. According to laboratory measurements on serpentinites of Christensen (1966) a serpentinisation of 20 to 30% is proposed. Serpentinites are characterised by a generally high Poisson ratio of 0.35, the highest observed within oceanic ophiolite complexes (Christensen, 1978). To

confirm and refine the suggestion of a partially serpentinised oceanic mantle, a systematic search for weak s-wave arrivals on the seismic sections has to be carried out. As serpentinisation is suggested to prefer tectonic weak zones the distribution of the Poisson ratio in the upper mantle would support the search for such localities (e.g. fractures). Beyond this a better density model can be calculated for solving conflicts with the results of density modelling (see next section).

7.2.3 Thermal construction of the lithosphere

Free-air gravity modelling along the transects off Kongsfjorden and Van Mijenfjorden using initial density models (by converting seismic velocity to density) reveal large positive deviations of calculated free-air gravity above the oceanic crustal sector. Off Van Mijenfjorden the effect of thin oceanic crust and a "normal density" mantle derives a mismatch of ~150 mGal. The presence of an oceanic layer 3 decreases the intensity of this effect, nevertheless a major residual effect remains.

Similar effects are reported by several authors who worked in the Arctic realm (e.g. off western Barents Sea, Breivik et al., 1999; East-Greenland's Fjordregion, Schmidt-Aursch, 2002; southwestern Labrador Sea, Funck & Louden, 1999). As discussed in section 4.3.5 one possible approximation is given by thermal modelling of the lithosphere. Breivik et al. (1999) model lithospheric thermal structure by heat conduction across the sheared Senja margin. After converting the modelled mantle temperatures to density, calculated free-air gravity was decreased by >100 mGal and provides a better fit to the observed gravity field. The proximity of the hot oceanic lithosphere off western Svalbard to the cooler continental margin is mentioned several times in this thesis. Induced convective partial melting was considered to derive slight amounts of melt along the margin off Kongsfjorden. Hence, the thermal construction of the deeper lithosphere of the northern Greenland/Svalbard region is supposed to be more complex. A "thermal" approach may derive a better fit in gravity modelling.

7.2.4 Magnetic modelling

The magnetic anomalies along Svalbard's west coast that coincide with the zones of slightly elevated seismic velocity are interpreted as magmatic bodies carrying a positive remanent magnetisation. Modelling of the magnetic field is necessary to constrain this assumption. This can clarify if only a remanent magnetisation of the uppermost magmatic body can induce the observed anomalies. A depth-to-source estimate may also provide additional constraints on the thermal structure of this region.

7.3 Proposals for future activities

7.3.1 Improving the plate tectonic break-up model

The plate tectonic model of Boebel (2000) should be improved by entering newly derived constraints on

- (i) the position of the Hornsund Lineament,
- (ii) the continuation of Molloy-, Spitsbergen and Fram Strait Fracture Zones (which separate),

- (iii) the continental margin into sheared and rifted sections and
- (iv) the magnetic signature along the Svalbard and Greenland margin.

The timing and duration of continental break-up is merely based on geometric constraints, since no spreading anomalies are present above oceanic crust. Further, the possible remanent magnetisation of the intrusives along the western Svalbard and Yermak Plateau margin may allow an age prediction for these anomalies and derive estimations on the break-up timing.

7.3.2 3D Gravity model

After the successful improvement of the plate tectonic break-up model (section 7.3.1) and the determination of the thermal state of the deeper lithosphere along the seismic transects (section 7.2.3), the crustal structure can be extrapolated to the Fram Strait/Northern Greenland region more reliably than before (i.e. Boebel, 2000). A spacial approach would enhance control on 3D effects due to steep bathymetric features like the Molloy Deep. The implementation of the regional 3D thermal structure of the lithosphere might answer questions concerning the sphere of influence of the North Atlantic mantle plume and possible astenospheric magma channelling below a lithospheric weak zones (thinspots).

7.3.3 Seismic data across the northern Yermak Plateau and at the conjugate margin

The new seismic refraction data discussed in this thesis, and further seismic experiments by the University of Bergen, Hokkaido University, etc. (e.g. Mjelde et al., 1998), showed that the crustal structure off Svalbard, the Yermak Plateau and the Barents Sea is more complex than previously resolved. The use of a close receiver spacing and a dense offshore shot pattern provides a good base to resolve such details. The western Svalbard margin is satisfyingly covered by seismic transects. But the break-up scenario for the Fram Strait and the structure of the northern Yermak Plateau, is only based on extrapolation from the southern seismically-constrained regions.

Seismic refraction data north of 81.5°N would give a detailed crustal model of the northern Yermak Plateau and its magnetic high zone. The proposed separation of the western margin and the crustal structure of the oceanic province of the Fram Strait can be clarified. The seismic investigations can be expanded to the conjugate, northern Greenland margin. The new knowledge about the crustal construction of the Svalbard margin, and the proposed plate tectonic model, gives a framework to guide the siting of seismic transects along the conjugate margin in order to test the suggested segmentation. As on the Svalbard margin, questions of magmatic influence, margin segmentation, geothermal construction, etc. can be addressed.

Seismic surveying in the Arctic realm is due to capricious ice-conditions for either the cruise planning or the field campaign, difficult to perform. During the German-American two-ship experiment in 2001 in the Gakkel Ridge region (Jokat et al., 2002), seismic refraction data were gathered using a leading "icebreaking" ship and a following "shooting" seismic ship. Wide-angle receivers were deployed on floes, to avoid risky deployment of ocean-bottom devices in a widely ice-covered region. This technique yielded a

deep seismic transect some 100 km long that provides detailed information on crustal structure. In order to improve the data base on Arctic crustal structure it is recommended to arrange further such international cooperations.

7.3.4 Local high-resolution seismic experiments along Caledonian detachments

As discussed in section 2.6.2 the simple shear tectonics of the southern Yermak Plateau are comparable to those inferred from onshore geological mapping (Friend et al., 1997; Woodfjorden Region). The Woodfjorden would provide an excellent opportunity to carry out seismic refraction and reflection experiments to compare geophysical information with the exposed onshore geology. In order to enhance resolution in the sedimentary record, the faulted block construction and image the detachment for the first time, a combined seismic reflection/refraction experiment may help. A 3D seismic refraction setup would provide enhanced geometrical information, since the dip of the proposed fault plane is not resolvable with a single 2D seismic line.

ACKNOWLEDGEMENTS

I thank sincerely my doctoral advisor Prof. Dr. Heinrich Miller who enabled me to write this thesis at the University of Bremen (Fachbereich 5 Geowissenschaften) and the Alfred Wegener Institute for Polar and Marine Research (AWI) in Bremerhaven. In addition many thanks go to the second referee of the University of Bremen, Prof. Dr. Ulrich Bleil.

I acknowledge the cooperation with Dr. Wilfried Jokat onboard *RV Polarstern* during the acquisition of the seismic data on the cruises ARK13/3 and ARK15/2 ('97/'99). Further, I thank him for many scientific discussions between a geologist and a geophysicist at the AWI in Bremerhaven :-)).

I kindly thank my Polish colleagues from the Polish Academy of Science: Prof. Dr. Alexander Guterch, Prof. Dr. Marek Grad, Wojciech Czbua and Dr. Piotr Sroda for sharing the Svalbard experiment in 1999 with *El Tanin* and the fruitful discussions during the cruise, on workshops and on meetings. Further, I am glad to have worked with Yuichi Nishimura during the same cruise, who acquired excellent obs-data along our transects.

I enjoyed the collaboration with the University of Bergen in Norway, especially with (Ass.) Prof. Dr. Rolf Mjelde and Dr. Asbjørn Breivik for acquisition of the seismic data of profiles 9 (OBS98) and 7 (*RV Håkon Mosby* '99). Further, I benefit from their proof reading of the manuscripts and helpful discussions on meetings. Here, I would like to acknowledge the participation of Dr. Hideki Shimamura from the Hokkaido University in Japan on the seismic refraction experiment OBS98.

In addition, many thanks to the crews of the involved ships *Polarstern*, *Håkon Mosby* and *El Tanin*.

Kind regards go to Dr. Graeme Eagles (AWI) for correction of the English manuscripts of the publications and thesis. No doubt that his work helped for a quick and successful review of the submitted publications!

Thanks are given to Dr. Tobias Boebel who performed the basic processing on airborne gravity data used for central Svalbard, and who compiled the gravity data as the regional grid used in this thesis.

For helpful discussions concerning geological and geophysical problems I thank sincerely Mechita Schmidt-Aursch, Dr. Johannes Rogenhagen, Dr. Vera Schlindwein, Etienne Wildeboer-Schut, Tom Schmitz, Daniel Birgel, Dr. Bernd Censarek, Sandra Jansen and the "Marine Geophysics" working group of the AWI. Additional standby was given by Dietrich Göttlicher, Sebastian Schaar and Jörg Wingender.

After all I thank my girlfriend Anja, my parents and brother for supporting me through the last few years.

REFERENCES

Amundsen, H.E.F., Griffin, W.L. & O'Reilly, S.Y., 1987. The lower crust and upper mantle beneath northwestern Spitsbergen: evidence from xenoliths and geophysics. Tectonophysics 139, 169-185.

Austegard, A., 1982. Velocity analysis of sonobuoy data from the northern Svalbard margin. Seismol. Obs. Scientific Report 9, University of Bergen, Bergen.

Austegard, A. & Sundvor, E., 1991. The Svalbard continental margin: Crustal structure from analysis of deep seismic profiles and gravity. Seismo-Series 53, University of Bergen, Bergen.

Barton, A.J. & White, R.S., 1997. Crustal structure of Edoras Bank continental margin and mantle thermal anomalies beneath the North Atlantic. J. Geophys. Res. 102 (B2), 3109-3129.

Baturin, D.G., 1990. Structure and Geodynamics of the Malloy Transform Fault Zone in the Mid-Oceanic Ridge System of the Norway-Greenland Basin. Oceanology 30 (3), 316-320.

Boebel, T., 2000. Airborne topography and gravimetry: System and application to Fram Strait, Svalbard and Northeast Greenland. Reports on Polar Research 366, Alfred Wegener Institute for Polar and Marine Research, Bremerhaven.

Bown, J.W. & White, R.S., 1994. Variation with spreading rate of oceanic crustal thickness and geochemistry. E. Planet. Sci. Lett. 121, 435-449.

Breivik, A.J., Verhoef, J. & Faleide, J.I., 1999. Effect of thermal constraints on gravity modeling at passive margins: Results from the western Barents Sea. J. Geophys. Res. 104 (B7), 15293-15311.

Chan, W.W. & Mitchell, B.J., 1982. Synthetic seismogram and surface wave contraints on crustal models of Spitsbergen. Tectonophysics 89, 51-76.

Christensen, N.I., 1966. The elasticity of ultrabasic rocks. J. Geophys. Res. 71, 5921-5931.

Christensen, N.I., 1978. Ophiolites, seismic velocities, and ocean crustal structure. Tectonophysics 47, 131-157.

Christensen, N.I. & Mooney, W.D., 1995. Seismic velocity structure and composition of the continental crust: A global view. J. Geophys. Res. 100 (B7), 9761-9788.

Crane, K., Sundvor, E., Buck, R. & Martinez, F., 1991. Rifting in the Northern Norwegian-Greenland Sea: Thermal Tests of Asymmetric Spreading. J. Geophys. Res. 96 (B9), 14529-14550.

Crane, K., Doss, H., Vogt, P., Sundvor, E., Cherkashov, G., Poroshima, I. & Joseph, D., 2001. The role of the Spitsbergen Shear Zone in determining morphology, segmentation and evolution of the Knipovich Ridge. Mar. Geophys. Res. 22, 153-205.

Czuba, W., Grad, M. & Guterch, A., 1999. Crustal structure of north-western Spitsbergen from DSS measurements. Polish Polar Research 20 (2), 131-148.

Czuba, W., Ritzmann, O., Nishimura, Y., Grad, M., Guterch, A., Jokat, W. & Mjelde, R., in preparation. Crustal structure of Northern Spitsbergen between the Molloy Deep and Nordaustlandet from SMORE II DSS profile.

DeMets, C., Gordon, R.G., Argus, D.F. & Stein, S., 1990. Current plate motions. Geophys. J. Int. 101, 425-478.

Detrick, R.S., White, R.S. & Purdy, G.M., 1993. Crustal structure of North Atlantic Fracture Zones. Rev. Geophys. 31 (4), 439-458.

Dimakis, P., Braathen, B.I., Faleide, J.I., Elverhøi, A. & Gudlaugsson, S.T., 1998. Cenozoic erosion and the preglacial uplift of the Svalbard-Barents Sea region. Tectonophysics 300, 311-327.

Doré, A.G. & Jensen, L.N., 1996. The impact of Late Cenozoic uplift and erosion on hydrocarbon exploration: offshore Norway and other uplifted basins. Global and Planetary Change 12, 415-436.

Edwards, R.A., Whitmarsh, R.B. & Scrutton, R.A., 1997. The crustal structure across the transform continental margin off Ghana, eastern equatorial Atlantic. J. Geophys. Res. 102 (B1), 747-772.

Eiken, O., 1993. An outline of the northwestern Svalbard continental margin. In: Vorren, T.O., Bergsager, E., Dahl-Stamnes, Ø.A., Holter, E., Johansen, B., Lie, E. & Lund, T.B. (Eds.), Arctic Geology and Petroleum Potential. NPF Special Publications 2, Elsevier, Amsterdam, pp. 619-629.

Eiken, O., 1994. Seismic Atlas of Western Svalbard - A selection of regional seismic transects. Meddelelser Nr. 130, Norsk Polarinstitutt, Oslo.

Eiken, O. & Austegard, A., 1987. The Tertiary orogenic belt of West-Spitsbergen: Seismic expressions of the offshore sedimentary basins. Norsk Geologisk Tidsskrift 67, 383-394.

Eiken, O. & Hinz, K., 1993. Contourites in the Fram Strait. Sedimentary Geology 92, 15-32.

Eldholm, O., Faleide, J.I. & Myhre, A.M., 1987. Continent-ocean transition at the western Barents Sea/Svalbard continental margin. Geology 15, 1118-1122.

Eldholm, O., Karasik, A.M. & Reksnes, P.A., 1990. The North American plate boundary. In: Grantz, A., Johnson, L. & Sweeney, J.F. (Eds.), The Arctic Ocean region. The Geology of North America Vol. L, Geological Society of America, Boulder, pp. 171-184.

Etheridge, M.A. & Vernon, R.H., 1983. Comment on "Seismic velocity and anisotropy in mylonites and the reflectivity of deep crustal fault zones". Geology 11, 487-489.

Faleide, J.I., Gudlaugsson, S.T., Eldholm, O., Myhre, A.M. & Jackson, H.R., 1991. Deep seismic transects across the sheared western Barents Sea-Svalbard continental margin. Tectonophysics 189, 73-89.

Fechner, N. & Jokat, W., 1996. Seismic refraction investigations on the crustal structure of the western Jameson Land Basin, East Greenland. J. Geophys. Res. 101 (B7), 15867-15881.

Feden, R.H., Vogt, P.R. & Fleming, H.S, 1979. Magnetic and Bathymetric Evidence for the "Yermak Hot Spot" northwest of Svalbard in the Arctic Basin. E. Planet. Sci. Lett. 44, 18-38.

Forsberg, R., 1984. A Study of Terrain Reductions, Density Anomalies and Geophysical Inversion Methods in Gravity Field Modeling. Reports of the Department of Geodetic Science and Surveying 355, Ohio State University, Columbus.

Fountain, D.M., Hurich, C.A. & Smithson, S.B., 1984. Seismic reflectivity of mylonite zones in the crust. Geology 12, 195-198.

Fowler, C.M.R., 1995. The Solid Earth - An Introduction to Global Geophysics. Cambridge University Press, Cambridge.

Friend, P.F., Harland, W.B., Rogers, D.A., Snape, I. & Thorney, S., 1997. Late Silurian and Early Devonian stratigraphy and probable strike-slip tectonism in north-western Spitsbergen. Geological Magazine 134, 459-479.

Funck, T. & Louden, K.E., 1999. Wide-angle seismic transect across the Torngat Orogen, northern Labrador: Evidence for a Proterozoic crustal root. J. Geophys. Res. 104 (B4), 7463-7480.

Gabrielsen, R.H., Oddbjørn, S.K., Haugsbø, H., Midbøe, P.S., Nøttvedt, A., Rasmussen, E. & Skott, P.H., 1992. A structural outline of Forlandsundet Graben, Prins Karls Forland, Svalbard. Norsk Geologisk Tidsskrift 72, 105-120.

Gardner, G.H.F., Gardner, L.W. & Gregory, A.R., 1974. Formation Velocity and Density - The Diagnostic Basic for Stratigraphic Traps. Geophysics 99 (6), 770-780.

Geissler, W.H., 2001. Marine seismische Untersuchungen am nördlichen Kontinentalrand von Svalbard (Spitzbergen). Unpublished diploma thesis, Institut für Geophysik der Technischen Universität Bergakademie Freiberg, Freiberg.

Guterch, A., Pajchel, J., Perchuc, E., Kowalski, J., Duda, S., Komber, G., Bojdys, G. & Sellevoll, M.A., 1978. Seismic reconnaissance measurements on the crustal structure in the Spitsbergen Region 1976. University of Bergen Seismological Observatory, Bergen.

Håkansson, E. & Pedersen, S.A.S., 1982. Late Paleozoic to Tertiary tectonic evolution of the continental margin in North Greenland. In: Embry, A.F. & Balkwill, H.R. (Eds.), Arctic Geology and Geophysics. Can. Soc. Pet. Geol. Mem. 8, Canadian Society of Petroleum Geologists, Calgary, pp. 331-348.

Håkansson, E. & Stemmerik, L., 1984. Wandel Sea Basin - The North Greenland equivalent to Svalbard and the Barents Shelf. In: Spencer, A.M. (Ed.), Petroleum geology of the North European margin. Graham & Trotham, London, pp. 97-108.

Hajnal, Z., Burianyk, M.J.A., Kesmarky, I. & Overton, A., 1990. Reflection Survey on Hobson's Choise Island, Arctic Ocean. Marine Geology 93, 211-224.

Harland, W.B., 1997a. Svalbard's geological frame. In: Harland, W.B. (Ed.), The Geology of Svalbard. Geological Survey Memoir 17, The Geological Society London, pp. 23-44.

Harland, W.B., 1997b. Devonian History. In: Harland, W.B. (Ed.), The Geology of Svalbard. Geological Survey Memoir 17, The Geological Society London, London, pp. 289-309.

Harland, W.B., 1997c. Northwestern Spitsbergen (with a contribution of Doubleday, P.A.). In: Harland, W.B. (Ed.), The Geology of Svalbard. Geological Survey Memoir 17, The Geological Society London, pp. 132-153.

Harland, W.B., 1997d. Northeastern Spitsbergen. In: Harland, W.B. (Ed.), The Geology of Svalbard. Geological Survey Memoir 17, The Geological Society London, pp. 110-131.

Harland, W.B., 1997e. Central Western Spitsbergen (with a contribution of Geddes, I. & Doubleday, P.A.). In: Harland, W.B. (Ed.), The Geology of Svalbard. Geological Survey Memoir 17, The Geological Society London, pp. 154-178.

Harland, W.B., 1997f. Paleogene History (with a contribution of Challinor, A. & Doubleday, P.A.). In: Harland, W.B. (Ed.), The Geology of Svalbard. Geological Survey Memoir 17, The Geological Society London, pp. 388-417.

Harland, W.B. & Wright, N.J.R., 1979. Alternative hypothesis for the pre-Carboniferous evolution of Svalbard. Norsk Polarinstitutt Skrifter 167, 89-117.

Hellebrand, E., 2000. Petrology. In: Jokat, W. (Ed.), The Expedition ARKTIS-XV/2 of "Polarstern" in 1999. Reports on Polar Research 368, Alfred Wegener Institute for Polar and Marine Research, Bremerhaven, pp. 59-60.

Hjelle, A., 1979. Aspects of the geology of northwest Spitsbergen. Norsk Polarinstitutt Skrifter 167, 37-63.

Hjelle, A. & Lauritzen, Ø., 1982. Geological Map of Svalbard 1 : 500 000 Sheet 3G, Spitsbergen northern part. Norsk Polarinstitutt, Oslo.

Holbrook, W.S., Mooney, W.D. & Christensen, N.I., 1992. The seismic velocity structure of the deep continental crust. In: Fountain, D.M., Arculus, R. & Kay, R.W. (Eds.), Continental Lower Crust. Developments in Geotectonics 23, Elsevier, Amsterdam, pp. 1-43.

Howells, K., Masson-Smith, D. & Maton, P.I., 1977. Some rock and formation densities from Svalbard. Norsk Polarinstitutt Årbok 1975, 53-67.

Horn, J.R., Clowes, R.M., Ellis, R.M. & Bird, D.N, 1984. The seismic structure across an active oceanic/continental transform fault zone. J. Geophys. Res. 89 (B5), 3107-3120.

Jackson, H.R., 1990. Evolution and Regional Stratigraphy of the Northeastern Canadian Polar Margin. Marine Geology 93, 179-192.

Jackson, H.R., Johnson, G.L., Sundvor, E. & Myhre, A., 1984. The Yermak Plateau: Formed at a Triple Junction. J. Geophys. Res. 89 (B5), 3223-3232.

Johannessen, E.P., & Steel, R.J., 1992. Mid-Carboniferous extension and rift-infill sequences in the Billefjorden Trough, Svalbard. Norsk Geologisk Tidsskrift 72, 35-48.

Jakobsson, M., Cherkis, N.Z., Woodward, J., Macnab, R. & Coakley, B., 2000. New grid of Arctic bathymetry aids scientists and mapmakers. EOS Transactions 81 (9), 89, 93, 96.

Jokat, W., 2000. The Sediment Distribution below the North Greenland Continental Margin and the adjacent Lena Trough. Polarforschung 68, 71-82.

Jokat, W., Eisen, O., Konn, B., Lensch, N., Martens, H., Ritzmann, O., Rogenhagen, J., Thalmann, K. & Weigelt, E., 1998. Marine Geophysics. In: Krause, G. (Ed.), The Expedition ARKTIS-XIII/3 of RV "Polarstern" in 1997. Reports on Polar Research 262, Alfred Wegener Institute for Polar and Marine Research, Bremerhaven, pp. 71-82.

Jokat, W., Czuba, W., Dzewas, J., Ehrhardt, A., Gierlichs, A., Kühn, D., Martens, H., Lensch, N., Nicolaus, M., Nishimura, Y., Ritzmann, O., Schmidt-Aursch, M., Sroda, P. & Wildeboer-Schut, E., 2000. Marine Geophysics. In: Jokat, W. (Ed.), The Expedition ARKTIS-XV/2 of "Polarstern" in 1999. Reports on Polar Research 368, Alfred Wegener Institute for Polar and Marine Research, Bremerhaven, pp. 8-26.

Jokat, W., Bohlmann, H., Drachev, S., Galaktionov, A., Karpinos, G., Lahrmann, B., Lensch, N., Miksch, U., Müller, K., Pignatelli, A., Ritzmann, O., Schmidt-Aursch, M., Schmidt, T., Schmitz, T. & Wüstefeld, A., 2002. Seismic Refraction Experiments along the Gakkel Ridge. In: Thiede, J. & the Shipboard Scientific Party (Eds.), Polarstern ARKTIS-XVII/2 Cruise Report: AMORE 2001 (Arctic Mid-Ocean Ridge Expedition). Reports on Polar Research 421, Alfred Wegener Institute for Polar and Marine Research, Bremerhaven, pp. 178-180.

Kearey, P. & Brooks, M., 1999. An introduction into geophysical exploration. Blackwell Science, Oxford.

Kellogg, H.E., 1975. Tertiary Stratigraphy and Tectonism in Svalbard and Continental Drift. AAPG Bull. 59 (3), 465-485.

Klingelhöfer, F., Géli, L., Matias, L., Steinsland, N. & Mohr, J., 2000. Crustal structure of a super-slow spreading centre: a seismic refraction study of Mohns Ridge, 72°N. Geophys. J. Int. 141, 509-526.

Kristoffersen, Y., 1990a. On the tectonic evolution and the paleoceanographic significance of the Fram Strait Gateway. In: Bleil, U. & Thiede, J. (Eds.), Geological History of the Polar Oceans: Arctic Versus Antarctic. NATO ASI Series C 308, Kluwer Academic Publishers, Dordrecht, pp. 63-76.

Kristoffersen, Y., 1990b. Eurasia Basin. In: Grantz, A., Johnson, L. & Sweeney, J.F. (Eds.), The Artic Ocean region. The Geology of North America Vol. L, Geological Society of America, Boulder, pp. 365-378.

Kurinin, R.G., 1970. Density and Magnetic Susceptibilities of Spitsbergen Rocks. In: Harland, W.B. (Ed.), Geology of Spitsbergen, 1965 Vol 2. National Lending Library for Science and Technology, Yorkshire, pp. 284-286.

Lawver, L.A., Müller, R.D., Srivastava, S.P. & Roest, W., 1990. The opening of the Arctic Ocean. In: Bleil, U. & Thiede, J. (Eds.), Geological History of the Polar Oceans: Arctic Versus Antarctic. NATO ASI Series C 308, Kluwer Academic Publishers, Dordrecht, pp. 29-62.

LCT, 1998. User's Guide. LCT Inc., Houston.

Lepvrier, C. & Geyssant, J., 1985. L'evolution structurale de la marge occidentale du Spitsberg: coulissement et rifting tertiares. Bulletin de la Société Géologique du Nord 103, 333-344.

Lin, J., Purdy, G.M., Schouten, H., Sempere, J.-C. & Zervas, C., 1990. Evidence from gravity data for focused magmatic accretion along the Mid-Atlantic Ridge. Nature 344, 627-632.

Lister, G.S., Etheridge, M.A. & Symonds, P.A., 1991. Detachment models for the formation of passive continental margins. Tectonics 10 (5), 1038-1064.

Ljones, F., Kuwano, A., Mjelde, R., Breivik, A., Shimamura, H., Murai, Y. & Nishimura, Y., submitted to Tectonophysics. Crustal transect from the Knipovich Ridge to the Svalbard Margin west of Hornsund.

Lorenzo, J.M., 1997. Sheared continent-ocean margins: an overview. Geo-Marine Letters 17, 1-3.

Lorenzo, J.M., Mutter, J.C., Larson, R.L., Buhl, P., Diebold, J., Mithal, R., Hopper, J., Falvey, D., Williamson, P. & Brassil, F., 1991. Development of the continent-ocean transform boundary of the southern Exmouth Plateau. Geology 19, 843-846.

Lowell, J.D., 1972. Spitsbergen Tertiary Orogenic Belt and the Spitsbergen Fracture Zone. Geol. Soc. Am. Bul. 83, 3091-3102.

Manby, G. & Lyberis, N., 1992. Tectonic evolution of the Devonian Basin of northern Svalbard. In: Dallmann, W.K., Andresen, A. & Krill, A. (Eds.), Post-Caledonian Tectonic Evolution of Svalbard. Norsk Geologisk Tidskrift 72, Scandinavian University Press, Oslo, pp. 7-19.

Mann, A. & Townsend, C., 1989. The post-Devonian tectonic evolution of southern Spitsbergen illustrated by structural cross-sections through Bellsund and Hornsund. Geological Magazine 126, 549-566.

Minshull, T.A., Muller, M.R., Robinson, C.J., White, R.S. & Bickle, M.J., 1998. Is the oceanic Moho a serpentinization front?. In: Mills, R.A. & Harrison, K. (Eds.), Modern Ocean Floor Processes and the Geological Record. Geol. Soc. Spec. Pub. 148, The Geological Society London, London, pp. 71-80.

Mjelde, R., Van Schaak, M. & Shimamura, H., 1998. OBS experiment in the Northern Barents Sea, 11. July - 31. August, 1998, Cruise report. University of Bergen, Bergen.

Mjelde, R. & Johansen, T.A., 1999. Cruise Report: Multichannel reflection survey west Spitsbergen, 17. September - 1. October 1999. University of Bergen, Bergen.

Müller, D. & Spielhagen, R.F., 1990. Evolution of the Central Tertiary Basin of Spitsbergen: towards a synthesis of sediment and plate tectonic history. Palaeogeography, Palaeoclimatology, Palaeoecology 80, 153-172.

Mutter, J.C., Buck, W.R. & Zehnder, C.M., 1988. Convective partial melting - A model for the formation of thick basaltic sequences durmg the initiation of spreading. J. Geophys. Res. 93 (B2), 1031-1048.

Myhre, A.M., Eldholm, O. & Sundvor, E., 1982. The margin between Senja and Spitsbergen fracture zones: Implications from plate tectonics. Tectonophysics 89, 1-32.

Myhre, A.M. & Eldholm, O., 1988. The Western Svalbard margin (74°-80°N). Marine and Petroleum Geology 5, 143-156.

Myhre, A.M., Thiede, J. & Firth, J.V., et al., 1995. Proceedings of the Ocean Drilling Program Initial Reports 151. Ocean Drilling Program Texas A&M University, College Station.

Neumann, E.-R. & Schilling, J.G., 1984. Petrology of basalts from the Mohns-Knipovich Ridge; the Norwegian-Greenland Sea. Contrib. Mineral. Petrol. 85, 209-223.

Nøttvedt, A., Livbjerg, F., Midbøe, P.S. & Rasmussen, E., 1993. Hydrocarbon potential of the Central Spitsbergen Basin. In: Vorren, T.O., Bergsager, E., Dahl-Stamnes, Ø.A., Holter, E., Johansen, B., Lie, E. & Lund, T.B. (Eds.), Arctic Geology and Petroleum Potential. NPF Special Publications 2, Elsevier, Amsterdam, pp. 333-361.

Oakey, G.N., Scott, R.A., Jackson, H.R. & Macnab, R., 1998. Circum-Arctic Magnetic Anomaly Map with Tectonic Overlay Polar Stereographic Projection, Geological Survey of Canada, Dartmouth.

Okay, N. & Crane, K., 1993. Thermal Rejuvenation of the Yermak Plateau. Mar. Geophys. Res. 15, 243-263.

Posewang, J. & Mienert, J., 1999. High-resolution seismic studies of gas hydrates west of Svalbard. Geo-Marine Letters 19, 150-156.

Reid, I.D., 1988. Crustal structure beneath the southern Grand Banks: seismic-refraction results and their implications. Can. J. Earth Sci. 25, 760-772.

Reid, I.D. & Jackson, H.R., 1997. A review of three transform margins off eastern Canada. Geo-Marine Letters 17, 87-93.

Ritzmann, O. & Jokat, W., 2003. Crustal structure of northwestern Svalbard and the adjacent Yermak Plateau: Evidence for Oligocene detachment tectonics and non-volcanic break-up. Geophys. J. Int. 152, 139-159.

Ritzmann, O., Jokat, W., Czuba, W., Guterch, A., Mjelde, R. & Nishimura, Y., submitted to Marine Geophysical Researches, see Chapter 3. A deep seismic transect in northwestern Svalbard at Kongsfjorden (Ny Ålesund) and the implications for Cenozoic break-up from Greenland: A sheared margin study.

Saunders, A.D., Storey, M., Kent, R.W. & Norry, M.J., 1992. Consequences of plume-lithosphere interactions. In: Storey, B.C., Alabaster, T. & Pankhurst, R.J. (Eds.), Magmatism and the Causes of Continental Break-up. Geol. Soc. Spec. Pub. 68. The Geological Society London, London, pp. 41-60.

Schmidt-Aursch, M.-C., 2002. Die Krustenstruktur der Fjordregion Ostgrönlands zwischen dem präkambrischen Schild und den rezenten mittelozeanischen Rücken: Ergebnisse seismischer und gravimetrischer Modellierungen. Dissertation, Universität Bremen, Bremen.

Schlindwein, V., 1998. Architecture and evolution of the continental crust of East Greenland from integrated geophysical studies. Reports on Polar Research 270, Alfred Wegener Institute for Polar and Marine Research, Bremerhaven.

Schlindwein, V. & Jokat, W., 1999. Structure and evolution of the continental crust of northern east Greenland from integrated geophysical studies. J. Geophys. Res. 104 (B7), 15227-15245.

Schlüter, H.U. & Hinz, K., 1978. The Continental margin of West Spitsbergen. Polarforschung 48 (1), 151-169.

Sellevoll, M.A., Duda, S.J., Guterch, A., Pajchel, J., Perchus, E. & Thyssen, F., 1991. Crustal structure in the Svalbard region from seismic measurements. Tectonophysics 189, 55-71.

Skogseid, J., Planke, S., Faleide, J.I., Pedersen, T., Eldholm, O. & Neverdal, F., 2000. NE Atlantic continental rifting and volcanic margin formation. In: Nøttvedt, A. (Ed.), Dynamics of the Norwegian Margin. Geol. Soc. Spec. Pub. 167. The Geological Society London, London, pp. 295-326.

Srivastava, S.P. & Tapscott, C.R., 1986. Plate kinematics of the North Atlantic. In: Vogt, P.R. & Tucholke, B.E. (Eds.), The Western North Atlantic Region. The Geology of North America Vol. M, Geological Society of America, Boulder, pp. 379-404.

Steel, R.J., Helland-Hansen, W., Kleinspehn, K., Nøttvedt, A. & Rye-Larsen, M., 1985. The Tertiary strike-slip basins and orogenic belt of Spitsbergen. In: Biddle, K.T. & Christie-Blick, N. (Eds.), Strike-slip deformation, Basin formation and Sedimentation. Special Publications Society of Economic Paleontologists and Mineralogists 37, Publisher SEPM Society for Sedimentary Geology, Tulsa, pp. 339-359.

Sundvor, E., Myhre, A.M., Austegard, A., Haugland, K., Eldholrn, O. & Gidskehaug, A., 1982. Marine geophysical survey on the Yermak Plateau. Seismological Observatory Sci. Rep. 7, University of Bergen, Bergen.

Sundvor, E. & Austegard, A., 1990. The Evolution of the Svalbard Margins: Synthesis and new Results. In: Bleil, U. & Thiede, J. (Eds.), Geological History of the Polar Oceans: Arctic Versus Antarctic. NATO ASI Series C 308, Kluwer Academic Publishers, Dordrecht, pp. 77-94.

Surlyk, F., 1991. Tectonostratigraphy of North Greenland. Bull. Grønlands Geol. Unders. 160, 25-47.

Talwani, M. & Eldholm, O., 1977. Evolution of the Norwegian-Greenland Sea. Geol. Soc. Am. Bul. 88, 969-999.

Thompson, R.N. & Gibson, S.A., 1991. Subcontinental mantle plumes, hotspots and pre-existing thinspots. Journal of the Geological Society London 147, 973-977.

Todd, B.J., Reid, I.D. & Keen, C.E., 1988. Crustal structure across the southwest Newfoundland transform margins. Can. J. Earth Sci. 25, 744-759.

Townsend, C. & Mann, A., 1989. The Tertiary Orogenic Belt of West Spitsbergen: seismic expressions of offshore sedimentary basins: A comment. Norsk Geologisk Tidsskrift 69, 135-136.

Vågnes, E. & Amundsen, H.E.F., 1993. Late Cenozoic uplift and volcanism on Spitsbergen caused by mantle convection?. Geology 21, 251-254.

Verhoef, J., Roest, W.R., Macnab, R., Arkani-Hamed, J. & Members of the Project Team, 1996. Magnetic anomalies of the Arctic and North Atlantic Oceans and adjacent land areas. GSC Open file 3125, Geological Survey of Canada, Dartmouth.

Weber, J.R. & Roots, E.F., 1990. Historical background; Explorations, concepts, and observations. In: Grantz, A., Johnson, L. & Sweeney, J.F. (Eds.), The Artic Ocean region. The Geology of North America Vol. L, Geological Society of America, Boulder, pp. 5-36.

Wernicke, B., 1985. Uniform-sense normal simple shear of the continental lithosphere. Can. J. Earth Sci. 22, 108-125.

White, R.S. & McKenzie, D., 1989. Magmatism at Rift Zones: The Generation of Volcanic Continental Margins and Flood Basalts. J. Geophys. Res. 94 (B6), 7685-7729.

White, R.S., McKenzie, D. & O'Nions, R.K., 1992. Oceanic Crustal Thickness From Seismic Measurements and Rare Earth Element Inversions. J. Geophys. Res. 97 (B13), 19683-19715.

White, R.S., Minshull, T.A., Bickle, M.J. & Robinson, C.J., 2001. Melt generation at very slow-spreading oceanic ridges; constraint from geochemical and geophysical data. J. Petr. 42 (6), 1171-1196.

Whitmarsh, R.B., Pinheiro, L.M., Miles, P.R., Recq, M. & Sibuet, J.-C., 1993. Thin crust at the western Iberia ocean-continent transition and ophiolites. Tectonics 12, 1230-1239.

Whitmarsh, R.B., Minshull, T.A, Russell, S.M., Dean, S.M., Louden, K.E. & Chain, D., 2001. The role of syn-rift magmatism in the rift-to-drift evolution of the West Iberia continental margin: geophysical observations. In: Wilson, R.C.L., Whitmarsh, R.B., Taylor, B. & Foitzheim, N. (Eds.), Non-volcanic Rifting of Continental Margins: A Comparision of Evidence from Land and Sea. Geol. Soc. Spec. Pub. 187, The Geological Society London, London, pp. 107-124.

Zelt, C.A. & Smith, R.B., 1992. Seismic travel time inversion for 2-D crustal velocity structure. Geophys. J. Int. 108, 16-34.

„Berichte zur Polarforschung"
Eine Titelübersicht der Hefte 1 bis 376 (1981 - 2000) erschien zuletzt im Heft 413 der nachfolgenden Reihe „Berichte zur Polar- und Meeresforschung". Ein Verzeichnis aller Hefte beider Reihen sowie eine Zusammenstellung der Abstracts in englischer Sprache finden sich im Internet unter der Adresse:
http://www.awi-bremerhaven.de/Resources/publications.html

Ab dem Heft Nr. 377 erscheint die Reihe unter dem Namen:
„Berichte zur Polar- und Meeresforschung"

Heft Nr. 377/2000 – „Rekrutierungsmuster ausgewählter Wattfauna nach unterschiedlich strengen Wintern", von Matthias Strasser

Heft Nr. 378/2001 – „Der Transport von Wärme, Wasser und Salz in den Arktischen Ozean", von Boris Cisewski

Heft Nr. 379/2001 – „Analyse hydrographischer Schnitte mit Satellitenaltimetrie", von Martin Losch

Heft Nr. 380/2001 – „Die Expeditionen ANTARKTIS XVI/1-2 des Forschungsschiffes ‚Polarstern' 1998/1999", herausgegeben von Eberhard Fahrbach und Saad El Naggar

Heft Nr. 381/2001 – „UV-Schutz- und Reparaturmechanismen bei antarktischen Diatomeen und *Phaeocystis antarctica*", von Lieselotte Rieger

Heft Nr. 382/2001 – "Age determination in polar Crustacea using the autofluorescent pigment lipofuscin", by Bodil Bluhm

Heft Nr. 383/2001 – „Zeitliche und räumliche Verteilung, Habitatspräferenzen und Populationsdynamik benthischer Copepoda Harpacticoida in der Potter Cove (King George Island, Antarktis)", von Gritta Veit-Köhler

Heft Nr. 384/2001 – „Beiträge aus geophysikalischen Messungen in Dronning Maud Land, Antarktis, zur Auffindung eines optimalen Bohrpunktes für eine Eiskerntiefbohrung", von Daniel Steinhage

Heft Nr. 385/2001 – „Actinium-227 als Tracer für Advektion und Mischung in der Tiefsee", von Walter Geibert

Heft Nr. 386/2001 – „Messung von optischen Eigenschaften troposphärischer Aerosole in der Arktis", von Rolf Schumacher

Heft Nr. 387/2001 – „Bestimmung des Ozonabbaus in der arktischen und subarktischen Stratosphäre", von Astrid Schulz

Heft Nr. 388/2001 – "Russian-German Cooperation SYSTEM LAPTEV SEA 2000: The Expedition LENA 2000", edited by Volker Rachold and Mikhail N. Grigoriev

Heft Nr. 389/2001 – "The Expeditions ARKTIS XVI/1 and ARKTIS XVI/2 of the Rearch Vessel 'Polarstern' in 2000", edited by Gunther Krause and Ursula Schauer

Heft Nr. 390/2001 – "Late Quaternary climate variations recorded in North Atlantic deep-sea benthic ostracodes", by Claudia Didié

Heft Nr. 391/2001 – "The polar and subpolar North Atlantic during the last five glacial-interglacial cycles", by Jan P. Helmke

Heft Nr. 392/2001 – „Geochemische Untersuchungen an hydrothermal beeinflußten Sedimenten der Bransfield Straße (Antarktis)", von Anke Dählmann

Heft Nr. 393/2001 – "The German-Russian Project on Siberian River Run-off (SIRRO): Scientific Cruise Report of the Kara Sea Expedition 'SIRRO 2000' of RV 'Boris Petrov' and first results", edited by Ruediger Stein and Oleg Stepanets

Heft Nr. 394/2001 – „Untersuchungen der Photooxidantien Wasserstoffperoxid, Methylhydroperoxid und Formaldehyd in der Troposphäre der Antarktis", von Katja Riedel

Heft Nr. 395/2001 – "Role of benthic cnidarians in the energy transfer processes in the Southern Ocean marine ecosystem (Antarctica)", by Covadonga Orejas Saco del Valle

Heft Nr. 396/2001 – "Biogeochemistry of Dissolved Carbohydrates in the Arctic", by Ralph Engbrodt

Heft Nr. 397/2001 – "Seasonality of marine algae and grazers of an Antarctic rocky intertidal, with emphasis on the role of the limpet *Nacilla concinna* Strebel (Gastropoda: Patellidae)", by Dohong Kim

Heft Nr. 398/2001 – „Polare Stratosphärenwolken und mesoskalige Dynamik am Polarwirbelrand", von Marion Müller

Heft Nr. 399/2001 – "North Antlantic Deep Water and Antarctic Bottom Water: Their Interaction and Influence on Modes of the Global Ocean Circulation", by Holger Brix

Heft Nr. 400/2001 – "The Expeditions ANTARKTIS XVIII/1-2 of the Research Vessel 'Polarstern' in 2000", edited by Victor Smetacek, Ulrich Bathmann, Saad El Naggar

Heft Nr. 401/2001 – „Variabilität von CH_2O (Formaldehyd) - untersucht mit Hilfe der solaren Absorptionsspektroskopie und Modellen", von Torsten Albrecht

Heft Nr. 402/2001 – "The Expedition ANTARKTIS XVII/3 (EASIZ III) of RV 'Polarstern' in 2000", edited by Wolf E. Arntz and Thomas Brey

Heft Nr. 403/2001 – „Mikrohabitatansprüche benthischer Foraminiferen in Sedimenten des Südatlantiks", von Stefanie Schumacher

Heft Nr. 404/2002 – „Die Expedition ANTARKTIS XVII/2 des Forschungsschiffes ‚Polarstern' 2000", herausgegeben von Jörn Thiede und Hans Oerter

Heft Nr. 405/2002 – "Feeding Ecology of the Arctic Ice-Amphipod *Gammarus wilkitzkii*. Physiological, Morphological and Ecological Studies", by Carolin E. Arndt

Heft Nr. 406/2002 – „Radiolarienfauna im Ochotskischen Meer - eine aktuopaläontologische Charakterisierung der Biozönose und Taphozönose", von Anja Nimmergut

Heft Nr. 407/2002 - "The Expedition ANTARKTIS XVIII/5b of the Research Vessel 'Polarstern' in 2001", edited by Ulrich Bathmann